Path Following Control of Wheeled Mobile Robots Combining Piecewise-Affine, Linear Parameter-Varying, and Backstepping Theories

Stefan LeBel

A Thesis

in

The Department

of

Mechanical and Industrial Engineering

Presented in Partial Fulfillment of the Requirements

for the Degree of Master of Applied Science (Mechanical Engineering) at

Concordia University

Montréal, Québec, Canada

August 2007

Your file Votre référence
ISBN: 978-0-494-34753-9
Our file Notre référence
ISBN: 978-0-494-34753-9

ABSTRACT

Path Following Control of Wheeled Mobile Robots Combining Piecewise-Affine, Linear Parameter-Varying, and Backstepping Theories

Stefan LeBel

This thesis presents a novel controller synthesis method for path following of a wheeled mobile robot (WMR). The proposed control method consists of a three-step procedure mixing piecewise-affine (PWA) and linear parameter-varying (LPV) techniques with backstepping. In the first step, two curvature limits and a curvature rate of change limit are defined for the desired path and the nonlinear WMR parameterized path kinematics are approximated by an uncertain piecewise-affine parameter-varying (PWAPV) system, while assuming that the WMR forward velocity is constant. A numerical method is proposed for determining PWA bounds on the uncertainty terms such that the original nonlinear parameter-dependent system is contained in the uncertain PWAPV system. Then, a PWAPV steering control law is designed using a parameter-dependent quadratic Lyapunov function. In the second step, a backstepping-type approach is used to include the vehicle dynamics and design the wheel control torques that guarantee convergence of the WMR forward and rotational velocities to the desired values. Finally, in the third step, the actuator dynamics are included and the input voltages are designed using backstepping. There are four primary advantages to the path following controller synthesis method proposed in this thesis. First, the PWAPV controller synthesis method can be formulated as a convex optimization program subject to a parameterized set of Linear Matrix Inequalities (LMIs), which will be approximated by a finite set of

LMIs using LPV theory and then solved efficiently using available software. Second, it includes both a general, non-singular path parameterization and the actuator dynamics. Third, the PWAPV control law can also stabilize the type of nonlinear parameter-dependent system considered here. And fourth, it is a first step toward including hard nonlinearities in the actuator dynamics, which are important PWA characteristics. The effectiveness of the proposed path following control method is demonstrated through numerical simulations.

ACKNOWLEDGEMENTS

First and foremost, I would like to thank my thesis adviser, Dr. Luis Rodrigues. Through your guidance and encouragement I have learned many things over the years, both about research and about myself. Thank you also to the professors and administrative staff in the department who helped throughout the time I was at Concordia.

I would also like to thank some of my research colleagues: Navid Dadkhah, Ralf Endress, Thomas Felder, Narendra Gollu, Henrique Paiva, Behzad Samadi, and Samer Shehab. Thank you all for the good laughs and the countless discussions of matters both related and unrelated to research. In particular, a big *merci* to Behzad for answering some of the really tough questions that others could not.

And last, but certainly not least, I would like to thank my wife, Karen, for supporting me and believing in me. You were there for me through all of it, both the good times and the bad.

CONTENTS

LIST OF FIGURES

NOMENCLATURE

$\{I\}$	inertial frame
$\{F\}$	Serret-Frenet frame
$C.G.$	center of gravity
$s = s(t)$	signed curvilinear abscissa
$c_c(t) = c_c(s(t))$	path curvature at given coordinate s
$P_{\{F\}}$	point of origin of Serret-Frenet frame $\{F\}$
P_{CG}	point of vehicle $C.G.$
$\mathbf{p}$	vector position of $P_{\{F\}}$, expressed in $\{I\}$
$\mathbf{q}$	vector position of P_{CG}, expressed in $\{I\}$
$\mathbf{r}$	vector position of P_{CG}, expressed in $\{F\}$
s_1	moving axis perpendicular to path curvature
y_1	moving axis tangent to path curvature
θ_v	angle of x body axis with respect to X inertial axis
θ_c	angle of s_1 moving axis with respect to X inertial axis
θ	heading error ($\theta = \theta_v - \theta_c$)
${}^F_I R$	rotation matrix from $\{I\}$ to $\{F\}$
u	velocity of vehicle along x body axis
v	velocity of vehicle along y body axis
r	angular velocity of vehicle about z body axis
M	vehicle mass
I	vehicle inertia about z body axis
r_w	radius of vehicle driving wheels
c	half-distance between vehicle driving wheels
T_R	torque applied to right driving wheel
T_L	torque applied to left driving wheel

ϕ_R	right wheel/motor angular position
ϕ_L	left wheel/motor angular position
L_a	DC motor electrical inductance
R_a	DC motor electrical resistance
K_b	DC motor back emf
K_m	DC motor constant
i_R	current in right driving motor
i_L	current in left driving motor
V_R	voltage applied to right driving motor
V_L	voltage applied to left driving motor
α	upper bound on the decay rate of state vector magnitude
$\rho(t)$	general time-varying parameter
$\mathbf{x}(t)$	general state vector
$\mathbf{u}(t)$	general input vector
$\mathbf{x}_1(t)$	vector of kinematic states
$\mathbf{x}_2(t)$	vector of kinematic and dynamic states
$\mathbf{x}_3(t)$	vector of kinematic, dynamic, and actuator states
LPV	linear parameter-varying
PWA	piecewise-affine
$PWAPV$	piecewise-affine parameter-varying
WMR	wheeled mobile robot

Chapter 1

Introduction

1.1 Motivation and Proposed Methodology

The problem of path following for autonomous vehicles is very important and has received a great deal of attention over the past few decades. In particular, the path following control of wheeled mobile robots (WMRs) allows for a wide range of applications. WMRs can be used in hazardous environments where human lives may be at risk, such as search and rescue operations, or in places where humans are unable to go, such as the exploration of extraterrestrial planets with the Mars Rover shown in Figure 1.1. This thesis proposes a novel path following controller synthesis method for WMRs that mixes piecewise-affine (PWA), linear parameter-varying (LPV), and backstepping methods.

The main motivation for the research proposed in this thesis stems from the need to develop more accurate models of WMRs. A broad range of nonlinear phenomena present in this type of vehicles, such as dead-zones, saturations, and hysteresis, are either already PWA or can be accurately approximated by PWA systems.

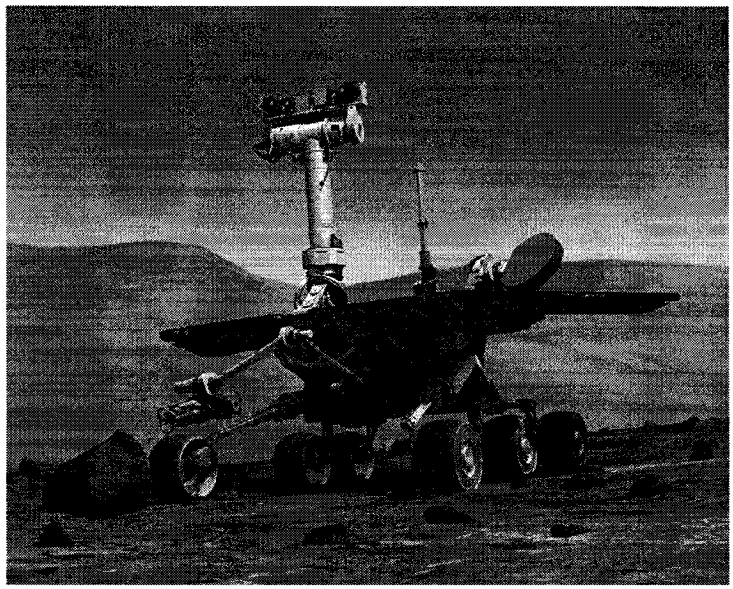

Figure 1.1: Mars Rover (Courtesy NASA/JPL-Caltech [1])

PWA systems represent a powerful modelling framework for complex dynamical systems involving nonlinear phenomena. However, existing PWA methods only consider the case where the dynamics are affine and constant within each region. By combining PWA and LPV methods, a new class of systems is introduced in this thesis, called piecewise-affine parameter-varying (PWAPV), whereby the dynamics in each region are affine and parameter-dependent. Furthermore, for nonlinear parameter-dependent systems that are approximated as PWAPV systems, the difference between the true and approximate dynamics leads to modelling uncertainties. A numerical method is proposed in this thesis for determining PWA bounds on the uncertainty terms such that the original nonlinear system is contained in the uncertain PWAPV system. This allows the synthesis of PWAPV controllers for nonlinear parameter-dependent systems.

The path following control method proposed in this thesis consists of a three-step procedure. In the first step, two curvature limits and a curvature rate of change

limit are defined for the desired path and the nonlinear WMR parameterized path kinematics are approximated by an uncertain PWAPV system, while assuming that the WMR forward velocity is constant. Then, a PWAPV steering control law is designed using a parameter-dependent quadratic Lyapunov function. In the second step, a backstepping-type approach is used to include the vehicle dynamics and design the wheel control torques that guarantee convergence of the WMR forward and rotational velocities to the desired values. Finally, in the third step, the actuator dynamics are included and the input voltages are designed using backstepping.

There are four primary advantages to the path following controller synthesis method proposed in this thesis. First, the PWAPV controller synthesis method can be formulated as a convex optimization program subject to a parameterized set of Linear Matrix Inequalities (LMIs), which will be approximated by a finite set of LMIs using LPV theory and then solved efficiently using available software [3]. Second, it includes both a general, non-singular path parameterization [2] and the actuator dynamics. Third, the PWAPV control law can also stabilize the class of nonlinear parameter-dependent systems considered here. And fourth, it is a first step toward including hard nonlinearities in the actuator dynamics, which are important PWA characteristics.

A review of the relevant literature on path following control and backstepping for WMRs, PWA techniques, and LPV methods is presented in the next section.

1.2 Literature Review

This section presents a review of the relevant literature on path following control and backstepping for WMR, PWA techniques, and LPV methods.

1.2.1 Path Following Control and Backstepping

The problem of path following for autonomous vehicles is very important and has received a great deal of attention over the past few decades. The importance of path following is made evident by the vast amount of work carried out in the area of path parameterization for the motion control of unicycle-type land robots [2,4,5], marine vehicles [6,7], and aerial vehicles (UAVs) [8–10].

Initial research in the area of path following and trajectory tracking for nonholonomic vehicles focused primarily on using only kinematic models. A thorough description of the kinematics for different types of WMRs is given by Zhao and BeMent [11]. Some of the different methods studied for path following and trajectory tracking using only WMR kinematics include discontinuous control [4, 12, 13], sliding mode control [14, 15], and dynamic feedback linearization [16–18]. A good survey of the work done on nonholonomic systems up until 1995 was conducted by Kolmanovsky and McClamroch [19].

An increasing amount of research is now examining the combination of kinematic and dynamic models. One of the first publications to use backstepping to include the vehicle dynamics is the work by Fierro and Lewis [20]. Since then, different control methods have been examined for the path following of WMRs, including adaptive backstepping [21–24], discontinuous backstepping [25], dynamic feedback linearization [26], approximate feedback linearization [27], and sliding mode control [28]. Some methods have also been developed to include dynamic constraints on the system [29,30], to combine position/force tracking control for nonholonomic systems [31], and to study the internal dynamic stability [32] as well as the zero dynamics [33] of mobile robots. Recently, some researchers have begun exploring

models with slipping motion [34–36]. A large body of research has focused on the robustness of controllers to unmodeled dynamics and parameter uncertainty [2,37–41]. It is only recently that research has been conducted in order to include the dynamics of the actuators in the controller design process [42–44]. This will be one of the major goals of this thesis. Moreover, as much as computer simulations are important in the development of models and controllers for WMRs, it is still important to conduct experiments to validate these models and controllers [26, 45–50].

One of the deficiencies of the path following methods mentioned thus far is their inability to effectively take into account hard nonlinearities in the system model. Since such nonlinear phenomena are important PWA characteristics, the use of PWA techniques is proposed in this thesis as a first step toward including such nonlinear phenomena.

1.2.2 Piecewise-Affine Methods

PWA systems represent a powerful modelling framework for complex dynamical systems involving nonlinear phenomena. With the emergence of promising new methods for stability analysis [51–54], state feedback controller synthesis [51, 55–60] and output feedback controller synthesis [61–63] for continuous-time PWA systems, this class of hybrid systems has become increasingly attractive for control purposes.

Although stability analysis and controller synthesis methods for continuous-time PWA systems have received a great deal of attention, it is only recently that modelling uncertainties have been taken into account. While Johansson [64] was able to analyze uncertain piecewise-linear (PWL) systems, Feng [65–69] is probably the first to examine the synthesis of stabilizing controllers for uncertain PWA systems. However, this problem is in general not convex and could only be transformed

into an LMI by assuming a special structure for the controller gain matrix [65–69]. Moreover, for nonlinear systems that are approximated as uncertain PWA systems, existing methods are unable to guarantee that the uncertainty terms include the nonlinear system. This will be another major goal of this thesis.

Given that PWA systems form a diverse and complex class of systems, formal synthesis methods must be targeted to systems with additional structure in order to cast the synthesis as a convex problem. In this sense, the work in this thesis departs considerably from previous work on controller synthesis for uncertain PWA systems and offers an interesting complementary approach. In fact, rather than imposing additional structure on the controller, this work will not constrain the controller and will focus instead on adding structure to the systems themselves. More specifically, a subclass of PWA systems is considered here: *PWA slab systems* [58]. Although not the most general class of PWA systems, PWA slab systems represent an important subclass because many practical systems are either already PWA slab systems or can be approximated by such systems with a high degree of accuracy. In fact, even for some systems that do not fall into this category, recent methods have been developed using backstepping techniques to transform the synthesis problem into the class of PWA slab systems [70, 71].

While research into PWA systems has been limited to systems where the dynamics are affine and constant within each region [70, 71], the new PWAPV systems introduced in this thesis, which combine PWA slab systems and LPV systems, are state-based switched systems whereby the dynamics in each region are affine and parameter-dependent.

1.2.3 Linear Parameter-Varying Methods

Initially, LPV methods received a great deal of attention because they provided a systematic means of designing gain-scheduled controllers [72, 73]. A good survey of the work up to 1999 is provided by Leith and Leithead [74]. Recently, LPV methods have been applied to a wide variety of systems, including spacecraft [75–77], high-performance aircraft [78, 79], missiles [80, 81], and vehicle engines [82].

Both quadratic and affine parameter-dependent Lyapunov functions were used for the analysis and controller synthesis of LPV systems [83–86]. Analysis methods were then proposed whereby the time-varying parameter was partitioned and the system described by different LPV dynamics in each region of the parameter [87, 88]. These methods used either continuous piecewise-affine parameter-dependent Lyapunov functions [87] or multiple parameter-dependent Lyapunov functions, which can be discontinuous at the switching boundaries [88]. Later, Lim and How extended their analysis method [87] to controller synthesis using quasi-piecewise-affine parameter-dependent Lyapunov functions [89]. More recently, a controller synthesis method was proposed using multiple parameter-dependent Lyapunov functions in which the time-varying parameter is partitioned and several LPV controllers are designed; the desired performance is then achieved by switching between the different controllers [90]. However, one drawback of this method is that it is restricted to a limited number of switches in any finite time interval.

Using the approach commonly taken in PWA methods, the PWAPV systems introduced in this thesis partition the state space, not the time-varying parameter. Additionally, the Lyapunov functions considered here are quadratic parameter-dependent. As will be seen in this thesis, the synthesis of PWAPV controllers for uncertain PWAPV slab systems can be cast as a convex program subject to a set

of LMIs. This is a major advantage of the proposed method.

The next section summarizes the main contributions and provides an outline of this thesis.

1.3 Contributions and Thesis Outline

The main contributions of this thesis are the following:

- Proposing a new class of systems, called uncertain piecewise-affine parameter-varying (PWAPV) systems.
- The formulation of the PWAPV controller synthesis problem for uncertain PWAPV slab systems as a convex program subject to a parameterized set of LMIs.
- The first successful combination of PWAPV controller synthesis methods with backstepping approaches for the control of nonlinear systems.
- Proposing a numerical method for determining PWA bounds on the uncertainty terms such that the original nonlinear system is contained in the uncertain PWAPV system. This allows the synthesis of PWAPV controllers for nonlinear parameter-dependent models.
- The first successful application of PWAPV controller synthesis methods to path following of a WMR.

The outline of the thesis is as follows:

- **Chapter 1** presents the introduction, contributions and thesis outline.

- **Chapter 2** presents the equations of motion for a WMR and reviews the path parameterization method used in this thesis. The path following problem considered in this thesis is also defined.

- **Chapter 3** defines the class of uncertain PWAPV systems introduced in this thesis. A method for approximating a nonlinear parameter-dependent system as an uncertain PWAPV system is described. A numerical method is also proposed for determining PWA bounds on the uncertainty terms such that the original nonlinear system is contained in the uncertain PWAPV system.

- **Chapter 4** proposes a convex PWAPV controller synthesis method for uncertain PWAPV slab systems, to be used in the following chapter.

- **Chapter 5** presents the three-step path following controller synthesis method proposed in this thesis.

- **Chapter 6** presents simulation results demonstrating the effectiveness of the proposed path following control method.

- **Chapter 7** states the conclusions and suggestions for future work.

The material presented in this thesis is based on the following work by the author:

- S. LeBel and L. Rodrigues, "PWL and PWA $\mathcal{H}_\infty$ Controller Synthesis for Uncertain PWA Slab Systems: LMI Approach," submitted to the *IEEE Trans. on Circuits and Systems I.*

- S. LeBel and L. Rodrigues, "Path Following of a Wheeled Mobile Robot Combining Piecewise-Affine Synthesis and Backstepping Approaches," in *Proc. of the 26th American Control Conf.*, New York, U.S.A., 11–13 July 2007, pp. 4513–4523.

• S. LeBel, L. Rodrigues, and A. Ng, "Piecewise-Affine Controller Synthesis for a Model of 2D Orbital Path Following," in *Proc. of the 2005 IEEE Conf. on Control Applications*, Toronto, Canada, 28–31 August 2005, pp. 571–576.

Chapter 2

Modelling of a WMR

This chapter presents the equations of motion for a wheeled mobile robot (WMR). We begin by describing the type of WMR under consideration, along with the coordinate systems used and the relevant parameters. Then, the WMR kinematic equations and path parameterization are described. This is followed by the WMR dynamic equations and the actuator dynamic equations. Finally, the WMR path following problem to be considered in this thesis is stated.

Consider the WMR shown in Figure 2.1, where $2c$ is the distance between the two driving wheels, r_w is the radius of the driving wheels, u is the velocity of the WMR in the direction of the x body axis, v is the velocity of the WMR in the direction of the y body axis, and r is the rotational velocity of the WMR about the z body axis. The heading angle of the WMR is given by θ_v and is measured from the positive X axis of the inertial frame. The mass of the WMR is M and its inertia about the z body axis is I. The origin of the body frame coincides with the center of gravity (C.G.) of the WMR and is located midway between the two driving wheels. Although other types of WMRs exist in the literature [11], a simple unicycle-type model is used here to demonstrate the methods proposed in this thesis and to make

use of the path parameterization method developed by Soeanto *et al.* [2]. The WMR is assumed to be rigid and to be driven by two wheels actuated by independently controlled DC motors. The subscripts $(\cdot)_R$ and $(\cdot)_L$ denote the right and left wheels and/or motors, respectively.

The inertial coordinate system is denoted by $\{I\}$ and the notation ${}^{I}(\cdot)$ means that the components of a vector are expressed in the inertial frame. The coordinate system $\{F\}$ is the Serret-Frenet frame that moves along the chosen path and represents the desired location and orientation of the vehicle. The notation ${}^{F}(\cdot)$ means that the components of a vector are expressed in the Serret-Frenet frame. The expression $\frac{d}{dt}\big|_F$ is the time derivative of a vector as measured by an observer in frame $\{F\}$.

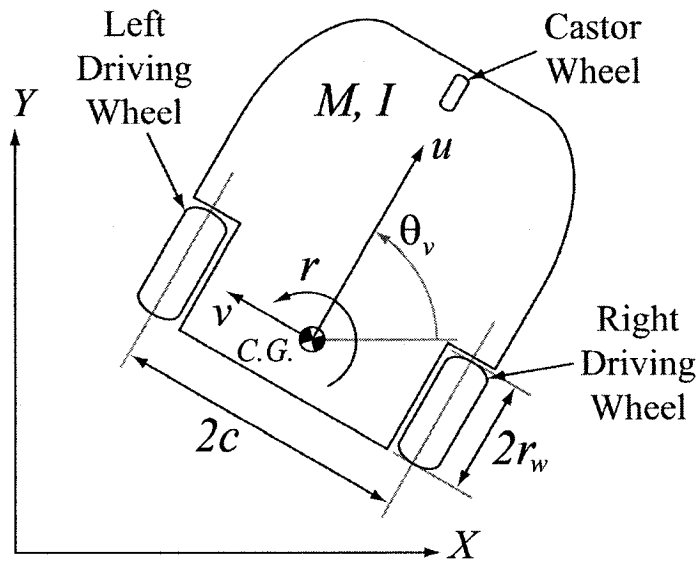

Figure 2.1: Diagram of wheeled mobile robot

The WMR kinematics and path parameterization are described in the next section.

2.1 WMR Kinematics and Path Parameterization

This section describes the WMR kinematics and reviews the parameterization method for path following of autonomous vehicles in the XY-plane developed by Soeanto *et al.* [2]. The main idea of the path parameterization method is to consider the position of the vehicle C.G. with respect to the desired position on the path, as well as the heading angle of the vehicle with respect to the tangent to the desired path, as the coordinates of an error space. A controller can then be designed that reduces these states to zero, which means that the vehicle is following the desired path.

Under the assumption that there is no sideslip velocity v, the WMR kinematic equations are given by

$$\begin{bmatrix} \dot{X} \\ \dot{Y} \\ \dot{\theta}_v \end{bmatrix} = \begin{bmatrix} \cos\theta_v & 0 \\ \sin\theta_v & 0 \\ 0 & 1 \end{bmatrix} \begin{bmatrix} u \\ r \end{bmatrix}. \tag{2.1}$$

Furthermore, it is assumed that the wheels roll without slipping. Thus, the driving wheel angular velocities $\dot{\phi}_R$ and $\dot{\phi}_L$ are directly related to the WMR forward and angular velocities according to

$$\begin{bmatrix} \dot{\phi}_R \\ \dot{\phi}_L \end{bmatrix} = \begin{bmatrix} \frac{1}{r_w} & \frac{c}{r_w} \\ \frac{1}{r_w} & -\frac{c}{r_w} \end{bmatrix} \begin{bmatrix} u \\ r \end{bmatrix}. \tag{2.2}$$

The path parameterization method is now described. The path parameters are shown in Figure 2.2. Consider a Serret-Frenet frame $\{F\}$ that moves along the chosen path and represents the desired location and orientation of the vehicle. The origin of this frame, point $P_{\{F\}}$, is not attached to the point on the path that is closest to the vehicle C.G., as is sometimes done [5], but is instead made to evolve according to some function of time [2]. Let vector $\mathbf{p}$ denote the position of point $P_{\{F\}}$ in $\{I\}$. Point P_{CG} is the position of the vehicle's C.G., which can either be

expressed by the vector ${}^{I}(\mathbf{q}) = (X,\ Y,\ 0)$ in the inertial frame $\{I\}$ or by the vector ${}^{F}(\mathbf{r}) = (s_1,\ y_1,\ 0)$ in the moving frame $\{F\}$. The heading angle of the vehicle is θ_v and the orientation of the Serret-Frenet frame is θ_c, both with respect to the X-axis of the inertial frame. Denoting by $s = s(t)$ the signed curvilinear abscissa of $P_{\{F\}}$ along the path, define $c_c(t) = c_c(s(t))$ as the path curvature and $\mathbf{t}$ as the unitary tangent vector at point $P_{\{F\}}$ on the path.

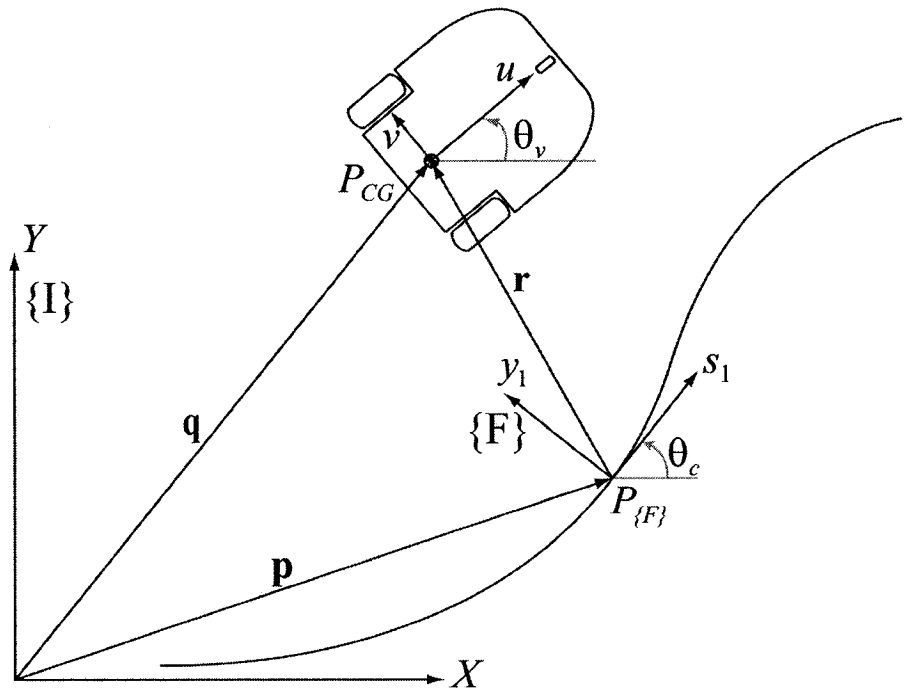

Figure 2.2: Path parameterization description (adapted from [2])

From the Coriolis Theorem [91], the inertial velocity of point P_{CG} expressed in $\{F\}$ is

$$ {}^{F}_{I}R \cdot {}^{I}\left(\frac{d\mathbf{q}}{dt}\right) = {}^{F}\left(\frac{d\mathbf{p}}{dt}\right) + {}^{F}\left(\frac{d\mathbf{r}}{dt}\bigg|_{F}\right) + {}^{F}(\boldsymbol{\omega}_c \times \mathbf{r}), \tag{2.3} $$

where the rotation matrix from $\{I\}$ to $\{F\}$ is

$$ {}^{F}_{I}R = \begin{bmatrix} \cos\theta_c & \sin\theta_c & 0 \\ -\sin\theta_c & \cos\theta_c & 0 \\ 0 & 0 & 1 \end{bmatrix}. \tag{2.4} $$

The inertial velocity of $P_{\{F\}}$ expressed in $\{F\}$ is

$$ {}^{F}\left(\frac{d\mathbf{p}}{dt}\right) = \dot{s} \cdot {}^{F}(\mathbf{t}) = \begin{bmatrix} \dot{s} \\ 0 \\ 0 \end{bmatrix}. \tag{2.5} $$

The inertial velocity of P_{CG} expressed in $\{I\}$ is

$$ {}^{I}\left(\frac{d\mathbf{q}}{dt}\right) = \begin{bmatrix} \dot{X} \\ \dot{Y} \\ 0 \end{bmatrix}, \tag{2.6} $$

while the velocity of P_{CG} as measured in $\{F\}$ and expressed in $\{F\}$ is

$$ {}^{F}\left(\left.\frac{d\mathbf{r}}{dt}\right|_{F}\right) = \begin{bmatrix} \dot{s}_1 \\ \dot{y}_1 \\ 0 \end{bmatrix}. \tag{2.7} $$

Since $\dot{\theta}_c = c_c(t)\dot{s}$, the cross product term of (2.3) is

$$ {}^{F}(\boldsymbol{\omega}_c \times \mathbf{r}) = \begin{bmatrix} 0 \\ 0 \\ c_c(t)\dot{s} \end{bmatrix} \times \begin{bmatrix} s_1 \\ y_1 \\ 0 \end{bmatrix} = \begin{bmatrix} -c_c(t)\dot{s}y_1 \\ c_c(t)\dot{s}s_1 \\ 0 \end{bmatrix}. \tag{2.8} $$

Combining and rearranging equations (2.3)–(2.8) yields

$$ \begin{cases} \dot{s}_1 = \dot{X}\cos\theta_c + \dot{Y}\sin\theta_c + c_c(t)\dot{s}y_1 - \dot{s} \\ \dot{y}_1 = -\dot{X}\sin\theta_c + \dot{Y}\cos\theta_c - c_c(t)\dot{s}s_1 \end{cases}. \tag{2.9} $$

It can be seen from (2.1) that the velocity of point P_{CG} expressed in $\{I\}$ is

$$\begin{bmatrix} \dot{X} \\ \dot{Y} \end{bmatrix} = u \begin{bmatrix} \cos\theta_v \\ \sin\theta_v \end{bmatrix}. \tag{2.10}$$

Introducing the variable $\theta = \theta_v - \theta_c$, we have

$$\dot{\theta} = \dot{\theta}_v - \dot{\theta}_c = r - c_c(t)\dot{s}, \tag{2.11}$$

where r is the angular velocity of the vehicle.

Finally, combining equations (2.9)–(2.11) yields

$$\begin{cases} \dot{\theta} = r - c_c(t)\dot{s} \\ \dot{s}_1 = u\cos\theta + c_c(t)\dot{s}y_1 - \dot{s} \\ \dot{y}_1 = u\sin\theta - c_c(t)\dot{s}s_1 \end{cases}. \tag{2.12}$$

The WMR dynamics are described in the next section.

2.2 WMR Dynamics

The WMR dynamic equations are given by

$$\begin{cases} \dot{u} = \frac{1}{Mr_w}(T_R + T_L) \\ \dot{r} = \frac{c}{Ir_w}(T_R - T_L) \end{cases}, \tag{2.13}$$

where T_R and T_L are the torques applied to the right and left wheels, respectively. The actuator dynamics are described in the next section.

2.3 Actuator Dynamics

The driving wheels of the WMR are actuated by two independently controlled DC motors. It is assumed that the right and left driving wheels and motors are identical

and thus possess the same physical characteristics. Furthermore, it is assumed that the shaft connecting the DC motors to their respective wheels is rigid and has zero inertia. The equations of the electrical component of the DC motors are [92]

$$\begin{cases} L_a \frac{d}{dt} i_R + R_a i_R + K_b \dot{\phi}_R = V_R \\ L_a \frac{d}{dt} i_L + R_a i_L + K_b \dot{\phi}_L = V_L \end{cases}, \tag{2.14}$$

where i_R and i_L are the motor currents, L_a is the electrical inductance, R_a is the electrical resistance, K_b is the back emf constant, and V_R and V_L are the input voltages. The torque produced by the DC motors is assumed to be linearly proportional to the armature current as

$$\begin{cases} T_R = K_m i_R \\ T_L = K_m i_L \end{cases}, \tag{2.15}$$

where K_m is the DC motor constant. Differentiating (2.15) and substituting the actuator dynamics (2.14) results in

$$\begin{cases} \dot{T}_R = -\frac{K_m R_a}{L_a} i_R - \frac{K_m K_b}{L_a} \dot{\phi}_R + \frac{K_m}{L_a} V_R \\ \dot{T}_L = -\frac{K_m R_a}{L_a} i_L - \frac{K_m K_b}{L_a} \dot{\phi}_L + \frac{K_m}{L_a} V_L \end{cases}. \tag{2.16}$$

The physical parameters used for the WMR are detailed in Chapter 6, when the path following controller synthesis method is applied in numerical simulations. After having derived the model of the WMR, the next section will state the path following problem to be solved in this thesis.

2.4 Problem Statement

The path following control problem considered in this thesis is now stated.

Problem 2.1 *Given a desired path, parameterized by a time-varying curvature $c_c(t)$, design a feedback control law for the actuator input voltages V_R and V_L for the system*

consisting of the WMR parameterized path kinematics (2.12), the WMR dynamics (2.13), and the actuator dynamics (2.16), such that the WMR follows the desired path. □

Chapter 5 proposes a three-step path following controller synthesis method to solve Problem 2.1. In the first step, two curvature limits and a curvature rate of change limit are defined for the desired path and the nonlinear WMR parameterized path kinematics are approximated by an uncertain piecewise-affine parameter-varying (PWAPV) system, while assuming that the WMR forward velocity is constant. Then, a PWAPV steering control law is designed using a parameter-dependent quadratic Lyapunov function. In the second step, a backstepping-type approach is used to include the vehicle dynamics and design the wheel control torques that guarantee convergence of the WMR forward and rotational velocities to the desired values. Finally, in the third step, the actuator dynamics are included and the input voltages are designed using backstepping.

However, before describing the proposed path following method in detail, Chapter 3 defines the class of uncertain PWAPV systems considered in this thesis and introduces a method for approximating nonlinear parameter-dependent systems by uncertain PWAPV slab systems such that the uncertainty bounds contain the nonlinear system. Then, Chapter 4 introduces the PWAPV controller synthesis problem for uncertain PWAPV slab systems, which will be used in the first step of the path following method proposed in Chapter 5.

Chapter 3

PWAPV Approximation of Nonlinear Systems

This chapter begins by defining the class of nonlinear and uncertain piecewise-affine parameter-varying (PWAPV) systems considered in this thesis. Then, a numerical method is described for approximating a nonlinear parameter-dependent system by a nominal PWAPV slab system. Finally, a numerical method is proposed for determining PWA bounds on the uncertainty terms in the PWAPV approximation such that the original nonlinear system is contained in the uncertain PWAPV system. The methods proposed in this chapter are valid for a nonlinear system that contains a nonlinear vector function of a scalar, which results in an uncertain PWAPV slab system. These methods will be used in Chapter 5.

3.1 Class of Systems

Consider a nonlinear parameter-dependent system of the form

$$\dot{\mathbf{x}}(t) = A(\rho)\mathbf{x}(t) + a(\rho) + f(\mathbf{x}) + B(\rho)\mathbf{u}(t), \tag{3.1}$$

where $\rho = \rho(t)$ is a time-varying parameter, $\mathbf{x}(t) \in \mathbb{R}^n$ is the state vector, and $\mathbf{u}(t) \in \mathbb{R}^{n_u}$ is the input vector. Matrices $A(\rho) \in \mathbb{R}^{n \times n}$, $a(\rho) \in \mathbb{R}^n$ and $B(\rho) \in \mathbb{R}^{n \times n_u}$ are affine in the time-varying parameter ρ, while the vector $f(\mathbf{x}) \in \mathbb{R}^n$ is nonlinear in the state vector $\mathbf{x}(t)$.

This thesis introduces the class of uncertain piecewise-affine parameter-varying (PWAPV) systems to approximate the nonlinear system (3.1). The dynamics of uncertain PWAPV systems are described by

$$\dot{\mathbf{x}}(t) = [A_i(\rho) + \Delta A(\mathbf{x})]\,\mathbf{x}(t) + [a_i(\rho) + \Delta a(\mathbf{x})] + B_i(\rho)\mathbf{u}(t), \quad \text{for } \mathbf{x}(t) \in \mathcal{R}_i, \quad (3.2)$$

where $\rho = \rho(t)$ is a time-varying parameter, $\mathbf{x}(t) \in \mathbb{R}^n$ is the state vector, and $\mathbf{u}(t) \in \mathbb{R}^{n_u}$ is the input vector. Matrices $A_i(\rho) \in \mathbb{R}^{n \times n}$, $a_i(\rho) \in \mathbb{R}^n$ and $B_i(\rho) \in \mathbb{R}^{n \times n_u}$ are affine in the time-varying parameter ρ and represent the nominal PWAPV system, while matrices $\Delta A(\mathbf{x}) \in \mathbb{R}^{n \times n}$ and $\Delta a(\mathbf{x}) \in \mathbb{R}^n$ are the uncertainty terms. The polytopic regions, $\mathcal{R}_i$, $i \in \mathcal{I} = \{1, \ldots, M\}$, partition a subset of the state space $\mathcal{X} \subset \mathbb{R}^n$ such that $\cup_{i=1}^{M} \overline{\mathcal{R}}_i = \mathcal{X}$, $\mathcal{R}_i \cap \mathcal{R}_j = \emptyset$, $i \neq j$, where $\overline{\mathcal{R}}_i$ denotes the closure of $\mathcal{R}_i$ (see [93] for generating such a partition). It is assumed that the desired closed-loop equilibrium point $\mathbf{x}^{cl}$ is the origin. The region in which $\mathbf{x}^{cl}$ lies is denoted as $\mathcal{R}_{i^*}$.

Following [51, 52, 94], each region is constructed as the intersection of a finite number (p_i) of half spaces

$$\mathcal{R}_i = \{\mathbf{x} \in \mathbb{R}^n \mid E_i\mathbf{x} + e_i \succ 0\}, \quad (3.3)$$

where $E_i \in \mathbb{R}^{p_i \times n}$ and $e_i \in \mathbb{R}^{p_i}$. The symbol $\succ$ denotes an element-wise inequality. Each polytopic region has a finite number of facets and vertices. Any two regions sharing a common facet will be called *level-1* neighbouring regions. Let $\mathcal{N}_i = \{$*level-1* neighbouring regions of $\mathcal{R}_i\}$. Vectors $H_{ij} \in \mathbb{R}^n$ and scalars h_{ij} exist such that the

facet boundary between regions $\mathcal{R}_i$ and $\mathcal{R}_j$ is contained in the hyperplane described by $\{\mathbf{x} \in \mathbb{R}^n \mid H_{ij}^T \mathbf{x} + h_{ij} = 0\}$, for $i = 1, \ldots, M$, $j \in \mathcal{N}_i$. A slab is a special case of a polyhedron, and is defined as follows.

Definition 3.1 *A slab is defined as*

$$\mathcal{S} = \{\boldsymbol{x} \in \mathbb{R}^n \mid h_1 < H^T \boldsymbol{x} < h_2\}, \tag{3.4}$$

where $H \in \mathbb{R}^n$ *and* $h_1, h_2 \in \mathbb{R}$. □

If $\mathcal{R}_i$ from (3.3) is a slab $\mathcal{S}$ defined as in (3.4), we have

$$E_i = \begin{bmatrix} H^T \\ -H^T \end{bmatrix}, \quad e_i = \begin{bmatrix} -h_1 \\ h_2 \end{bmatrix}. \tag{3.5}$$

Definition 3.2 *A piecewise-affine parameter-varying (PWAPV) slab system is a PWAPV system for which the regions are slabs.* □

For PWAPV slab systems, each region $\mathcal{R}_i$ can be outer approximated by a degenerate ellipsoid $\mathcal{E}_i$, such that $\mathcal{R}_i \subseteq \mathcal{E}_i$, where

$$\mathcal{E}_i = \{\mathbf{x} \in \mathbb{R}^n \mid \|L_i \mathbf{x} + l_i\|_2 < 1\}, \tag{3.6}$$

For PWAPV slab systems this covering is in fact exact, *i.e.* $\mathcal{R}_i \subseteq \mathcal{E}_i$ and $\mathcal{E}_i \subseteq \mathcal{R}_i$, and is described by

$$\begin{cases} L_i = 2H^T/(h_2 - h_1) \\ l_i = -(h_2 + h_1)/(h_2 - h_1) \end{cases}. \tag{3.7}$$

Finally, the following *a priori* assumptions, adapted from previous work in the robust piecewise-linear (PWL) control literature [65], are made for the uncertainty terms:

$$\begin{cases} \Delta A^T(\mathbf{x}) \Delta A(\mathbf{x}) \leq U_{A_i}^T U_{A_i} \\ \Delta a(\mathbf{x}) \Delta a^T(\mathbf{x}) \leq U_{a_i} U_{a_i}^T \end{cases}, \quad \text{for } \mathbf{x}(t) \in \mathcal{R}_i. \tag{3.8}$$

As shown in the proof of the following theorem, the nonlinear parameter-dependent system (3.1) is equivalent to an uncertain PWAPV system of the form (3.2) under certain conditions.

Theorem 3.1 *The nonlinear parameter-dependent system (3.1) is equivalent to the uncertain PWAPV system (3.2) if the constraint*

$$f(\boldsymbol{x}) - \tilde{A}_i\boldsymbol{x}(t) - \tilde{a}_i = \Delta A(\boldsymbol{x})\boldsymbol{x}(t) + \Delta a(\boldsymbol{x}), \quad \textit{for } \boldsymbol{x}(t) \in \mathcal{R}_i, \tag{3.9}$$

is satisfied. □

Proof: System (3.1) can be rewritten as

$$\dot{\mathbf{x}}(t) = A(\rho)\mathbf{x}(t) + a(\rho) + f(\mathbf{x}) + [\tilde{A}_i\mathbf{x}(t) + \tilde{a}_i] - [\tilde{A}_i\mathbf{x}(t) + \tilde{a}_i] + B(\rho)\mathbf{u}(t). \tag{3.10}$$

Using the constraint (3.9), this last equation becomes

$$\dot{\mathbf{x}}(t) = A(\rho)\mathbf{x}(t) + a(\rho) + \tilde{A}_i\mathbf{x}(t) + \tilde{a}_i + \Delta A(\mathbf{x})\mathbf{x}(t) + \Delta a(\mathbf{x}) + B(\rho)\mathbf{u}(t). \tag{3.11}$$

This can be rewritten as

$$\dot{\mathbf{x}}(t) = [A_i(\rho) + \Delta A(\mathbf{x})]\mathbf{x}(t) + [a_i(\rho) + \Delta a(\mathbf{x})] + B_i(\rho)\mathbf{u}(t), \tag{3.12}$$

where

$$\begin{cases} A_i(\rho) = A(\rho) + \tilde{A}_i \\ a_i(\rho) = a(\rho) + \tilde{a}_i \\ B_i(\rho) = B(\rho) \end{cases}.$$

This concludes the proof. □

In order to obtain the uncertain PWAPV system (3.2), the following steps must be carried out:

1. The nonlinear system (3.1) is approximated by a nominal PWAPV system.

2. The PWA uncertainty bounds (3.8) are determined such that the original nonlinear system is contained in the uncertain PWAPV system.

The next two section address these steps.

3.2 PWAPV Approximation

The first step in approximating the nonlinear system (3.1) by the uncertain PWAPV system (3.2) is to obtain a nominal PWAPV system of the form

$$\dot{\mathbf{x}}(t) = A_i(\rho)\mathbf{x}(t) + a_i(\rho) + B_i(\rho)\mathbf{u}(t), \quad \text{for } \mathbf{x}(t) \in \mathcal{R}_i, \tag{3.13}$$

with

$$\begin{cases} A_i(\rho) = A(\rho) + \tilde{A}_i \\ a_i(\rho) = a(\rho) + \tilde{a}_i \\ B_i(\rho) = B(\rho) \end{cases}, \tag{3.14}$$

where matrices $A(\rho)$, $a(\rho)$ and $B(\rho)$ in (3.14) are from (3.1), and matrices $\tilde{A}_i$ and $\tilde{a}_i$ in (3.14) come from the PWA approximation of the nonlinear function $f(\mathbf{x})$ in (3.1):

$$f(\mathbf{x}) \approx \tilde{A}_i\mathbf{x}(t) + \tilde{a}_i, \quad \text{for } \mathbf{x}(t) \in \mathcal{R}_i. \tag{3.15}$$

A numerical method for obtaining $\tilde{A}_i$ and $\tilde{a}_i$ is given by Samadi and Rodrigues [95], and is now described. Given a partition of the state space $\mathcal{X}$, the PWA approximation (3.15) of the nonlinear function $f(\mathbf{x})$ in (3.1) is defined in this case as the PWA function that minimizes the sum of squares of the error between the PWA function and the nonlinear function over the sampling points $\mathbf{x}_k$, $k = 1, \ldots, N_s$. Sampling points corresponding to the boundary between two neighbouring regions $\mathcal{R}_i$ and $\mathcal{R}_j$ for $i = 1, \ldots, M$, $j \in \mathcal{N}_i$, are denoted by $\mathbf{x}_{k^*}$.

Let the difference between the nonlinear function $f(\mathbf{x})$ in (3.1) and its PWA approximation (3.15), at the sampling points $\mathbf{x}_k$, be described by the error function

$$\mathbf{e}(\mathbf{x}_k) = f(\mathbf{x}_k) - \tilde{A}_i\mathbf{x}_k - \tilde{a}_i, \quad \text{for } \mathbf{x}_k \in \mathcal{R}_i,\ k = 1, \ldots, N_s, \tag{3.16}$$

which comes from the left-hand side of condition (3.9). Continuity of the PWA approximation (3.15) at the boundary points $\mathbf{x}_{k^\star}$ can be written as a set of linear constraints:

$$(\tilde{A}_i - \tilde{A}_j)\mathbf{x}_{k^\star} + (\tilde{a}_i - \tilde{a}_j) = 0, \quad \text{for } i = 1, \ldots, M,\ j \in \mathcal{N}_i. \tag{3.17}$$

Additionally, the PWA approximation (3.15) in region $\mathcal{R}_{i^\star}$ is made to be equal to the linear approximation of the nonlinear function $f(\mathbf{x})$ in (3.1) at $\mathbf{x}^{cl}$, given by $\tilde{A}_L\mathbf{x}(t) + \tilde{a}_L$. This can be ensured with the equality constraints

$$\begin{cases} \tilde{A}_{i^\star} = \tilde{A}_L \\ \tilde{a}_{i^\star} = \tilde{a}_L \end{cases}. \tag{3.18}$$

The PWA approximation (3.15) of the nonlinear function $f(\mathbf{x})$ in (3.1) can be obtained by solving the following convex optimization problem [95]:

Problem 3.1 *Given a partition of the state space $\mathcal{X}$, the sampling points $\boldsymbol{x}_k$, $k = 1, \ldots, N_s$, and matrices $\tilde{A}_L$ and $\tilde{a}_L$:*

$$\begin{aligned} \min \quad & \textstyle\sum_{k=1}^{N_s} \boldsymbol{e}^T(\boldsymbol{x}_k)\boldsymbol{e}(\boldsymbol{x}_k) \\ s.t. \quad & (3.16),\ (3.17),\ (3.18), \\ & i = 1, \ldots, M,\ j \in \mathcal{N}_i, \\ & k = 1, \ldots, N_s, \end{aligned}$$

where M is the number of state space partitions and $\boldsymbol{x}_{k^\star}$ are the sampling points corresponding to the boundary between two neighbouring regions. □

A numerical method for determining the PWA uncertainty bounds (3.8) is proposed in the next section.

3.3 PWA Uncertainty Bounds

Once the nominal PWAPV approximation (3.13) of the nonlinear parameter-dependent system (3.1) has been obtained, the PWA bounds (3.8) on the uncertainty terms in (3.2) can be determined such that the original nonlinear system is contained in the uncertain piecewise-affine parameter-varying (PWAPV) system.

The following function is proposed to describe the error function (3.16), at the sampling points $\mathbf{x}_k$,

$$\Delta A(\mathbf{x}_k)\mathbf{x}_k + \Delta a(\mathbf{x}_k) = \mathbf{e}(\mathbf{x}_k), \quad \text{for } i = 1, \ldots, M, \ k = 1, \ldots, N_s, \tag{3.19}$$

which comes from the right-hand side of condition (3.9), where matrices $\Delta A(\mathbf{x}_k)$ and $\Delta a(\mathbf{x}_k)$ are the uncertainty terms in (3.2) and are assumed to be polynomial functions in $\mathbf{x}_k$ of order n_p. Moreover, defining $W_{A_i} = U_{A_i}^T U_{A_i}$ and $W_{a_i} = U_{a_i} U_{a_i}^T$, the PWA constraints (3.8) can be written as the LMIs

$$\begin{bmatrix} W_{A_i} & \Delta A^T(\mathbf{x}_k) \\ \Delta A(\mathbf{x}_k) & I_{(n)} \end{bmatrix} \geq 0, \quad \text{for } \mathbf{x}_k \in \mathcal{R}_i, \ k = 1, \ldots, N_s, \tag{3.20}$$

and

$$\begin{bmatrix} W_{a_i} & \Delta a(\mathbf{x}_k) \\ \Delta a^T(\mathbf{x}_k) & 1 \end{bmatrix} \geq 0, \quad \text{for } \mathbf{x}_k \in \mathcal{R}_i, \ k = 1, \ldots, N_s. \tag{3.21}$$

The PWA uncertainty bounds (3.8) can be obtained by solving the following convex optimization problem:

Problem 3.2 *Given the sampling points $\boldsymbol{x}_k$, $k = 1, \ldots, N_s$, the scalar n_p, and the*

nominal PWAPV system (3.13):

$$\begin{aligned} \min \quad & \textstyle\sum_{i=1}^{M} trace\,[W_{A_i} + W_{a_i}] \\ s.t. \quad & (3.19),\ (3.20),\ (3.21) \\ & i = 1, \ldots, M, \\ & k = 1, \ldots, N_s, \end{aligned}$$

where $\Delta A(\boldsymbol{x}_k)$ *and* $\Delta a(\boldsymbol{x}_k)$ *are assumed to be polynomial functions in* $\boldsymbol{x}_k$ *of order* n_p. □

Remark 3.1 *Note that the PWA uncertainty bounds (3.8) resulting from the solution of Problem 3.2 are dependent on the sampling points* $\boldsymbol{x}_k$. *Therefore, it can not be guaranteed that the uncertainties resulting from the difference between the nonlinear parameter-dependent system (3.1) and the nominal PWAPV system (3.13) satisfy the PWA bounds (3.8) for* $\forall \boldsymbol{x}(t) \in \mathbb{R}^n$. □

This chapter defined the class of uncertain piecewise-affine parameter-varying (PWAPV) systems considered in this thesis. A numerical method was described for approximating nonlinear functions by PWA functions, which yields the nominal PWAPV system. A numerical method was then proposed for determining PWA bounds on the uncertainty terms such that the original nonlinear system is contained in the uncertain PWAPV system. The next chapter introduces the PWAPV controller synthesis problem for uncertain PWAPV slab systems.

Chapter 4

PWAPV Controller Synthesis

This chapter defines and solves the piecewise-affine parameter-varying (PWAPV) controller synthesis problem for the class of uncertain PWAPV slab systems defined in the previous chapter. The synthesis of a PWAPV controller will be used in the first step of the path following method proposed in the next chapter.

4.1 Design Objectives

The objective is to design a feedback control law that globally exponentially stabilizes the uncertain PWAPV system (3.2) (repeated here for convenience),

$$\dot{\mathbf{x}}(t) = [A_i(\rho) + \Delta A(\mathbf{x})]\,\mathbf{x}(t) + [a_i(\rho) + \Delta a(\mathbf{x})] + B_i(\rho)\mathbf{u}(t), \quad \text{for } \mathbf{x}(t) \in \mathcal{R}_i, \quad (4.1)$$

to the origin. The PWAPV state feedback control law proposed here is of the form

$$\mathbf{u}(t) = K_i(\rho)\mathbf{x}(t) + k_i(\rho), \quad \text{for } \mathbf{x}(t) \in \mathcal{R}_i. \quad (4.2)$$

Substituting (4.2) into (4.1) yields the closed-loop uncertain PWAPV system

$$\begin{aligned}\dot{\mathbf{x}}(t) = &\{[A_i(\rho) + \Delta A(\mathbf{x})] + B_i(\rho)K_i(\rho)\}\,\mathbf{x}(t) \\ &+ \{[a_i(\rho) + \Delta a(\mathbf{x})] + B_i(\rho)k_i(\rho)\}\end{aligned}, \quad \text{for } \mathbf{x}(t) \in \mathcal{R}_i, \quad (4.3)$$

which can be rewritten as

$$\dot{\mathbf{x}}(t) = \bar{A}_i^{cl}(\rho)\mathbf{x}(t) + \bar{a}_i^{cl}(\rho), \quad \text{for } \mathbf{x}(t) \in \mathcal{R}_i, \tag{4.4}$$

where

$$\begin{cases} \bar{A}_i^{cl}(\rho) = \{[A_i(\rho) + \Delta A(\mathbf{x})] + B_i(\rho)K_i(\rho)\} \\ \bar{a}_i^{cl}(\rho) = \{[a_i(\rho) + \Delta a(\mathbf{x})] + B_i(\rho)k_i(\rho)\} \end{cases}. \tag{4.5}$$

The PWA uncertainty bounds are given by (3.8) (repeated here for convenience),

$$\begin{cases} \Delta A^T(\mathbf{x})\Delta A(\mathbf{x}) \leq U_{A_i}^T U_{A_i} \\ \Delta a(\mathbf{x})\Delta a^T(\mathbf{x}) \leq U_{a_i} U_{a_i}^T \end{cases}, \quad \text{for } \mathbf{x}(t) \in \mathcal{R}_i. \tag{4.6}$$

Some background material must be reviewed before the PWAPV controller synthesis problem is stated.

4.2 Mathematical Preliminaries

This section presents two lemmas and one theorem to be used in the ensuing development.

Lemma 4.1 *[96] Let X and Y be real constant matrices of compatible dimensions, then the following equation*

$$X^TY + Y^TX \leq \epsilon X^TX + \epsilon^{-1}Y^TY$$

holds for any $\epsilon > 0$. □

Lemma 4.2 *If $M \geq 0$, then*

$$BMB^T \leq \text{trace}(M)BB^T$$

for any matrix B with appropriate dimensions. □

Proof: It suffices to show that $\text{trace}(M)I - M \geq 0$. This is true because the eigenvalues $\lambda_i(\beta I - M)$ are equal to $\beta - \lambda_i(M)$ for any β. Therefore, since the trace is the sum of all eigenvalues and since $M \geq 0$, the eigenvalues of $[\text{trace}(M)I - M]$ are all greater than or equal to zero, which finishes the proof. □

In the following theorem, ρ_{min} and ρ_{max} are limits on ρ, and $\bar{\rho}_{max}$ is a limit on the magnitude of $\dot{\rho}$.

Theorem 4.1 *Consider the closed-loop system (4.4), and let $\boldsymbol{x}^{cl} = 0$ be an equilibrium point of this system. Let $V : \mathbb{R}^n \to \mathbb{R}$ be a continuously differentiable function such that*

$$V(\boldsymbol{x}, \rho) = \boldsymbol{x}^T P(\rho) \boldsymbol{x} \tag{4.7}$$

with $P(\rho) = P^T(\rho) > 0$, and

$$\begin{aligned} \dot{V}(\boldsymbol{x}, \rho, \dot{\rho}) &= \dot{\boldsymbol{x}}^T P(\rho)\boldsymbol{x} + \boldsymbol{x}^T \dot{P}(\rho)\boldsymbol{x} + \boldsymbol{x}^T P(\rho)\dot{\boldsymbol{x}} \\ &= \dot{\boldsymbol{x}}^T P(\rho)\boldsymbol{x} + \boldsymbol{x}^T \dot{\rho}\tfrac{dP}{d\rho}\boldsymbol{x} + \boldsymbol{x}^T P(\rho)\dot{\boldsymbol{x}} \\ &< -\alpha V(\boldsymbol{x}, \rho) \end{aligned} \tag{4.8}$$

for $\forall \rho \in [\rho_{min}, \rho_{max}]$, $|\dot{\rho}| \leq \bar{\rho}_{max}$ and $\forall t \geq 0$, where $\alpha \geq 0$. Then the system (4.4) is globally exponentially stable to $\boldsymbol{x}^{cl}$ and the function $V(\boldsymbol{x}, \rho)$ is called a parameter-dependent quadratic Lyapunov function, where $\alpha \geq 0$ is an upper bound on the decay rate of the magnitude of the state vector $\boldsymbol{x}(t)$.

Proof: Integrating inequality (4.8) from t_0 to t yields [86]

$$V(\mathbf{x}(t), \rho(t)) \leq V(\mathbf{x}(t_0), \rho(t_0))e^{-\alpha(t-t_0)}, \tag{4.9}$$

for $\forall \rho \in [\rho_{min}, \rho_{max}]$. A quadratic positive definite function of the form (4.7) can be bounded according to

$$\lambda_{min}[P(\rho)]\|\mathbf{x}(t)\|_2^2 \leq V(\mathbf{x}(t), \rho) \leq \lambda_{max}[P(\rho)]\|\mathbf{x}(t)\|_2^2, \tag{4.10}$$

where $\lambda_{min}[P(\rho)]$ and $\lambda_{max}[P(\rho)]$ denote the minimum and maximum eigenvalues of $P(\rho)$, respectively. From the left-hand side inequality in (4.10),

$$\|\mathbf{x}(t)\|_2 \leq \left[\frac{1}{\lambda_{min}[P(\rho)]} V(\mathbf{x}(t), \rho)\right]^{\frac{1}{2}}. \tag{4.11}$$

With (4.9), inequality (4.11) can be bounded by

$$\|\mathbf{x}(t)\|_2 \leq \left[\frac{1}{\lambda_{min}[P(\rho)]} V(\mathbf{x}(t_0), \rho) e^{-\alpha(t-t_0)})\right]^{\frac{1}{2}}. \tag{4.12}$$

Then, using the right-hand side inequality in (4.10) at $t = t_0$, inequality (4.12) can be bounded by

$$\|\mathbf{x}(t)\|_2 \leq \left[\frac{\lambda_{max}[P(\rho)]}{\lambda_{min}[P(\rho)]} \|\mathbf{x}(t_0)\|_2^2 e^{-\alpha(t-t_0)}\right]^{\frac{1}{2}}. \tag{4.13}$$

This last expression is rewritten as

$$\|\mathbf{x}(t)\|_2 \leq \sqrt{\sigma[P(\rho)]}\ \|\mathbf{x}(t_0)\|_2\ e^{-\frac{\alpha}{2}(t-t_0)}, \tag{4.14}$$

for $\forall \rho \in [\rho_{min}, \rho_{max}]$, where $\sigma[P(\rho)] = \frac{\lambda_{max}[P(\rho)]}{\lambda_{min}[P(\rho)]}$ is the condition number of $P(\rho)$. □

The PWAPV controller synthesis problem is introduced in the next section.

4.3 PWAPV Controller Synthesis

The synthesis of piecewise-affine parameter-varying (PWAPV) controllers for uncertain PWAPV slab systems is presented as a theorem, followed by the proof.

Theorem 4.2 *Consider the uncertain PWAPV slab system (4.1) and the PWAPV state feedback (4.2). Let $I_{(n)}$ be an identity matrix of dimension n, where n is the number of state variables. Given $\alpha \geq 0$, $k_{lim} > 0$, $\mu_i < 0$, $i = 1, \ldots, M$, $\epsilon_j > 0$, $j = 1, \ldots, 6$, and λ_{max}, for $\forall \rho \in [\rho_{min}, \rho_{max}]$ and $|\dot{\rho}| \leq \bar{\rho}_{max}$, if $Q(\rho) = Q^T(\rho) > 0$,*

$\frac{dQ}{d\rho} - \lambda_{max} I_{(n)} \leq 0$, *inequality*

$$\begin{bmatrix} \Omega_i & I_{(n)} & I_{(n)} & Q(\rho)U_{A_i}^T \\ I_{(n)} & -\bar{\rho}_{max}^{-1}|\lambda_{max}|^{-1} I_{(n)} & 0 & 0 \\ I_{(n)} & 0 & -\epsilon_1 I_{(n)} & 0 \\ U_{A_i} Q(\rho) & 0 & 0 & -\epsilon_1^{-1} I_{(n)} \end{bmatrix} < 0, \tag{4.15}$$

is verified for $i = i^\star$, *and inequality*

$$\begin{bmatrix} \bar{\Omega}_i & I_{(n)} & I_{(n)} & Q(\rho)U_{A_i}^T & Q(\rho)L_i^T \\ I_{(n)} & -\bar{\rho}_{max}^{-1}|\lambda_{max}|^{-1} I_{(n)} & 0 & 0 & 0 \\ I_{(n)} & 0 & -\epsilon_1 I_{(n)} & 0 & 0 \\ U_{A_i} Q(\rho) & 0 & 0 & -\epsilon_1^{-1} I_{(n)} & 0 \\ L_i Q(\rho) & 0 & 0 & 0 & -\Gamma_i^{-1} \end{bmatrix} < 0, \tag{4.16}$$

is verified for $i \neq i^\star$ *with* $1 - l_i^2 < 0$, *where*

$$\Omega_i = A_i(\rho)Q(\rho) + B_i(\rho)Y_i(\rho) + Q(\rho)A_i^T(\rho) + Y_i^T(\rho)B_i^T(\rho) + \alpha Q(\rho)$$

for $i = i^\star$ *and*

$$\begin{aligned} \bar{\Omega}_i = {} & A_i(\rho)Q(\rho) + B_i(\rho)Y_i(\rho) + Q(\rho)A_i^T(\rho) + Y_i^T(\rho)B_i^T(\rho) + \alpha Q(\rho) \\ & + \mu_i[1 + l_i^2(1 - l_i^2)^{-1}][(1 + \epsilon_2^{-1})a_i(\rho)a_i^T(\rho) + (1 + \epsilon_2)U_{a_i}U_{a_i}^T] \\ & + \mu_i[1 + l_i^2(1 - l_i^2)^{-1}][a_i(\rho)k_i^T(\rho)B_i^T(\rho) + B_i(\rho)k_i(\rho)a_i^T(\rho)] \\ & + [\mu_i\epsilon_3 k_{lim}^2 + \mu_i\epsilon_4 k_{lim}^2 + \epsilon_5]U_{a_i}U_{a_i}^T + l_i(1 - l_i^2)^{-1}[a_i(\rho)L_iQ(\rho) + Q(\rho)L_i^T a_i^T(\rho)] \\ & + [\mu_i\epsilon_3^{-1} + \mu_i\epsilon_4^{-1}l_i^4(1 - l_i^2)^{-2} + \epsilon_6 + \mu_i k_{lim}^2\{1 + l_i^2(1 - l_i^2)^{-1}\}]B_i(\rho)B_i^T(\rho) \end{aligned}$$

with $\Gamma_i = [\epsilon_5^{-1}l_i^2(1 - l_i^2)^{-2} + \epsilon_6^{-1}l_i^2(1 - l_i^2)^{-2}k_{lim}^2 + \mu_i^{-1}(1 - l_i^2)^{-1}]$ *for* $i \neq i^\star$ *and if*

$$\begin{bmatrix} k_{lim}^2 & k_i(\rho) \\ k_i^T(\rho) & 1 \end{bmatrix} > 0, \ i = 1, \ldots, M, \tag{4.17}$$

then the closed-loop uncertain PWAPV system (4.4) is globally exponentially stable to the origin. □

Proof: The proof is given for the case where $i \neq i^\star$; the proof for the case where $i = i^\star$ is similar. Using the closed-loop uncertain PWAPV system (4.4), the sufficient conditions (4.7) and (4.8) become $\alpha \geq 0$, $P(\rho) = P(\rho)^T > 0$, and

$$\begin{aligned} &\left[\bar{A}_i^{cl}(\rho)\mathbf{x} + \bar{a}_i^{cl}(\rho)\right]^T P(\rho)\mathbf{x} + \mathbf{x}^T P(\rho)\left[\bar{A}_i^{cl}(\rho)\mathbf{x} + \bar{a}_i^{cl}(\rho)\right] \\ &\quad + \alpha \mathbf{x}^T P(\rho)\mathbf{x} + \mathbf{x}^T \dot{\rho}\tfrac{dP}{d\rho}\mathbf{x} < 0, \end{aligned} \qquad \text{for } \mathbf{x}(t) \in \mathcal{R}_i, \quad (4.18)$$

for $\forall \rho \in [\rho_{min}, \rho_{max}]$ and $|\dot{\rho}| \leq \bar{\rho}_{max}$, which can be written in matrix form as

$$\begin{bmatrix} \mathbf{x} \\ 1 \end{bmatrix}^T \begin{bmatrix} \Xi_i & \left[P(\rho)\bar{a}_i^{cl}(\rho)\right] \\ \left[P(\rho)\bar{a}_i^{cl}(\rho)\right]^T & 0 \end{bmatrix} \begin{bmatrix} \mathbf{x} \\ 1 \end{bmatrix} < 0, \quad (4.19)$$

where $\Xi_i = P(\rho)\left[\bar{A}_i^{cl}(\rho)\right] + \left[\bar{A}_i^{cl}(\rho)\right]^T P(\rho) + \alpha P(\rho) + \dot{\rho}\frac{dP}{d\rho}$. This condition can be relaxed to $\mathbf{x}(t) \in \mathcal{E}_i$ using the $\mathcal{S}-$*procedure* [97] with multipliers $\lambda_i < 0$ and the ellipsoidal covering (3.6) from Chapter 3, yielding the sufficient conditions $\alpha \geq 0$, $P(\rho) = P^T(\rho) > 0$, and

$$\begin{bmatrix} \Xi_i + \lambda_i L_i^T L_i & \left[P(\rho)\bar{a}_i^{cl}(\rho) + \lambda_i L_i^T l_i\right] \\ \left[P(\rho)\bar{a}_i^{cl}(\rho) + \lambda_i L_i^T l_i\right]^T & -\lambda_i\left[1 - l_i^T l_i\right] \end{bmatrix} < 0, \quad (4.20)$$

for $\forall \rho \in [\rho_{min}, \rho_{max}]$ and $|\dot{\rho}| \leq \bar{\rho}_{max}$. Using Schur complement twice, inequality (4.20) is equivalent to $1 - l_i^T l_i < 0$ and

$$\begin{aligned} &P(\rho)\left[\bar{A}_i^{cl}(\rho)\right] + \left[\bar{A}_i^{cl}(\rho)\right]^T P(\rho) + \alpha P(\rho) + \dot{\rho}\tfrac{dP}{d\rho} + \lambda_i L_i^T L_i \\ &\quad + \lambda_i^{-1}\left[P(\rho)\bar{a}_i^{cl}(\rho) + \lambda_i L_i^T l_i\right]\left[1 - l_i^T l_i\right]^{-1}\left[P(\rho)\bar{a}_i^{cl}(\rho) + \lambda_i L_i^T l_i\right]^T < 0. \end{aligned} \quad (4.21)$$

Expanding the first two terms of (4.21) using (4.5) yields

$$\begin{aligned} &P(\rho)A_i(\rho) + P(\rho)B_i(\rho)K_i(\rho) + A_i^T(\rho)P(\rho) + K_i^T(\rho)B_i^T(\rho)P(\rho) \\ &\quad + \alpha P(\rho) + \dot{\rho}\tfrac{dP}{d\rho} + P(\rho)\Delta A(\mathbf{x}) + \Delta A^T(\mathbf{x})P(\rho) + \lambda_i L_i^T L_i \\ &\quad + \lambda_i^{-1}\left[P(\rho)\bar{a}_i^{cl}(\rho) + \lambda_i L_i^T l_i\right]\left[1 - l_i^T l_i\right]^{-1}\left[P(\rho)\bar{a}_i^{cl}(\rho) + \lambda_i L_i^T l_i\right]^T < 0. \end{aligned} \quad (4.22)$$

Applying Lemma 4.1 yields (the order of the factors is arbitrary)

$$P(\rho)\Delta A(\mathbf{x}) + \Delta A^T(\mathbf{x})P(\rho) \leq \epsilon_1 \Delta A^T(\mathbf{x})\Delta A(\mathbf{x}) + \epsilon_1^{-1} P^2(\rho)$$

with constant $\epsilon_1 > 0$. The left-hand side (L.H.S) of inequality (4.22) can then be bounded as

$$\begin{aligned} L.H.S. \leq\ & P(\rho)A_i(\rho) + P(\rho)B_i(\rho)K_i(\rho) + A_i^T(\rho)P(\rho) + K_i^T(\rho)B_i^T(\rho)P(\rho) \\ & +\alpha P(\rho) + \dot{\rho}\tfrac{dP}{d\rho} + \epsilon_1 \Delta A^T(\mathbf{x})\Delta A(\mathbf{x}) + \epsilon_1^{-1}P^2(\rho) + \lambda_i L_i^T L_i \\ & +\lambda_i^{-1}\left[P(\rho)\bar{a}_i^{cl}(\rho) + \lambda_i L_i^T l_i\right]\left[1 - l_i^T l_i\right]^{-1}\left[P(\rho)\bar{a}_i^{cl}(\rho) + \lambda_i L_i^T l_i\right]^T. \end{aligned} \tag{4.23}$$

Defining $\mu_i = \lambda_i^{-1}$, pre-multiplying by $Q^T(\rho)$ and post-multiplying by $Q(\rho)$, where $Q(\rho) = Q^T(\rho) = P^{-1}(\rho)$ and [98]

$$\frac{dQ}{d\rho} = -P^{-1}\frac{dP}{d\rho}P^{-1} = -Q\frac{dP}{d\rho}Q, \tag{4.24}$$

the sufficient conditions become $\mu_i < 0$, $\alpha \geq 0$, $1 - l_i^T l_i < 0$, $Q(\rho) = Q^T(\rho) > 0$, and

$$\begin{aligned} & A_i(\rho)Q(\rho) + B_i(\rho)K_i(\rho)Q(\rho) + Q(\rho)A_i^T(\rho) + Q(\rho)K_i^T(\rho)B_i^T(\rho) \\ & +\alpha Q(\rho) - \dot{\rho}\tfrac{dQ}{d\rho} + \epsilon_1 Q(\rho)\Delta A^T(\mathbf{x})\Delta A(\mathbf{x})Q(\rho) + \epsilon_1^{-1}I_{(n)} + \mu_i^{-1}Q(\rho)L_i^T L_i Q(\rho) \\ & +\mu_i\left[\bar{a}_i^{cl}(\rho) + \mu_i^{-1}Q(\rho)L_i^T l_i\right]\left[1 - l_i^T l_i\right]^{-1}\left[\bar{a}_i^{cl}(\rho) + \mu_i^{-1}Q(\rho)L_i^T l_i\right]^T < 0, \end{aligned} \tag{4.25}$$

for $\forall \rho \in [\rho_{min}, \rho_{max}]$ and $|\dot{\rho}| \leq \bar{\rho}_{max}$. Using the Matrix Inversion Lemma, Rodrigues and Boyd [58] have shown that

$$\begin{aligned} & A_i Q + Q A_i^T + \alpha Q + \mu_i^{-1} Q L_i^T L_i Q \\ & \quad +\mu_i(a_i + \mu_i^{-1}QL_i^T l_i)(1 - l_i^T l_i)^{-1}(a_i + \mu_i^{-1}QL_i^T l_i)^T < 0 \end{aligned} \tag{4.26}$$

is equivalent to

$$\begin{aligned} & A_i Q + Q A_i^T + \alpha Q + \mu_i a_i a_i^T \\ & \quad +\mu_i^{-1}(\mu_i a_i l_i^T + QL_i^T)(I - l_i l_i^T)^{-1}(\mu_i a_i l_i^T + QL_i^T)^T < 0. \end{aligned} \tag{4.27}$$

The difference between inequalities (4.25) and (4.26) is that $A_i(\rho)$, $\bar{a}_i^{cl}(\rho)$, and $Q(\rho)$ in (4.25) are replaced by A_i, a_i, and Q in (4.26), respectively, and (4.25) has the extra terms

$$\begin{aligned} & B_i(\rho)K_i(\rho)Q(\rho) + Q(\rho)K_i^T(\rho)B_i^T(\rho) - \dot{\rho}\tfrac{dQ}{d\rho} \\ & +\epsilon_1 Q(\rho)\Delta A^T(\mathbf{x})\Delta A(\mathbf{x})Q(\rho) + \epsilon_1^{-1}I_{(n)}. \end{aligned}$$

However, following a similar procedure as the one used by Rodrigues and Boyd [58], it can be concluded that (4.25) is equivalent to

$$\begin{aligned} &A_i(\rho)Q(\rho) + B_i(\rho)K_i(\rho)Q(\rho) + Q(\rho)A_i^T(\rho) + Q(\rho)K_i^T(\rho)B_i^T(\rho) \\ &+\alpha Q(\rho) - \dot{\rho}\tfrac{dQ}{d\rho} + \epsilon_1 Q(\rho)\Delta A^T(\mathbf{x})\Delta A(\mathbf{x})Q(\rho) + \epsilon_1^{-1}I_{(n)} + \mu_i[\bar{a}_i^{cl}(\rho)][\bar{a}_i^{cl}(\rho)]^T \\ &+\mu_i^{-1}(1-l_i^2)^{-1}\left[\mu_i l_i \bar{a}_i^{cl}(\rho) + Q(\rho)L_i^T\right]\left[\mu_i l_i \bar{a}_i^{cl}(\rho) + Q(\rho)L_i^T\right]^T < 0, \end{aligned} \tag{4.28}$$

using the fact that $l_i = l_i^T$ is a scalar for slab systems. Expanding terms using (4.5) yields

$$\begin{aligned} &A_i(\rho)Q(\rho) + B_i(\rho)K_i(\rho)Q(\rho) + Q(\rho)A_i^T(\rho) + Q(\rho)K_i^T(\rho)B_i^T(\rho) \\ &+\alpha Q(\rho) - \dot{\rho}\tfrac{dQ}{d\rho} + \epsilon_1 Q(\rho)\Delta A^T(\mathbf{x})\Delta A(\mathbf{x})Q(\rho) + \epsilon_1^{-1}I_{(n)} \\ &+\mu_i[1 + l_i^2(1-l_i^2)^{-1}][a_i(\rho)a_i^T(\rho) + a_i(\rho)\Delta a^T(\mathbf{x}) + \Delta a(\mathbf{x})a_i^T(\rho) + \Delta a(\mathbf{x})\Delta a^T(\mathbf{x})] \\ &+\mu_i[a_i(\rho)k_i^T(\rho)B_i^T(\rho) + \Delta a(\mathbf{x})k_i^T(\rho)B_i^T(\rho) + B_i(\rho)k_i(\rho)a_i^T(\rho) + B_i(\rho)k_i(\rho)\Delta a^T(\mathbf{x})] \\ &+\mu_i l_i^2(1-l_i^2)^{-1}[a_i(\rho)k_i^T(\rho)B_i^T(\rho) + \Delta a(\mathbf{x})k_i^T(\rho)B_i^T(\rho) \\ &\qquad +B_i(\rho)k_i(\rho)a_i^T(\rho) + B_i(\rho)k_i(\rho)\Delta a^T(\mathbf{x})] \\ &+l_i(1-l_i^2)^{-1}[a_i(\rho)L_iQ(\rho) + \Delta a(\mathbf{x})L_iQ(\rho) + Q(\rho)L_i^T a_i^T(\rho) + Q(\rho)L_i^T\Delta a^T(\mathbf{x})] \\ &+l_i(1-l_i^2)^{-1}[B_i(\rho)k_i(\rho)L_iQ(\rho) + Q(\rho)L_i^T k_i^T(\rho)B_i^T(\rho)] \\ &+\mu_i^{-1}(1-l_i^2)^{-1}Q(\rho)L_i^T L_iQ(\rho) + \mu_i[1 + l_i^2(1-l_i^2)^{-1}]B_i(\rho)k_i(\rho)k_i^T(\rho)B_i^T(\rho) < 0. \end{aligned} \tag{4.29}$$

Using Lemma 4.2 with trace $\left[k_i(\rho)k_i(\rho)^T\right]$ = trace $\left[k_i(\rho)^T k_i(\rho)\right] = \|k_i(\rho)\|_2^2$, $\forall \rho \in [\rho_{min}, \rho_{max}]$, the left-hand side (L.H.S.) of (4.29) can be bounded as

$$\begin{aligned} L.H.S. \leq\ &A_i(\rho)Q(\rho) + B_i(\rho)K_i(\rho)Q(\rho) + Q(\rho)A_i^T(\rho) + Q(\rho)K_i^T(\rho)B_i^T(\rho) \\ &+\alpha Q(\rho) - \dot{\rho}\tfrac{dQ}{d\rho} + \epsilon_1 Q(\rho)\Delta A^T(\mathbf{x})\Delta A(\mathbf{x})Q(\rho) + \epsilon_1^{-1}I_{(n)} \\ &+\mu_i[1 + l_i^2(1-l_i^2)^{-1}][a_i(\rho)a_i^T(\rho) + a_i(\rho)\Delta a^T(\mathbf{x}) + \Delta a(\mathbf{x})a_i^T(\rho) + \Delta a(\mathbf{x})\Delta a^T(\mathbf{x})] \\ &+\mu_i[a_i(\rho)k_i^T(\rho)B_i^T(\rho) + \Delta a(\mathbf{x})k_i^T(\rho)B_i^T(\rho) + B_i(\rho)k_i(\rho)a_i^T(\rho) + B_i(\rho)k_i(\rho)\Delta a^T(\mathbf{x})] \\ &+\mu_i l_i^2(1-l_i^2)^{-1}[a_i(\rho)k_i^T(\rho)B_i^T(\rho) + \Delta a(\mathbf{x})k_i^T(\rho)B_i^T(\rho) \\ &\qquad +B_i(\rho)k_i(\rho)a_i^T(\rho) + B_i(\rho)k_i(\rho)\Delta a^T(\mathbf{x})] \\ &+l_i(1-l_i^2)^{-1}[a_i(\rho)L_iQ(\rho) + \Delta a(\mathbf{x})L_iQ(\rho) + Q(\rho)L_i^T a_i^T(\rho) + Q(\rho)L_i^T\Delta a^T(\mathbf{x})] \\ &+l_i(1-l_i^2)^{-1}[B_i(\rho)k_i(\rho)L_iQ(\rho) + Q(\rho)L_i^T k_i^T(\rho)B_i^T(\rho)] \\ &+\mu_i^{-1}(1-l_i^2)^{-1}Q(\rho)L_i^T L_iQ(\rho) + \mu_i\|k_i\|_2^2[1 + l_i^2(1-l_i^2)^{-1}]B_i(\rho)B_i^T(\rho). \end{aligned} \tag{4.30}$$

Applying Lemma 4.1 again yields

$$
\begin{cases}
a_i(\rho)\Delta a^T(\mathbf{x}) + \Delta a(\mathbf{x})a_i^T(\rho) \\
\qquad\qquad \leq \epsilon_2 \Delta a(\mathbf{x})\Delta a^T(\mathbf{x}) + \epsilon_2^{-1} a_i(\rho)a_i^T(\rho) \\
\Delta a(\mathbf{x})k_i^T(\rho)B_i^T(\rho) + B_i(\rho)k_i(\rho)\Delta a^T(\mathbf{x}) \\
\qquad\qquad \leq \epsilon_3 \Delta a(\mathbf{x})k_i^T(\rho)k_i(\rho)\Delta a^T(\mathbf{x}) + \epsilon_3^{-1} B_i(\rho)B_i^T(\rho) \\
l_i^2(1-l_i^2)^{-1}\Delta a(\mathbf{x})k_i^T(\rho)B_i^T(\rho) + l_i^2(1-l_i^2)^{-1}B_i(\rho)k_i(\rho)\Delta a^T(\mathbf{x}) \\
\qquad\qquad \leq \epsilon_4 \Delta a(\mathbf{x})k_i^T(\rho)k_i(\rho)\Delta a^T(\mathbf{x}) + \epsilon_4^{-1} l_i^4(1-l_i^2)^{-2} B_i(\rho)B_i^T(\rho) \\
l_i(1-l_i^2)^{-1}\Delta a(\mathbf{x})L_iQ(\rho) + l_i(1-l_i^2)^{-1}Q(\rho)L_i^T\Delta a^T(\mathbf{x}) \\
\qquad\qquad \leq \epsilon_5 \Delta a(\mathbf{x})\Delta a^T(\mathbf{x}) + \epsilon_5^{-1} l_i^2(1-l_i^2)^{-2} Q(\rho)L_i^T L_iQ(\rho) \\
l_i(1-l_i^2)^{-1}B_i(\rho)k_i(\rho)L_iQ(\rho) + l_i(1-l_i^2)^{-1}Q(\rho)L_i^T k_i^T(\rho)B_i^T(\rho) \\
\qquad\qquad \leq \epsilon_6 B_i(\rho)B_i^T(\rho) + \epsilon_6^{-1} l_i^2(1-l_i^2)^{-2} Q(\rho)L_i^T k_i^T(\rho)k_i(\rho)L_iQ(\rho)
\end{cases}
$$

with constants $\epsilon_j > 0,\ j = 2, \ldots, 6$. The right-hand side (R.H.S) of inequality (4.30) can then be bounded as

$$
\begin{aligned}
R.H.S. \leq\ & A_i(\rho)Q(\rho) + B_i(\rho)K_i(\rho)Q(\rho) + Q(\rho)A_i^T(\rho) + Q(\rho)K_i^T(\rho)B_i^T(\rho) \\
& + \alpha Q(\rho) - \dot{\rho}\tfrac{dQ}{d\rho} + \epsilon_1 Q(\rho)\Delta A^T(\mathbf{x})\Delta A(\mathbf{x})Q(\rho) + \epsilon_1^{-1} I_{(n)} \\
& + \mu_i[1 + l_i^2(1-l_i^2)^{-1}][(1+\epsilon_2^{-1})a_i(\rho)a_i^T(\rho) + (1+\epsilon_2)\Delta a(\mathbf{x})\Delta a^T(\mathbf{x})] \\
& + \mu_i[1 + l_i^2(1-l_i^2)^{-1}][a_i(\rho)k_i^T(\rho)B_i^T(\rho) + B_i(\rho)k_i(\rho)a_i^T(\rho)] \\
& + \mu_i[\epsilon_3 \Delta a(\mathbf{x})k_i^T(\rho)k_i(\rho)\Delta a^T(\mathbf{x}) + \epsilon_3^{-1} B_i(\rho)B_i^T(\rho)] \\
& + \mu_i[\epsilon_4 \Delta a(\mathbf{x})k_i^T(\rho)k_i(\rho)\Delta a^T(\mathbf{x}) + \epsilon_4^{-1} l_i^4(1-l_i^2)^{-2} B_i(\rho)B_i^T(\rho)] \\
& + l_i(1-l_i^2)^{-1}[a_i(\rho)L_iQ(\rho) + Q(\rho)L_i^T a_i^T(\rho)] \\
& + \epsilon_5 \Delta a(\mathbf{x})\Delta a^T(\mathbf{x}) + \epsilon_5^{-1} l_i^2(1-l_i^2)^{-2} Q(\rho)L_i^T L_iQ(\rho) \\
& + \epsilon_6 B_i(\rho)B_i^T(\rho) + \epsilon_6^{-1} l_i^2(1-l_i^2)^{-2} Q(\rho)L_i^T k_i^T(\rho)k_i(\rho)L_iQ(\rho) \\
& + \mu_i^{-1}(1-l_i^2)^{-1} Q(\rho)L_i^T L_iQ(\rho) \\
& + \mu_i \|k_i(\rho)\|_2^2[1 + l_i^2(1-l_i^2)^{-1}] B_i(\rho)B_i^T(\rho).
\end{aligned}
\tag{4.31}
$$

Note that (4.17) is equivalent to $k_i^T(\rho)k_i(\rho) \leq k_{lim}^2$ for $\forall \rho \in [\rho_{min}, \rho_{max}]$. Using this fact and the uncertainty bounds (4.6), the right-hand side (R.H.S) of (4.31) verifies

$$\begin{aligned}
R.H.S. \leq\ & A_i(\rho)Q(\rho) + B_i(\rho)K_i(\rho)Q(\rho) + Q(\rho)A_i^T(\rho) + Q(\rho)K_i^T(\rho)B_i^T(\rho) \\
& +\alpha Q(\rho) - \dot{\rho}\frac{dQ}{d\rho} + \epsilon_1 Q(\rho)U_{A_i}^T U_{A_i} Q(\rho) + \epsilon_1^{-1} I_{(n)} \\
& +\mu_i[1 + l_i^2(1-l_i^2)^{-1}][(1+\epsilon_2^{-1})a_i(\rho)a_i^T(\rho) + (1+\epsilon_2)U_{a_i}U_{a_i}^T] \\
& +\mu_i[1 + l_i^2(1-l_i^2)^{-1}][a_i(\rho)k_i^T(\rho)B_i^T(\rho) + B_i(\rho)k_i(\rho)a_i^T(\rho)] \\
& +\mu_i[\epsilon_3 k_{lim}^2 U_{a_i}U_{a_i}^T + \epsilon_3^{-1}B_i(\rho)B_i^T(\rho)] \\
& +\mu_i[\epsilon_4 k_{lim}^2 U_{a_i}U_{a_i}^T + \epsilon_4^{-1}l_i^4(1-l_i^2)^{-2}B_i(\rho)B_i^T(\rho)] \\
& +l_i(1-l_i^2)^{-1}[a_i(\rho)L_iQ(\rho) + Q(\rho)L_i^T a_i^T(\rho)] \\
& +\epsilon_5 U_{a_i}U_{a_i}^T + \epsilon_5^{-1}l_i^2(1-l_i^2)^{-2}Q(\rho)L_i^T L_i Q(\rho) \\
& +\epsilon_6 B_i(\rho)B_i^T(\rho) + \epsilon_6^{-1}l_i^2(1-l_i^2)^{-2}k_{lim}^2 Q(\rho)L_i^T L_i Q(\rho) \\
& +\mu_i^{-1}(1-l_i^2)^{-1}Q(\rho)L_i^T L_i Q(\rho) + \mu_i k_{lim}^2[1 + l_i^2(1-l_i^2)^{-1}]B_i(\rho)B_i^T(\rho).
\end{aligned} \tag{4.32}$$

With the additional constraint $\frac{dQ}{d\rho} - \lambda_{max} I_{(n)} \leq 0$, where λ_{max} is given, the right-hand side (R.H.S) of (4.32) can be bounded by

$$\begin{aligned}
R.H.S. \leq\ & A_i(\rho)Q(\rho) + B_i(\rho)K_i(\rho)Q(\rho) + Q(\rho)A_i^T(\rho) + Q(\rho)K_i^T(\rho)B_i^T(\rho) \\
& +\alpha Q(\rho) + \bar{\rho}_{max}|\lambda_{max}|I_{(n)} + \epsilon_1 Q(\rho)U_{A_i}^T U_{A_i} Q(\rho) + \epsilon_1^{-1} I_{(n)} \\
& +\mu_i[1 + l_i^2(1-l_i^2)^{-1}][(1+\epsilon_2^{-1})a_i(\rho)a_i^T(\rho) + (1+\epsilon_2)U_{a_i}U_{a_i}^T] \\
& +\mu_i[1 + l_i^2(1-l_i^2)^{-1}][a_i(\rho)k_i^T(\rho)B_i^T(\rho) + B_i(\rho)k_i(\rho)a_i^T(\rho)] \\
& +\mu_i[\epsilon_3 k_{lim}^2 U_{a_i}U_{a_i}^T + \epsilon_3^{-1}B_i(\rho)B_i^T(\rho)] \\
& +\mu_i[\epsilon_4 k_{lim}^2 U_{a_i}U_{a_i}^T + \epsilon_4^{-1}l_i^4(1-l_i^2)^{-2}B_i(\rho)B_i^T(\rho)] \\
& +l_i(1-l_i^2)^{-1}[a_i(\rho)L_iQ(\rho) + Q(\rho)L_i^T a_i^T(\rho)] \\
& +\epsilon_5 U_{a_i}U_{a_i}^T + \epsilon_5^{-1}l_i^2(1-l_i^2)^{-2}Q(\rho)L_i^T L_i Q(\rho) \\
& +\epsilon_6 B_i(\rho)B_i^T(\rho) + \epsilon_6^{-1}l_i^2(1-l_i^2)^{-2}k_{lim}^2 Q(\rho)L_i^T L_i Q(\rho) \\
& +\mu_i^{-1}(1-l_i^2)^{-1}Q(\rho)L_i^T L_i Q(\rho) + \mu_i k_{lim}^2[1 + l_i^2(1-l_i^2)^{-1}]B_i(\rho)B_i^T(\rho).
\end{aligned} \tag{4.33}$$

Thus, changing variables to $Y_i(\rho) = K_i(\rho)Q(\rho)$, $\forall \rho \in [\rho_{min}, \rho_{max}]$, the constraints (4.7) and (4.8) are guaranteed to be satisfied if the following are verified

$$
\begin{aligned}
&\begin{bmatrix} k_{lim}^2 & k_i(\rho) \\ k_i^T(\rho) & 1 \end{bmatrix} > 0, \quad 1 - l_i^2 < 0, \quad \mu_i < 0, \quad \alpha \geq 0, \\
&\epsilon_j > 0,\ j = 1, \ldots, 6, \quad Q(\rho) = Q^T(\rho) > 0, \frac{dQ}{d\rho} - \lambda_{max} I_{(n)} \leq 0, \\
&\forall \rho \in [\rho_{min}, \rho_{max}],\ |\dot{\rho}| \leq \bar{\rho}_{max}, \\
&A_i(\rho)Q(\rho) + B_i(\rho)Y_i(\rho) + Q(\rho)A_i^T(\rho) + Y_i^T(\rho)B_i^T(\rho) \\
&\quad + \alpha Q(\rho) + \bar{\rho}_{max}|\lambda_{max}|I_{(n)} + \epsilon_1 Q(\rho)U_{A_i}^T U_{A_i} Q(\rho) + \epsilon_1^{-1} I_{(n)} \\
&\quad + \mu_i[1 + l_i^2(1 - l_i^2)^{-1}][(1 + \epsilon_2^{-1})a_i(\rho)a_i^T(\rho) + (1 + \epsilon_2)U_{a_i}U_{a_i}^T] \\
&\quad + \mu_i[1 + l_i^2(1 - l_i^2)^{-1}][a_i(\rho)k_i^T(\rho)B_i^T(\rho) + B_i(\rho)k_i(\rho)a_i^T(\rho)] \\
&\quad + [\mu_i\epsilon_3 k_{lim}^2 + \mu_i\epsilon_4 k_{lim}^2 + \epsilon_5]U_{a_i}U_{a_i}^T + l_i(1 - l_i^2)^{-1}[a_i(\rho)L_iQ(\rho) + Q(\rho)L_i^T a_i^T(\rho)] \\
&\quad + [\mu_i\epsilon_3^{-1} + \mu_i\epsilon_4^{-1}l_i^4(1 - l_i^2)^{-2} + \epsilon_6 + \mu_i k_{lim}^2\{1 + l_i^2(1 - l_i^2)^{-1}\}]B_i(\rho)B_i^T(\rho) \\
&\quad + [\epsilon_5^{-1}l_i^2(1 - l_i^2)^{-2} + \epsilon_6^{-1}l_i^2(1 - l_i^2)^{-2}k_{lim}^2 + \mu_i^{-1}(1 - l_i^2)^{-1}]Q(\rho)L_i^T L_i Q(\rho) \leq 0.
\end{aligned}
\tag{4.34}
$$

This last expression can be written in matrix form by successive uses of the Schur complement, yielding the inequality (4.16).

Since inequalities (4.34) ensure that the Lyapunov conditions (4.7) and (4.8) are verified for $\forall \rho \in [\rho_{min}, \rho_{max}]$ and $|\dot{\rho}| \leq \bar{\rho}_{max}$, from Theorem 4.1 the closed-loop uncertain PWAPV system (4.4) is globally exponentially stable to the origin. □

The next section describes a numerical method to approximate the parameterized inequalities of Theorem 4.2 by a finite set of LMIs, which can be solved efficiently using available software [3].

4.4 Numerical Solution

Note that Theorem 4.2 results in a parameterized set of inequalities, which can not be solved in practice. However, it has been suggested in the LPV literature [86] that such a parameterized set of inequalities can be solved numerically by creating a set of N_ρ grid points in the interval $[\rho_{min}, \rho_{max}]$ and solving one set of inequalities for each grid point.

To make the inequalities in Theorem 4.2 LMIs, one can fix the parameters α, μ_i and ϵ_j, $j = 1, \ldots, 6$. Furthermore, it will be assumed that $Q(\rho)$, $Y_i(\rho)$ and $k_i(\rho)$ are linearly dependent on the time-varying parameter $\rho(t)$, that is,

$$\begin{cases} Q(\rho) = \overline{Q0} \cdot \rho(t) + \overline{Q1} \\ Y_i(\rho) = \overline{Y0}_i \cdot \rho(t) + \overline{Y1}_i \\ k_i(\rho) = \overline{k0}_i \cdot \rho(t) + \overline{k1}_i \end{cases} . \tag{4.35}$$

Based on these assumptions, the PWAPV controller synthesis problem can be formulated as follows:

Problem 4.1 *For given scalars* $\alpha \geq 0$, $\epsilon_j > 0$, $j = 1, \ldots, 6$, $k_{lim} > 0$, $\mu_i < 0$, ρ_{min}, ρ_{max}, $\bar{\rho}_{max}$, λ_{max}, *vectors* Y_i^{lim}, *and a set of grid points* ρ_k, $k = 1, \ldots, N_\rho$:

$$\begin{aligned} \text{find} \quad & \overline{Q0},\ \overline{Q1},\ \overline{Y0}_i,\ \overline{Y1}_i,\ \overline{k0}_i,\ \overline{k1}_i \\ s.t. \quad & Q(\rho_k) = \overline{Q0} \cdot \rho_k + \overline{Q1},\ Q(\rho_k) = Q^T(\rho_k) > 0, \\ & \overline{Q0} - \lambda_{max} I_{(n)} \leq 0, \\ & Y_i(\rho_k) = \overline{Y0}_i \cdot \rho_k + \overline{Y1}_i,\ -Y_i^{lim} \prec Y_i(\rho_k) \prec Y_i^{lim}, \\ & k_i(\rho_k) = \overline{k0}_i \cdot \rho_k + \overline{k1}_i,\ \begin{bmatrix} k_{lim}^2 & k_i(\rho_k) \\ k_i(\rho_k)^T & 1 \end{bmatrix} > 0, \\ & i = 1, \ldots, M,\ k = 1, \ldots, N_\rho, \end{aligned}$$

and

$$\begin{bmatrix} \Omega_i & I_{(n)} & I_{(n)} & Q(\rho_k)U_{A_i}^T \\ I_{(n)} & -\bar{\rho}_{max}^{-1}|\lambda_{max}|^{-1}I_{(n)} & 0 & 0 \\ I_{(n)} & 0 & -\epsilon_1 I_{(n)} & 0 \\ U_{A_i}Q(\rho_k) & 0 & 0 & -\epsilon_1^{-1}I_{(n)} \end{bmatrix} < 0,$$

for $i = i^\star$,

$$\begin{bmatrix} \bar{\Omega}_i & I_{(n)} & I_{(n)} & Q(\rho_k)U_{A_i}^T & Q(\rho_k)L_i^T \\ I_{(n)} & -\bar{\rho}_{max}^{-1}|\lambda_{max}|^{-1}I_{(n)} & 0 & 0 & 0 \\ I_{(n)} & 0 & -\epsilon_1 I_{(n)} & 0 & 0 \\ U_{A_i}Q(\rho_k) & 0 & 0 & -\epsilon_1^{-1}I_{(n)} & 0 \\ L_iQ(\rho_k) & 0 & 0 & 0 & -\Gamma_i^{-1} \end{bmatrix} < 0,$$

for $i \neq i^\star$ *with* $1 - l_i^2 < 0$, *where*

$$\Omega_i = A_i(\rho_k)Q(\rho_k) + B_i(\rho_k)Y_i(\rho_k) + Q(\rho_k)A_i^T(\rho_k) + Y_i^T(\rho_k)B_i^T(\rho_k) + \alpha Q(\rho_k)$$

for $i = i^\star$ *and*

$$\begin{aligned} \bar{\Omega}_i = {} & A_i(\rho_k)Q(\rho_k) + B_i(\rho_k)Y_i(\rho_k) + Q(\rho_k)A_i^T(\rho_k) + Y_i^T(\rho_k)B_i^T(\rho_k) + \alpha Q(\rho_k) \\ & + \mu_i[1 + l_i^2(1 - l_i^2)^{-1}][(1 + \epsilon_2^{-1})a_i(\rho_k)a_i^T(\rho_k) + (1 + \epsilon_2)U_{a_i}U_{a_i}^T] \\ & + \mu_i[1 + l_i^2(1 - l_i^2)^{-1}][a_i(\rho_k)k_i^T(\rho_k)B_i^T(\rho_k) + B_i(\rho_k)k_i(\rho_k)a_i^T(\rho_k)] \\ & + [\mu_i\epsilon_3 k_{lim}^2 + \mu_i\epsilon_4 k_{lim}^2 + \epsilon_5]U_{a_i}U_{a_i}^T + l_i(1 - l_i^2)^{-1}[a_i(\rho_k)L_iQ(\rho_k) + Q(\rho_k)L_i^T a_i^T(\rho_k)] \\ & + [\mu_i\epsilon_3^{-1} + \mu_i\epsilon_4^{-1}l_i^4(1 - l_i^2)^{-2} + \epsilon_6 + \mu_i k_{lim}^2\{1 + l_i^2(1 - l_i^2)^{-1}\}]B_i(\rho_k)B_i^T(\rho_k) \end{aligned}$$

with $\Gamma_i = [\epsilon_5^{-1}l_i^2(1 - l_i^2)^{-2} + \epsilon_6^{-1}l_i^2(1 - l_i^2)^{-2}k_{lim}^2 + \mu_i^{-1}(1 - l_i^2)^{-1}]$ *for* $i \neq i^\star$. *The symbols* $\succ$ *and* $\prec$ *denote component-wise inequalities.* □

Remark 4.1 *Note that, in Problem 4.1, the scalars* $\alpha \geq 0$, $\epsilon_j > 0$, $j = 1, \ldots, 6$, $k_{lim} > 0$, $\mu_i < 0$, ρ_{min}, ρ_{max}, $\bar{\rho}_{max}$, λ_{max}, *vectors* Y_i^{lim}, *and the set of grid points* ρ_k, $k = 1, \ldots, N_\rho$ *are parameters that must be chosen by the designer.*

The gains for the PWAPV control law (4.2) resulting from the solution of Problem 4.1 are given by

$$\begin{cases} K_i(\rho) = Y_i(\rho)Q^{-1}(\rho) \\ k_i(\rho) = \overline{k0}_i \cdot \rho(t) + \overline{k1}_i \end{cases} \tag{4.36}$$

and the Lyapunov function (4.7) is parameterized by $P(\rho) = Q^{-1}(\rho)$, where $Y_i(\rho)$ and $Q(\rho)$ are given in (4.35).

This chapter defined and solved the piecewise-affine parameter-varying (PWAPV) controller synthesis problem for uncertain PWAPV slab systems. The next chapter describes the three-step path following controller synthesis method proposed in this thesis to solve the path following problem defined in Chapter 2, *i.e.*, Problem 2.1.

Chapter 5

Path Following Controller Synthesis for a WMR

This chapter proposes a three-step controller synthesis method to solve the path following problem defined in Chapter 2, namely, Problem 2.1. In the first step, two curvature limits $c_{c_{min}}$ and $c_{c_{max}}$ and a curvature rate of change limit $\bar{c}_{c_{max}}$ are defined for the desired path and the nonlinear WMR parameterized path kinematics are approximated by an uncertain piecewise-affine parameter-varying (PWAPV) system, while assuming that the WMR forward velocity is constant, *i.e.*, $u = u_{des}$. Then, a PWAPV steering control law $r(t)$ is designed using a parameter-dependent quadratic Lyapunov function. In the second step, a backstepping-type approach is used to include the vehicle dynamics and design the wheel control torques T_R and T_L that guarantee convergence of the WMR forward and rotational velocities to the desired values. Finally, in the third step, the actuator dynamics are included and the input voltages V_R and V_L are designed using backstepping.

5.1 PWAPV Kinematic Controller Synthesis

In the first step of the path following controller synthesis method proposed here, a PWAPV steering control law $r(t)$ is designed for the WMR parameterized path kinematics. A diagram of the kinematic closed-loop system is shown in Figure 5.1.

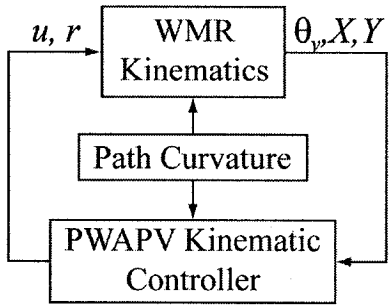

Figure 5.1: Diagram of kinematic closed-loop system

Considering only the WMR parameterized path kinematics (2.12) with constant velocity $u = u_{des}$, rewritten as

$$\begin{bmatrix} \dot{\theta} \\ \dot{s}_1 \\ \dot{y}_1 \end{bmatrix} = \begin{bmatrix} 0 & 0 & 0 \\ 0 & 0 & c_c(t)\dot{s} \\ 0 & -c_c(t)\dot{s} & 0 \end{bmatrix} \begin{bmatrix} \theta \\ s_1 \\ y_1 \end{bmatrix} + \begin{bmatrix} -c_c(t)\dot{s} \\ -\dot{s} \\ 0 \end{bmatrix} + \begin{bmatrix} 0 \\ u_{des}\cos\theta \\ u_{des}\sin\theta \end{bmatrix} + \begin{bmatrix} 1 \\ 0 \\ 0 \end{bmatrix} r(t), \quad (5.1)$$

which is a nonlinear system of the form (3.1) (repeated here for convenience),

$$\dot{\mathbf{x}}_1(t) = A(c_c)\mathbf{x}_1(t) + a(c_c) + f(\mathbf{x}_1) + B(c_c)\mathbf{u}_1(t), \quad (5.2)$$

where the state vector is $\mathbf{x}_1(t) = [\theta,\ s_1,\ y_1]^T$, the input vector is $\mathbf{u}_1(t) = r(t)$, and $c_c = c_c(t)$ is the time-varying parameter $\rho(t)$. The desired closed-loop equilibrium point is $\mathbf{x}_1^{cl} = [0,\ 0,\ 0]^T$.

Partitioning the state variable θ into M regions and using the methods described in Chapter 3, the nonlinear parameter-dependent system (5.2) can be approximated by an uncertain piecewise-affine parameter-varying (PWAPV) system

of the form (3.2) (repeated here for convenience),

$$\dot{\mathbf{x}}_1(t) = [A_i(c_c) + \Delta A(\mathbf{x}_1)]\,\mathbf{x}_1(t) + [a_i(c_c) + \Delta a(\mathbf{x}_1)] + B_i(c_c)\mathbf{u}_1(t), \quad \text{for } \mathbf{x}_1(t) \in \mathcal{R}_i, \tag{5.3}$$

where the PWA uncertainty bounds are given by

$$\begin{cases} \Delta A^T(\mathbf{x}_1)\Delta A(\mathbf{x}_1) \leq U_{A_i}^T U_{A_i} \\ \Delta a(\mathbf{x}_1)\Delta a^T(\mathbf{x}_1) \leq U_{a_i} U_{a_i}^T \end{cases}, \quad \text{for } \mathbf{x}_1(t) \in \mathcal{R}_i. \tag{5.4}$$

With the PWAPV steering control law (4.2) from Chapter 4, *i.e.*,

$$r(t) = K_i(c_c)\mathbf{x}_1(t) + k_i(c_c), \quad \text{for } \mathbf{x}_1(t) \in \mathcal{R}_i, \tag{5.5}$$

the resulting closed-loop uncertain PWAPV system is

$$\dot{\mathbf{x}}_1(t) = \bar{A}_i^{cl}(c_c)\mathbf{x}_1(t) + \bar{a}_i^{cl}(c_c), \quad \text{for } \mathbf{x}_1(t) \in \mathcal{R}_i, \tag{5.6}$$

where

$$\begin{cases} \bar{A}_i^{cl}(c_c) = \{[A_i(c_c) + \Delta A(\mathbf{x}_1)] + B_i(c_c)K_i(c_c)\} \\ \bar{a}_i^{cl}(c_c) = \{[a_i(c_c) + \Delta a(\mathbf{x}_1)] + B_i(c_c)k_i(c_c)\} \end{cases}.$$

It was shown in Chapter 4 that a PWAPV control law of the form (5.5) can be designed such that the closed-loop uncertain PWAPV system (5.6) satisfies the Lyapunov conditions

$$V_1(\mathbf{x}_1, c_c) = \mathbf{x}_1^T P_1(c_c)\mathbf{x}_1 \tag{5.7}$$

with $P_1(c_c) = P_1^T(c_c) > 0$, and

$$\begin{aligned} \dot{V}_1(\mathbf{x}_1, c_c, \dot{c}_c) &= \dot{\mathbf{x}}_1^T P_1(c_c)\mathbf{x}_1 + \mathbf{x}_1^T \dot{P}_1(c_c)\mathbf{x}_1 + \mathbf{x}_1^T P_1(c_c)\dot{\mathbf{x}}_1 \\ &= \dot{\mathbf{x}}_1^T P_1(c_c)\mathbf{x}_1 + \mathbf{x}_1^T \dot{c}_c \tfrac{dP_1}{dc_c}\mathbf{x}_1 + \mathbf{x}_1^T P_1(c_c)\dot{\mathbf{x}}_1 \\ &< -\alpha V_1(\mathbf{x}_1, c_c) \end{aligned} \tag{5.8}$$

for $\forall c_c \in [c_{c_{min}}, c_{c_{max}}]$, $|\dot{c}_c| \leq \bar{c}_{c_{max}}$, and $\forall t \geq 0$, where $\alpha \geq 0$. The PWAPV control law (5.5) can be obtained by solving Problem 4.1 (repeated here for convenience):

Problem 5.1 *For given scalars* $\alpha \geq 0$, $\epsilon_j > 0$, $j = 1, \ldots, 6$, $k_{lim} > 0$, $\mu_i < 0$, $c_{c_{min}}$, $c_{c_{max}}$, $\bar{c}_{c_{max}}$, λ_{max}, *vectors* Y_i^{lim}, *and a set of grid points* c_{c_k}, $k = 1, \ldots, N_{c_c}$:

$$
\begin{aligned}
\text{find} \quad & \overline{Q0},\ \overline{Q1},\ \overline{Y0}_i,\ \overline{Y1}_i,\ \overline{k0}_i,\ \overline{k1}_i \\
s.t. \quad & Q_1(c_{c_k}) = \overline{Q0} \cdot c_{c_k} + \overline{Q1},\ Q_1(c_{c_k}) = Q_1^T(c_{c_k}) > 0, \\
& \overline{Q0} - \lambda_{max} I_{(n)} \leq 0, \\
& Y_i(c_{c_k}) = \overline{Y0}_i \cdot c_{c_k} + \overline{Y1}_i,\ -Y_i^{lim} \prec Y_i(c_{c_k}) \prec Y_i^{lim}, \\
& k_i(c_{c_k}) = \overline{k0}_i \cdot c_{c_k} + \overline{k1}_i,\ \begin{bmatrix} k_{lim}^2 & k_i(c_{c_k}) \\ k_i(c_{c_k})^T & 1 \end{bmatrix} > 0, \\
& i = 1, \ldots, M,\ k = 1, \ldots, N_{c_c},
\end{aligned}
$$

and

$$
\begin{bmatrix}
\Omega_i & I_{(n)} & I_{(n)} & Q_1(c_{c_k}) U_{A_i}^T \\
I_{(n)} & -\bar{c}_{c_{max}}^{-1} |\lambda_{max}|^{-1} I_{(n)} & 0 & 0 \\
I_{(n)} & 0 & -\epsilon_1 I_{(n)} & 0 \\
U_{A_i} Q_1(c_{c_k}) & 0 & 0 & -\epsilon_1^{-1} I_{(n)}
\end{bmatrix} < 0, \tag{5.9}
$$

for $i = i^\star$,

$$
\begin{bmatrix}
\bar{\Omega}_i & I_{(n)} & I_{(n)} & Q_1(c_{c_k}) U_{A_i}^T & Q_1(c_{c_k}) L_i^T \\
I_{(n)} & -\bar{c}_{c_{max}}^{-1} |\lambda_{max}|^{-1} I_{(n)} & 0 & 0 & 0 \\
I_{(n)} & 0 & -\epsilon_1 I_{(n)} & 0 & 0 \\
U_{A_i} Q_1(c_{c_k}) & 0 & 0 & -\epsilon_1^{-1} I_{(n)} & 0 \\
L_i Q_1(c_{c_k}) & 0 & 0 & 0 & -\Gamma_i^{-1}
\end{bmatrix} < 0, \tag{5.10}
$$

for $i \neq i^\star$ *with* $1 - l_i^2 < 0$, *where*

$$
\begin{aligned}
\Omega_i = {} & A_i(c_{c_k}) Q_1(c_{c_k}) + B_i(c_{c_k}) Y_i(c_{c_k}) + Q_1(c_{c_k}) A_i^T(c_{c_k}) \\
& + Y_i^T(c_{c_k}) B_i^T(c_{c_k}) + \alpha Q_1(c_{c_k})
\end{aligned}
$$

for $i = i^\star$ *and*

$$\begin{aligned}\bar{\Omega}_i = {} & A_i(c_{c_k})Q_1(c_{c_k}) + B_i(c_{c_k})Y_i(c_{c_k}) + Q_1(c_{c_k})A_i^T(c_{c_k}) + Y_i^T(c_{c_k})B_i^T(c_{c_k}) + \alpha Q_1(c_{c_k}) \\ & + \mu_i[1 + l_i^2(1-l_i^2)^{-1}][(1+\epsilon_2^{-1})a_i(c_{c_k})a_i^T(c_{c_k}) + (1+\epsilon_2)U_{a_i}U_{a_i}^T] \\ & + \mu_i[1 + l_i^2(1-l_i^2)^{-1}][a_i(c_{c_k})k_i^T(c_{c_k})B_i^T(c_{c_k}) + B_i(c_{c_k})k_i(c_{c_k})a_i^T(c_{c_k})] \\ & + [\mu_i\epsilon_3 k_{lim}^2 + \mu_i\epsilon_4 k_{lim}^2 + \epsilon_5]U_{a_i}U_{a_i}^T + l_i(1-l_i^2)^{-1}[a_i(c_{c_k})L_iQ_1(c_{c_k}) + Q_1(c_{c_k})L_i^T a_i^T(c_{c_k})] \\ & + [\mu_i\epsilon_3^{-1} + \mu_i\epsilon_4^{-1}l_i^4(1-l_i^2)^{-2} + \epsilon_6 + \mu_i k_{lim}^2\{1 + l_i^2(1-l_i^2)^{-1}\}]B_i(c_{c_k})B_i^T(c_{c_k})\end{aligned}$$

with $\Gamma_i = [\epsilon_5^{-1}l_i^2(1-l_i^2)^{-2} + \epsilon_6^{-1}l_i^2(1-l_i^2)^{-2}k_{lim}^2 + \mu_i^{-1}(1-l_i^2)^{-1}]$ *for* $i \neq i^\star$. *The symbols* $\succ$ *and* $\prec$ *denote component-wise inequalities.* □

Remark 5.1 *Note that, in Problem 5.1, the scalars* $\alpha \geq 0$, $\epsilon_j > 0$, $j = 1, \ldots, 6$, $k_{lim} > 0$, $\mu_i < 0$, $c_{c_{min}}$, $c_{c_{max}}$, $\bar{c}_{c_{max}}$, λ_{max}, *vectors* Y_i^{lim}, *and the set of grid points* c_{c_k}, $k = 1, \ldots, N_{c_c}$ *are parameters that must be chosen by the designer.*

The gains for the PWAPV control law (5.5) resulting from the solution of Problem 5.1 are given by

$$\begin{cases} K_i(c_c) = Y_i(c_c)Q_1^{-1}(c_c) \\ k_i(c_c) = \overline{k0}_i \cdot c_c(t) + \overline{k1}_i \end{cases} \tag{5.11}$$

and the Lyapunov function (5.7) is parameterized by $P_1(c_c) = Q_1^{-1}(c_c)$.

In the proof of the following theorem, it will be shown that the PWAPV steering control law (5.5) designed for the uncertain PWAPV system (5.3) can also globally exponentially stabilize the nonlinear system (5.2) to $\theta = 0$, $s_1 = 0$, and $y_1 = 0$.

Theorem 5.1 *The PWAPV control law (5.5) resulting from the solution of Problem 5.1 can globally exponentially stabilize the nonlinear parameter-dependent system (5.2) to the origin.* □

Proof: It was shown in Chapter 4 that the PWAPV control law (5.5) resulting from the solution of Problem 5.1 globally exponentially stabilizes the uncertain PWAPV system (5.3) for all uncertainties contained within the PWA bounds (5.4). Using the numerical methods of Chapter 3, suppose that PWA uncertainty bounds (5.4) are obtained such that the uncertainties resulting from the difference between the nonlinear parameter-dependent system (3.1) and the nominal PWAPV system (3.13) satisfy these bounds for $\forall \mathbf{x}_1(t) \in \mathbb{R}^n$. Therefore, it can be concluded that the closed-loop nonlinear parameter-dependent system given by

$$\dot{\mathbf{x}}_1(t) = [A(c_c) + B(c_c)K_i(c_c)]\mathbf{x}_1(t) + [a(c_c) + B(c_c)k_i(c_c)] + f(\mathbf{x}_1) \tag{5.12}$$

satisfies

$$\begin{aligned} \dot{V}_1(\mathbf{x}_1, c_c, \dot{c}_c) &= \dot{\mathbf{x}}_1^T P_1(c_c)\mathbf{x}_1 + \mathbf{x}_1^T \dot{c}_c \tfrac{dP_1}{dc_c}\mathbf{x}_1 + \mathbf{x}_1^T P_1(c_c)\dot{\mathbf{x}}_1 \\ &< -\alpha V_1(\mathbf{x}_1, c_c), \end{aligned} \tag{5.13}$$

for $\forall c_c \in [c_{c_{min}}, c_{c_{max}}]$ and $|\dot{c}_c| \leq \bar{c}_{c_{max}}$. □

The next section uses a backstepping-type approach to include the vehicle dynamics and design the wheel control torques T_R and T_L that guarantee convergence of the WMR forward and rotational velocities to the desired values.

5.2 Dynamic Controller Synthesis

In the second step of the path following controller synthesis method proposed here, a backstepping-type approach [99] is used to include the vehicle dynamics and design the wheel control torques T_R and T_L that guarantee convergence of the WMR forward and rotational velocities to the desired values. A diagram of the dynamic closed-loop system is shown in Figure 5.2.

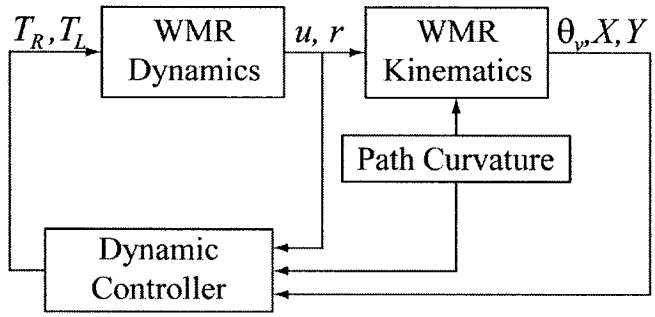

Figure 5.2: Diagram of dynamic closed-loop system

Consider the WMR kinematics (5.1), rewritten as

$$\begin{bmatrix} \dot{\theta} \\ \dot{s}_1 \\ \dot{y}_1 \end{bmatrix} = \begin{bmatrix} -c_c(t)\dot{s} \\ c_c(t)\dot{s}y_1 - \dot{s} \\ -c_c(t)\dot{s}s_1 \end{bmatrix} + \begin{bmatrix} 0 \\ \cos\theta \\ \sin\theta \end{bmatrix} u + \begin{bmatrix} 1 \\ 0 \\ 0 \end{bmatrix} r \tag{5.14}$$

or as

$$\dot{\mathbf{x}}_1 = g(\mathbf{x}_1, c_c) + g_u(\mathbf{x}_1)u + g_r(\mathbf{x}_1)r. \tag{5.15}$$

Combining the kinematics (5.15) with the WMR dynamics (2.13) results in

$$\begin{cases} \dot{\mathbf{x}}_1 = g(\mathbf{x}_1, c_c) + g_u(\mathbf{x}_1)u + g_r(\mathbf{x}_1)r \\ \dot{u} = \frac{1}{Mr_w}(T_R + T_L) \\ \dot{r} = \frac{c}{Ir_w}(T_R - T_L) \end{cases} . \tag{5.16}$$

We now consider r a *virtual control*, and call the PWAPV steering control law (5.5) a *stabilizing function* and denote it by r_{des}. The new control inputs to the augmented system (5.16) are the wheel torques T_R and T_L. In the proof of the

following theorem, it will be shown that the control laws

$$\begin{cases} T_R = \frac{Mr_w}{2}\left\{\dot{u}_{des} - \frac{\alpha}{2}\xi_u - \left(\frac{\partial V_1}{\partial \mathbf{x}_1}\right)^T g_u(\mathbf{x}_1)\right\} \\ \qquad\qquad + \frac{Ir_w}{2c}\left\{\dot{r}_{des} - \frac{\alpha}{2}\xi_r - \left(\frac{\partial V_1}{\partial \mathbf{x}_1}\right)^T g_r(\mathbf{x}_1)\right\} \\ T_L = \frac{Mr_w}{2}\left\{\dot{u}_{des} - \frac{\alpha}{2}\xi_u - \left(\frac{\partial V_1}{\partial \mathbf{x}_1}\right)^T g_u(\mathbf{x}_1)\right\} \\ \qquad\qquad - \frac{Ir_w}{2c}\left\{\dot{r}_{des} - \frac{\alpha}{2}\xi_r - \left(\frac{\partial V_1}{\partial \mathbf{x}_1}\right)^T g_r(\mathbf{x}_1)\right\} \end{cases}, \quad \text{for } \mathbf{x}_1(t) \in \mathcal{R}_i, \tag{5.17}$$

can globally exponentially stabilize the system (5.16) to $u = u_{des}$, $r = r_{des}$, $\theta = 0$, $s_1 = 0$, and $y_1 = 0$ for $\forall c_c \in [c_{c_{min}}, c_{c_{max}}]$ and $|\dot{c}_c| \leq \bar{c}_{c_{max}}$, where $\left(\frac{\partial V_1}{\partial \mathbf{x}_1}\right)^T = 2P_1(c_c)\mathbf{x}_1$.

Theorem 5.2 *Consider the system (5.16). Let there exist a constant forward velocity u_{des} and a stabilizing function r_{des} given by (5.5), as well as a parameter-dependent quadratic Lyapunov function $V_1(\boldsymbol{x}_1, c_c)$ that satisfies (5.7) and (5.8). Then the wheel control torques T_R and T_L given by (5.17) render the system (5.16) globally exponentially stable to $u = u_{des}$, $r = r_{des}$, $\theta = 0$, $s_1 = 0$, and $y_1 = 0$ for $\forall c_c \in [c_{c_{min}}, c_{c_{max}}]$ and $|\dot{c}_c| \leq \bar{c}_{c_{max}}$.* □

Proof: Introducing the error variables

$$\begin{cases} \xi_u = u - u_{des} \\ \xi_r = r - r_{des} \end{cases} \tag{5.18}$$

and differentiating with respect to time yields

$$\begin{cases} \dot{\xi}_u = \dot{u} - \dot{u}_{des} \\ \dot{\xi}_r = \dot{r} - \dot{r}_{des} \end{cases}, \tag{5.19}$$

where $\dot{u}$ and $\dot{r}$ are given in (5.16), and $\dot{u}_{des}$ and $\dot{r}_{des}$ are given by

$$\begin{cases} \dot{u}_{des} = 0 \\ \dot{r}_{des} = K_i(c_c)\dot{\mathbf{x}}_1 \end{cases}, \quad \text{for } \mathbf{x}_1(t) \in \mathcal{R}_i. \tag{5.20}$$

System (5.16) can now be rewritten in terms of the error states as

$$\begin{cases} \dot{\mathbf{x}}_1 = g(\mathbf{x}_1, c_c) + g_u(\mathbf{x}_1)\left[\xi_u + u_{des}\right] + g_r(\mathbf{x}_1)\left[\xi_r + r_{des}\right] \\ \dot{\xi}_u = \dot{u} - \dot{u}_{des} \\ \dot{\xi}_r = \dot{r} - \dot{r}_{des} \end{cases} . \tag{5.21}$$

Using the constant forward velocity u_{des} and the stabilizing function r_{des} given by (5.5), it was shown in the previous section that the function

$$\nabla_{V_1}(\mathbf{x}_1, c_c, \dot{c}_c) = \left(\frac{\partial V_1}{\partial \mathbf{x}_1}\right)^T \{g(\mathbf{x}_1, c_c) + g_u(\mathbf{x}_1)u_{des} + g_r(\mathbf{x}_1)r_{des}\} \tag{5.22}$$

verifies

$$\nabla_{V_1}(\mathbf{x}_1, c_c, \dot{c}_c) < -\alpha V_1(\mathbf{x}_1, c_c). \tag{5.23}$$

A candidate parameter-dependent quadratic control Lyapunov function (CLF) for system (5.21) is thus proposed by augmenting $V_1(\mathbf{x}_1, c_c)$ in (5.7) as follows

$$V_2(\mathbf{x}_2, c_c) = \frac{1}{2}\xi_u^2 + \frac{1}{2}\xi_r^2 + V_1(\mathbf{x}_1, c_c), \tag{5.24}$$

where $\mathbf{x}_2 = [u,\ r,\ \theta,\ s_1,\ y_1]^T$. The derivative of (5.24) along the state trajectories of the system (5.21) is given by

$$\begin{aligned} \dot{V}_2(\mathbf{x}_2, c_c, \dot{c}_c) &= \left(\tfrac{\partial V_1}{\partial \mathbf{x}_1}\right)^T \dot{\mathbf{x}}_1 + \xi_u\dot{\xi}_u + \xi_r\dot{\xi}_r \\ &= \left(\tfrac{\partial V_1}{\partial \mathbf{x}_1}\right)^T \{g(\mathbf{x}_1, c_c) + g_u(\mathbf{x}_1)[\xi_u + u_{des}] + g_r(\mathbf{x}_1)[\xi_r + r_{des}]\} \\ &\qquad +\xi_u\dot{\xi}_u + \xi_r\dot{\xi}_r \\ &= \left(\tfrac{\partial V_1}{\partial \mathbf{x}_1}\right)^T \{g(\mathbf{x}_1, c_c) + g_u(\mathbf{x}_1)u_{des} + g_r(\mathbf{x}_1)r_{des}\} \\ &\qquad +\xi_u\left\{\dot{\xi}_u + \left(\tfrac{\partial V_1}{\partial \mathbf{x}_1}\right)^T g_u(\mathbf{x}_1)\right\} \\ &\qquad +\xi_r\left\{\dot{\xi}_r + \left(\tfrac{\partial V_1}{\partial \mathbf{x}_1}\right)^T g_r(\mathbf{x}_1)\right\} \\ &= \nabla_{V_1}(\mathbf{x}_1, c_c, \dot{c}_c) + \xi_u\left\{\dot{\xi}_u + \left(\tfrac{\partial V_1}{\partial \mathbf{x}_1}\right)^T g_u(\mathbf{x}_1)\right\} \\ &\qquad +\xi_r\left\{\dot{\xi}_r + \left(\tfrac{\partial V_1}{\partial \mathbf{x}_1}\right)^T g_r(\mathbf{x}_1)\right\} \end{aligned} \tag{5.25}$$

where all the terms containing the error states ξ_u and ξ_r have been grouped together. Using (5.18), (5.19) and (5.23), equation (5.25) is bounded by

$$\begin{aligned}\dot{V}_2(\mathbf{x}_2, c_c, \dot{c}_c) \quad < -\alpha V_1(\mathbf{x}_1, c_c) + (u - u_{des}) \left\{ (\dot{u} - \dot{u}_{des}) + \left(\frac{\partial V_1}{\partial \mathbf{x}_1}\right)^T g_u(\mathbf{x}_1) \right\} \\ + (r - r_{des}) \left\{ (\dot{r} - \dot{r}_{des}) + \left(\frac{\partial V_1}{\partial \mathbf{x}_1}\right)^T g_r(\mathbf{x}_1) \right\}.\end{aligned} \tag{5.26}$$

The control laws T_R and T_L given by (5.17) then guarantee that

$$\dot{V}_2(\mathbf{x}_2, c_c, \dot{c}_c) < -\alpha V_2(\mathbf{x}_2, c_c). \tag{5.27}$$

Given that $V_2(\mathbf{x}_2, c_c)$ is positive definite and radially unbounded, condition (5.27) yields global exponential stability of the system (5.16) to $u = u_{des}$, $r = r_{des}$, $\theta = 0$, $s_1 = 0$, and $y_1 = 0$ for $\forall c_c \in [c_{c_{min}}, c_{c_{max}}]$ and $|\dot{c}_c| \leq \bar{c}_{c_{max}}$. □

The next section uses backstepping to include the actuator dynamics and design the input voltages V_R and V_L.

5.3 Actuator Controller Synthesis

In the third step of the path following controller synthesis method proposed here, the actuator dynamics are included and the input voltages V_R and V_L are designed using backstepping. A diagram of the complete closed-loop system is shown in Figure 5.3.

Consider the WMR kinematics and dynamics (5.16), rewritten as

$$\begin{bmatrix} \dot{u} \\ \dot{r} \\ \dot{\theta} \\ \dot{s}_1 \\ \dot{y}_1 \end{bmatrix} = \begin{bmatrix} 0 \\ 0 \\ r - c_c(t)\dot{s} \\ u\cos\theta + c_c(t)\dot{s}y_1 - \dot{s} \\ u\sin\theta - c_c(t)\dot{s}s_1 \end{bmatrix} + \begin{bmatrix} \frac{1}{Mr_w} \\ \frac{c}{Ir_w} \\ 0 \\ 0 \\ 0 \end{bmatrix} T_R + \begin{bmatrix} \frac{1}{Mr_w} \\ \frac{-c}{Ir_w} \\ 0 \\ 0 \\ 0 \end{bmatrix} T_L \tag{5.28}$$

or as

$$\dot{\mathbf{x}}_2 = g(\mathbf{x}_2, c_c) + g_{T_R}(\mathbf{x}_2)T_R + g_{T_L}(\mathbf{x}_2)T_L. \tag{5.29}$$

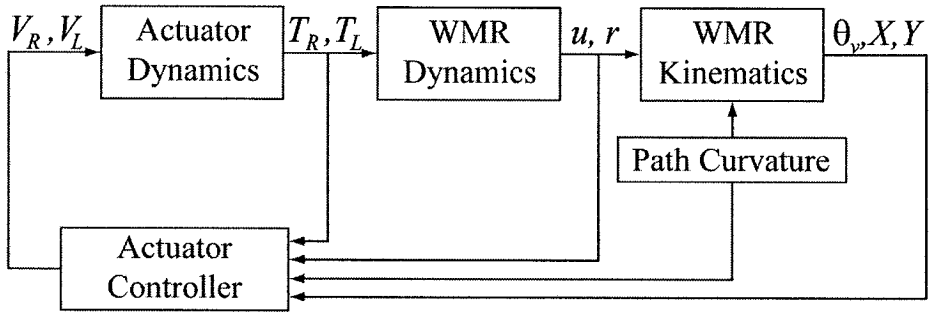

Figure 5.3: Diagram of complete closed-loop system

Combining the WMR kinematics and dynamics (5.29) with the actuator dynamics (2.16) results in

$$\begin{cases} \dot{\mathbf{x}}_2 = g(\mathbf{x}_2, c_c) + g_{T_R}(\mathbf{x}_2)T_R + g_{T_L}(\mathbf{x}_2)T_L \\ \dot{T}_R = -\frac{K_m R_a}{L_a} i_R - \frac{K_m K_b}{L_a}\dot{\phi}_R + \frac{K_m}{L_a} V_R \\ \dot{T}_L = -\frac{K_m R_a}{L_a} i_L - \frac{K_m K_b}{L_a}\dot{\phi}_L + \frac{K_m}{L_a} V_L \end{cases} . \tag{5.30}$$

We now consider T_R and T_L *virtual controls*, and call the torque control laws (5.17) *stabilizing functions* and denote them by $T_{R_{des}}$ and $T_{L_{des}}$. The new control inputs to the augmented system (5.30) are the actuator voltages V_R and V_L. In the proof of the following theorem, it will be shown that the control laws

$$\begin{cases} V_R = \frac{L_a}{K_m}\dot{T}_{R_{des}} - \frac{\alpha}{2}\frac{L_a}{K_m}\xi_{T_R} \\ \qquad -\frac{L_a}{K_m}\left(\frac{\partial V_2}{\partial \mathbf{x}_2}\right)^T g_{T_R}(\mathbf{x}_2) + K_b\dot{\phi}_R + R_a i_R \\ V_L = \frac{L_a}{K_m}\dot{T}_{L_{des}} - \frac{\alpha}{2}\frac{L_a}{K_m}\xi_{T_L} \\ \qquad -\frac{L_a}{K_m}\left(\frac{\partial V_2}{\partial \mathbf{x}_2}\right)^T g_{T_L}(\mathbf{x}_2) + K_b\dot{\phi}_L + R_a i_L \end{cases} , \quad \text{for } \mathbf{x}_1(t) \in \mathcal{R}_i, \tag{5.31}$$

can globally exponentially stabilize the system (5.30) to $T_R = T_{R_{des}}$, $T_L = T_{L_{des}}$, $u = u_{des}$, $r = r_{des}$, $\theta = 0$, $s_1 = 0$, and $y_1 = 0$ for $\forall c_c \in [c_{c_{min}}, c_{c_{max}}]$ and $|\dot{c}_c| \leq \bar{c}_{c_{max}}$,

where $\left(\frac{\partial V_2}{\partial \mathbf{x}_2}\right)^T = 2P_2(c_c)(\mathbf{x}_2 - \mathbf{x}_2^{cl})$ with

$$P_2(c_c) = \begin{bmatrix} \frac{1}{2} & 0 & 0 \\ 0 & \frac{1}{2} & 0 \\ 0 & 0 & P_1(c_c) \end{bmatrix}. \tag{5.32}$$

Theorem 5.3 *Consider the system (5.30). Let there exist stabilizing functions T_R and T_L given by (5.17), as well as a parameter-dependent quadratic Lyapunov function $V_2(\boldsymbol{x}_2, c_c)$ that satisfies (5.24) and (5.27). Then the actuator input voltages V_R and V_L given by (5.31) render the system (5.30) globally exponentially stable to $T_R = T_{R_{des}}$, $T_L = T_{L_{des}}$, $u = u_{des}$, $r = r_{des}$, $\theta = 0$, $s_1 = 0$, and $y_1 = 0$ for $\forall c_c \in [c_{c_{min}}, c_{c_{max}}]$ and $|\dot{c}_c| \leq \bar{c}_{c_{max}}$.* □

Proof: Introducing the two error variables

$$\begin{cases} \xi_{T_R} = T_R - T_{R_{des}} \\ \xi_{T_L} = T_L - T_{L_{des}} \end{cases}, \tag{5.33}$$

and differentiating with respect to time yields

$$\begin{cases} \dot{\xi}_{T_R} = \dot{T}_R - \dot{T}_{R_{des}} \\ \dot{\xi}_{T_L} = \dot{T}_L - \dot{T}_{L_{des}} \end{cases}, \tag{5.34}$$

where $\dot{T}_R$ and $\dot{T}_L$ are given in (5.30), and $\dot{T}_{R_{des}}$ and $\dot{T}_{L_{des}}$ are given by

$$\begin{cases} \dot{T}_{R_{des}} = \frac{Mr_w}{2}\left\{\ddot{u}_{des} - \frac{\alpha}{2}\dot{\xi}_u - \frac{d}{dt}\left[\left(\frac{\partial V_1}{\partial \mathbf{x}_1}\right)^T\right] g_u(\mathbf{x}_1) - \left(\frac{\partial V_1}{\partial \mathbf{x}_1}\right)^T \frac{d}{dt}\left[g_u(\mathbf{x}_1)\right]\right\} \\ \qquad\qquad + \frac{Ir_w}{2c}\left\{\ddot{r}_{des} - \frac{\alpha}{2}\dot{\xi}_r - \frac{d}{dt}\left[\left(\frac{\partial V_1}{\partial \mathbf{x}_1}\right)^T\right] g_r(\mathbf{x}_1) - \left(\frac{\partial V_1}{\partial \mathbf{x}_1}\right)^T \frac{d}{dt}\left[g_r(\mathbf{x}_1)\right]\right\} \\ \dot{T}_{L_{des}} = \frac{Mr_w}{2}\left\{\ddot{u}_{des} - \frac{\alpha}{2}\dot{\xi}_u - \frac{d}{dt}\left[\left(\frac{\partial V_1}{\partial \mathbf{x}_1}\right)^T\right] g_u(\mathbf{x}_1) - \left(\frac{\partial V_1}{\partial \mathbf{x}_1}\right)^T \frac{d}{dt}\left[g_u(\mathbf{x}_1)\right]\right\} \\ \qquad\qquad - \frac{Ir_w}{2c}\left\{\ddot{r}_{des} - \frac{\alpha}{2}\dot{\xi}_r - \frac{d}{dt}\left[\left(\frac{\partial V_1}{\partial \mathbf{x}_1}\right)^T\right] g_r(\mathbf{x}_1) - \left(\frac{\partial V_1}{\partial \mathbf{x}_1}\right)^T \frac{d}{dt}\left[g_r(\mathbf{x}_1)\right]\right\} \end{cases}, \tag{5.35}$$

for $\mathbf{x}_1(t) \in \mathcal{R}_i$, with

$$\frac{d}{dt}\left[\left(\frac{\partial V_1}{\partial \mathbf{x}_1}\right)^T\right] = 2\dot{c}_c \frac{dP_1}{dc_c}\mathbf{x}_1 + 2P_1(c_c)\dot{\mathbf{x}}_1, \tag{5.36}$$

and

$$\frac{d}{dt}\left[g_u(\mathbf{x}_1)\right] = \begin{bmatrix} 0 \\ -\dot{\theta}\sin\theta \\ \dot{\theta}\cos\theta \end{bmatrix}, \qquad \frac{d}{dt}\left[g_r(\mathbf{x}_1)\right] = \begin{bmatrix} 0 \\ 0 \\ 0 \end{bmatrix}. \tag{5.37}$$

System (5.30) can now be rewritten in terms of the error states as

$$\begin{cases} \dot{\mathbf{x}}_2 = g(\mathbf{x}_2, c_c) + g_{T_R}(\mathbf{x}_2)\left[\xi_{T_R} + T_{R_{des}}\right] + g_{T_L}(\mathbf{x}_2)\left[\xi_{T_L} + T_{L_{des}}\right] \\ \dot{\xi}_{T_R} = \dot{T}_R - \dot{T}_{R_{des}} \\ \dot{\xi}_{T_L} = \dot{T}_L - \dot{T}_{L_{des}} \end{cases}. \tag{5.38}$$

Using the stabilizing functions $T_{R_{des}}$ and $T_{L_{des}}$ given by (5.17), it was shown in the previous section that the function

$$\nabla_{V_2}(\mathbf{x}_2, c_c, \dot{c}_c) = \left(\frac{\partial V_2}{\partial \mathbf{x}_2}\right)^T \left\{g(\mathbf{x}_2, c_c) + g_{T_R}(\mathbf{x}_2)T_{R_{des}} + g_{T_L}(\mathbf{x}_2)T_{L_{des}}\right\} \tag{5.39}$$

verifies

$$\nabla_{V_2}(\mathbf{x}_2, c_c, \dot{c}_c) < -\alpha V_2(\mathbf{x}_2, c_c). \tag{5.40}$$

A candidate parameter-dependent quadratic CLF for the system (5.38) is thus proposed by augmenting $V_2(\mathbf{x}_2, c_c)$ in (5.24) as follows

$$V_3(\mathbf{x}_3, c_c) = \frac{1}{2}\xi_{T_R}^2 + \frac{1}{2}\xi_{T_L}^2 + V_2(\mathbf{x}_2, c_c), \tag{5.41}$$

where $\mathbf{x}_3 = [T_R,\ T_L,\ u,\ r,\ \theta,\ s_1,\ y_1]^T$. The derivative of (5.41) along the state

trajectories of the system (5.38) is given by

$$\begin{aligned}
\dot{V}_3(\mathbf{x}_3, c_c, \dot{c}_c) &= \left(\frac{\partial V_2}{\partial \mathbf{x}_2}\right)^T \dot{\mathbf{x}}_2 + \xi_{T_R}\dot{\xi}_{T_R} + \xi_{T_L}\dot{\xi}_{T_L} \\
&= \left(\frac{\partial V_2}{\partial \mathbf{x}_2}\right)^T \{g(\mathbf{x}_2, c_c) + g_{T_R}(\mathbf{x}_2)\left[\xi_{T_R} + T_{R_{des}}\right] + g_{T_L}(\mathbf{x}_2)\left[\xi_{T_L} + T_{L_{des}}\right]\} \\
&\qquad + \xi_{T_R}\dot{\xi}_{T_R} + \xi_{T_L}\dot{\xi}_{T_L} \\
&= \left(\frac{\partial V_2}{\partial \mathbf{x}_2}\right)^T \{g(\mathbf{x}_2, c_c) + g_{T_R}(\mathbf{x}_2)T_{R_{des}} + g_{T_L}(\mathbf{x}_2)T_{L_{des}}\} \\
&\qquad + \xi_{T_R}\left\{\dot{\xi}_{T_R} + \left(\frac{\partial V_2}{\partial \mathbf{x}_2}\right)^T g_{T_R}(\mathbf{x}_2)\right\} \\
&\qquad + \xi_{T_L}\left\{\dot{\xi}_{T_L} + \left(\frac{\partial V_2}{\partial \mathbf{x}_2}\right)^T g_{T_L}(\mathbf{x}_2)\right\} \\
&= \nabla_{V_2}(\mathbf{x}_2, c_c, \dot{c}_c) + \xi_{T_R}\left\{\dot{\xi}_{T_R} + \left(\frac{\partial V_2}{\partial \mathbf{x}_2}\right)^T g_{T_R}(\mathbf{x}_2)\right\} \\
&\qquad + \xi_{T_L}\left\{\dot{\xi}_{T_L} + \left(\frac{\partial V_2}{\partial \mathbf{x}_2}\right)^T g_{T_L}(\mathbf{x}_2)\right\}
\end{aligned} \tag{5.42}$$

where all the terms containing ξ_{T_R} and ξ_{T_L} have been grouped together. Using (5.33), (5.34) and (5.40), equation (5.42) is bounded by

$$\begin{aligned}
\dot{V}_3(\mathbf{x}_3, c_c, \dot{c}_c) &< -\alpha V_2(\mathbf{x}_2, c_c) + (T_R - T_{R_{des}})\left\{(\dot{T}_R - \dot{T}_{R_{des}}) + \left(\frac{\partial V_2}{\partial \mathbf{x}_2}\right)^T g_{T_R}(\mathbf{x}_2)\right\} \\
&\qquad + (T_L - T_{L_{des}})\left\{(\dot{T}_L - \dot{T}_{L_{des}}) + \left(\frac{\partial V_2}{\partial \mathbf{x}_2}\right)^T g_{T_L}(\mathbf{x}_2)\right\}.
\end{aligned} \tag{5.43}$$

The actuator input voltages V_R and V_L given by (5.31) then guarantee that

$$\dot{V}_3(\mathbf{x}_3, c_c, \dot{c}_c) < -\alpha V_3(\mathbf{x}_3, c_c). \tag{5.44}$$

Given that $V_3(\mathbf{x}_3, c_c)$ is positive definite and radially unbounded, condition (5.44) yields global exponential stability of the system (5.30) to $T_R = T_{R_{des}}$, $T_L = T_{L_{des}}$, $u = u_{des}$, $r = r_{des}$, $\theta = 0$, $s_1 = 0$, and $y_1 = 0$ for $\forall c_c \in [c_{c_{min}}, c_{c_{max}}]$ and $|\dot{c}_c| \leq \bar{c}_{c_{max}}$. □

This chapter proposed a three-step path following controller synthesis method to solve Problem 2.1. This path following method will be applied to numerical simulations in the next chapter.

Chapter 6

Simulation Results

This chapter presents simulation results for the three-step path following controller synthesis method presented in the previous chapter for a wheeled mobile robot (WMR). In the first step, two curvature limits $c_{c_{min}}$ and $c_{c_{max}}$ and a curvature rate of change limit $\bar{c}_{c_{max}}$ are defined for the desired path and the nonlinear WMR parameterized path kinematics are approximated by an uncertain piecewise-affine parameter-varying (PWAPV) system, while assuming that the WMR forward velocity u_{des} is constant. Then, a PWAPV steering control law $r(t)$ is designed using a parameter-dependent quadratic Lyapunov function. In the second step, a backstepping-type approach is used to include the vehicle dynamics and design the wheel control torques T_R and T_L that guarantee convergence of the WMR forward and rotational velocities to the desired values. Finally, in the third step, the actuator dynamics are included and the input voltages V_R and V_L are designed using backstepping.

Consider the WMR shown in Figure 2.1 with the following physical parameters: $M = 6.0\ kg$, $I = 8.0\ kg \cdot m^2$, $c = 0.20\ m$, $r_w = 0.05\ m$, $K_b = 0.0001\ V \cdot s/rad$, $K_m = 1.0\ N \cdot m/A$, $R_a = 10.0\ \Omega$, and $L_a = 0.001\ H$. We choose $\dot{s} = 0.10\ m/s$, such

that $u_{des} = 0.10\ m/s$ and is constant. The curvature limits are set for a minimum turning radius $R = \pm 1.0\ m$; thus $c_{c_{min}} = -1.0\ m^{-1}$ and $c_{c_{max}} = +1.0\ m^{-1}$. The curvature rate of change magnitude limit is set as $\bar{c}_{c_{max}} = +2.0\ m^{-1}s^{-1}$.

6.1 PWAPV Kinematic Controller Synthesis

We begin by considering only the WMR parameterized path kinematics (5.1) with constant velocity $u = u_{des}$ and a time-varying path curvature $c_c(t)$

$$\begin{bmatrix} \dot{\theta} \\ \dot{s}_1 \\ \dot{y}_1 \end{bmatrix} = \begin{bmatrix} 0 & 0 & 0 \\ 0 & 0 & 0.10c_c(t) \\ 0 & -0.10c_c(t) & 0 \end{bmatrix} \begin{bmatrix} \theta \\ s_1 \\ y_1 \end{bmatrix} + \begin{bmatrix} -0.10c_c(t) \\ -0.10 \\ 0 \end{bmatrix} + \begin{bmatrix} 0 \\ 0.10\cos\theta \\ 0.10\sin\theta \end{bmatrix} + \begin{bmatrix} 1 \\ 0 \\ 0 \end{bmatrix} r(t), \tag{6.1}$$

which is of the form (5.2) (repeated here for convenience),

$$\dot{\mathbf{x}}_1(t) = A(c_c)\mathbf{x}_1(t) + a(c_c) + f(\mathbf{x}_1) + B(c_c)\mathbf{u}_1(t), \tag{6.2}$$

where the state vector is $\mathbf{x}_1(t) = [\theta,\ s_1,\ y_1]^T$ and the input vector is $\mathbf{u}_1(t) = r(t)$.

Solving Problem 3.1 from Chapter 3 with the state variable θ partitioned according to the grid

$$\theta = \left\{-\pi,\ -\tfrac{1}{2}\pi,\ -\tfrac{1}{4}\pi,\ +\tfrac{1}{4}\pi,\ +\tfrac{1}{2}\pi,\ +\pi\right\}, \tag{6.3}$$

$N_s = 200$ sampling points over the interval $\theta = [-\pi,\ +\pi]$, and the matrices

$$\tilde{A}_L = \begin{bmatrix} 0 & 0 & 0 \\ 0 & 0 & 0 \\ +0.10 & 0 & 0 \end{bmatrix}, \quad \tilde{a}_L = \begin{bmatrix} 0 \\ 0 \\ 0 \end{bmatrix}, \tag{6.4}$$

the nonlinear parameter-dependent system (6.2) is approximated by the nominal PWAPV system

$$\dot{\mathbf{x}}_1(t) = A_i(c_c)\mathbf{x}_1(t) + a_i(c_c) + B_i(c_c)\mathbf{u}_1(t), \quad \text{for } \mathbf{x}_1(t) \in \mathcal{R}_i, \tag{6.5}$$

with the matrices

$$
\begin{aligned}
A_1(c_c) &= \begin{bmatrix} 0 & 0 & 0 \\ +0.0836 & 0 & +0.10c_c \\ -0.0795 & -0.10c_c & 0 \end{bmatrix}, \quad a_1(c_c) = \begin{bmatrix} -0.10c_c \\ +0.0314 \\ -0.2499 \end{bmatrix}, \\
A_2(c_c) &= \begin{bmatrix} 0 & 0 & 0 \\ +0.1273 & 0 & +0.10c_c \\ +0.0591 & -0.10c_c & 0 \end{bmatrix}, \quad a_2(c_c) = \begin{bmatrix} -0.10c_c \\ +0.1000 \\ -0.0321 \end{bmatrix}, \\
A_3(c_c) &= \begin{bmatrix} 0 & 0 & 0 \\ 0 & 0 & +0.10c_c \\ +0.1000 & -0.10c_c & 0 \end{bmatrix}, \quad a_3(c_c) = \begin{bmatrix} -0.10c_c \\ 0 \\ 0 \end{bmatrix}, \\
A_4(c_c) &= \begin{bmatrix} 0 & 0 & 0 \\ -0.1273 & 0 & +0.10c_c \\ +0.0591 & -0.10c_c & 0 \end{bmatrix}, \quad a_4(c_c) = \begin{bmatrix} -0.10c_c \\ +0.1000 \\ +0.0321 \end{bmatrix}, \\
A_5(c_c) &= \begin{bmatrix} 0 & 0 & 0 \\ -0.0836 & 0 & +0.10c_c \\ -0.0795 & -0.10c_c & 0 \end{bmatrix}, \quad a_5(c_c) = \begin{bmatrix} -0.10c_c \\ +0.0314 \\ +0.2499 \end{bmatrix},
\end{aligned}
\tag{6.6}
$$

and

$$
B_i(c_c) = \begin{bmatrix} 1 \\ 0 \\ 0 \end{bmatrix}, \quad \text{for } i = 1, \ldots, 5. \tag{6.7}
$$

The nonlinear functions **cos** and **sin**, along with their PWA approximations, are plotted in Figure 6.1.

Solving Problem 3.2 from Chapter 3 with the nominal PWAPV matrices (6.6) and (6.7), $N_s = 200$ sampling points over the interval $\theta = [-\pi, \ +\pi]$, and the polynomial order $n_p = 2$, the following PWA uncertainty bounds W_{A_i} and W_{a_i} are

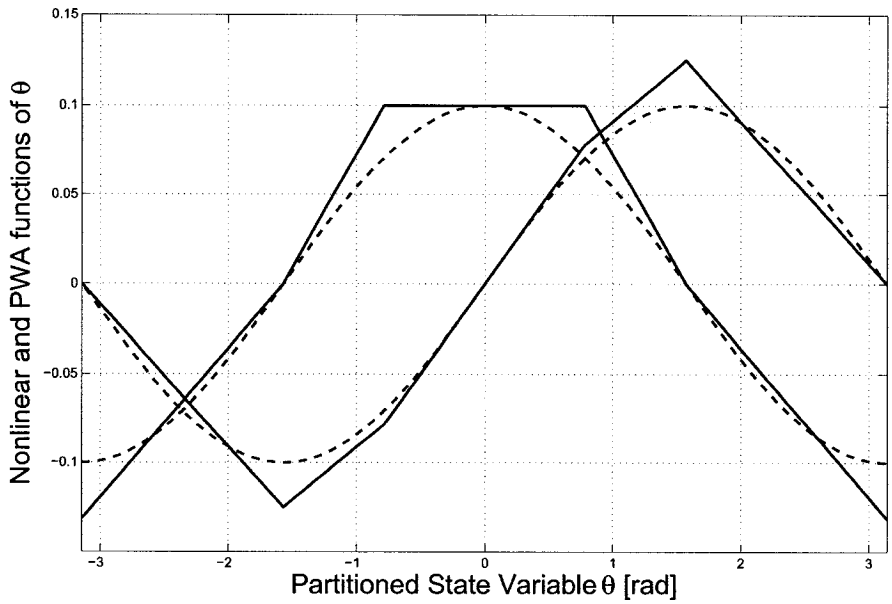

Figure 6.1: Nonlinear functions **cos** and **sin** with their PWA approximations

obtained:

$$
\begin{aligned}
W_{A_1} &= \begin{bmatrix} +0.0002390 & 0 & 0 \\ 0 & +0.0002273 & 0 \\ 0 & 0 & +0.0002273 \end{bmatrix}, \\
W_{A_2} &= \begin{bmatrix} +0.0003036 & 0 & 0 \\ 0 & +0.0001657 & 0 \\ 0 & 0 & +0.0001657 \end{bmatrix}, \\
W_{A_3} &= \begin{bmatrix} +0.0002702 & 0 & 0 \\ 0 & +0.0002262 & 0 \\ 0 & 0 & +0.0002262 \end{bmatrix}, \\
W_{A_4} &= \begin{bmatrix} +0.0003036 & 0 & 0 \\ 0 & +0.0001657 & 0 \\ 0 & 0 & +0.0001657 \end{bmatrix}, \\
W_{A_5} &= \begin{bmatrix} +0.0002390 & 0 & 0 \\ 0 & +0.0002273 & 0 \\ 0 & 0 & +0.0002273 \end{bmatrix},
\end{aligned}
\tag{6.8}
$$

and

$$
\begin{aligned}
W_{a_1} &= \begin{bmatrix} +0.0002273 & 0 & 0 \\ 0 & +0.0002281 & 0 \\ 0 & 0 & +0.0002295 \end{bmatrix}, \\
W_{a_2} &= \begin{bmatrix} +0.0001657 & 0 & 0 \\ 0 & +0.0003099 & 0 \\ 0 & 0 & +0.0001855 \end{bmatrix}, \\
W_{a_3} &= \begin{bmatrix} +0.0002262 & 0 & 0 \\ 0 & +0.0002965 & 0 \\ 0 & 0 & +0.0002305 \end{bmatrix}, \\
W_{a_4} &= \begin{bmatrix} +0.0001657 & 0 & 0 \\ 0 & +0.0003099 & 0 \\ 0 & 0 & +0.0001855 \end{bmatrix}, \\
W_{a_5} &= \begin{bmatrix} +0.0002273 & 0 & 0 \\ 0 & +0.0002281 & 0 \\ 0 & 0 & +0.0002295 \end{bmatrix}.
\end{aligned} \tag{6.9}
$$

The bounding ellipsoids (3.6) corresponding to the state space partition (6.3) are defined by

$$
\begin{aligned}
L_1 &= \begin{bmatrix} +1.2732 & 0 & 0 \end{bmatrix}, \quad l_1 = +3.0, \\
L_2 &= \begin{bmatrix} +2.5465 & 0 & 0 \end{bmatrix}, \quad l_2 = +3.0, \\
L_3 &= \begin{bmatrix} +1.2732 & 0 & 0 \end{bmatrix}, \quad l_3 = \ 0.0, \\
L_4 &= \begin{bmatrix} +2.5465 & 0 & 0 \end{bmatrix}, \quad l_4 = -3.0, \\
L_5 &= \begin{bmatrix} +1.2732 & 0 & 0 \end{bmatrix}, \quad l_5 = -3.0.
\end{aligned} \tag{6.10}
$$

For the synthesis of the PWAPV steering control law

$$
r(t) = K_i(c_c)\mathbf{x}_1(t) + k_i(c_c), \quad \text{for } \mathbf{x}_1(t) \in \mathcal{R}_i, \tag{6.11}
$$

Problem 5.1 from the previous chapter is solved with $\alpha = 0.01$, $\mu_i = -100$, $k_{lim} = 1$, $c_{c_{min}} = -1.0\ m^{-1}$, $c_{c_{max}} = +1.0\ m^{-1}$, $\bar{c}_{c_{max}} = +2.0\ m^{-1}s^{-1}$, $Y_i^{lim} = [20,\ 20,\ 20]^T$,

$\lambda_{max} = 1.0 \times 10^{-6}$, a set of $N_{c_c} = 20$ grid points over the interval $c_c = [-1.0, \ +1.0]$, and

$$\epsilon_1 = 7.2 \times 10^{+6}, \quad \epsilon_2 = 5.0 \times 10^{+1}, \quad \epsilon_3 = 1.0 \times 10^{+2},$$
$$\epsilon_4 = 5.0 \times 10^{+2}, \quad \epsilon_5 = 5.0 \times 10^{+1}, \quad \epsilon_6 = 5.0 \times 10^{-1}.$$

The solution of Problem 5.1 gives

$$\begin{cases} \overline{Y0}_1 = [+0.0933, \ -0.0539, \ -0.0920] \\ \overline{Y0}_2 = [+0.1574, \ -0.0700, \ -0.0966] \\ \overline{Y0}_3 = [-0.0429, \ +0.0010, \ +0.0012] \\ \overline{Y0}_4 = [+0.1728, \ -0.0752, \ -0.0966] \\ \overline{Y0}_5 = [+0.1219, \ -0.0640, \ -0.0305] \end{cases} \tag{6.12}$$

and

$$\begin{cases} \overline{Y1}_1 = [-14.1638, \ -7.4153, \ -7.3965] \\ \overline{Y1}_2 = [-14.5909, \ -7.6757, \ -6.7744] \\ \overline{Y1}_3 = [-16.2819, \ -0.0025, \ -0.0218] \\ \overline{Y1}_4 = [-14.5921, \ -7.6726, \ -6.7730] \\ \overline{Y1}_5 = [-14.1668, \ -7.4026, \ -7.3873] \end{cases} \tag{6.13}$$

for $Y_i(c_c) = \overline{Y0}_i \cdot c_c + \overline{Y1}_i$,

$$\begin{cases} \overline{k0}_1 = +0.0710 \\ \overline{k0}_2 = +0.0771 \\ \overline{k0}_3 = +0.1000 \\ \overline{k0}_4 = +0.0754 \\ \overline{k0}_5 = +0.0668 \end{cases} \tag{6.14}$$

and

$$\begin{cases} \overline{k1}_1 = -0.0802 \\ \overline{k1}_2 = +0.0165 \\ \overline{k1}_3 = \ 0.0 \\ \overline{k1}_4 = +0.0468 \\ \overline{k1}_5 = +0.1014 \end{cases} \tag{6.15}$$

for $k_i(c_c) = \overline{k0}_i \cdot c_c + \overline{k1}_i$, and

$$\overline{Q0} = \begin{bmatrix} -0.0447 & -0.0000 & +0.0000 \\ -0.0000 & -0.0000 & -0.0001 \\ +0.0000 & -0.0001 & -0.0001 \end{bmatrix} \tag{6.16}$$

and

$$\overline{Q1} = \begin{bmatrix} +0.1680 & +0.0000 & -0.0010 \\ +0.0000 & +0.0001 & +0.0000 \\ -0.0010 & +0.0000 & +0.0002 \end{bmatrix} \tag{6.17}$$

for $Q_1(c_c) = \overline{Q0} \cdot c_c + \overline{Q1}$. Thus, the gains for the PWAPV control law (6.11) are defined by

$$\begin{cases} K_i(c_c) = Y_i(c_c) \cdot Q_1^{-1}(c_c) \\ k_i(c_c) = \overline{k0}_i \cdot c_c + \overline{k1}_i \end{cases},$$

and the Lyapunov function (5.7) (repeated here for convenience),

$$V_1(\mathbf{x}_1, c_c) = \mathbf{x}_1^T P_1(c_c) \mathbf{x}_1, \tag{6.18}$$

is parameterized by $P_1(c_c) = Q_1^{-1}(c_c)$.

The next section gives the wheel control torques T_R and T_L.

6.2 Dynamic Controller Synthesis

The WMR parameterized path kinematics and dynamics (5.16) are given by

$$\begin{cases} \dot{u} = \frac{1}{0.3}(T_R + T_L) \\ \dot{r} = \frac{0.1}{0.4}(T_R - T_L) \\ \dot{\theta} = r - 0.10c_c(t) \\ \dot{s}_1 = 0.10\cos\theta + 0.10c_c(t)y_1 - 0.10 \\ \dot{y}_1 = 0.10\sin\theta - 0.10c_c(t)s_1 \end{cases} . \tag{6.19}$$

The dynamic control laws (5.17) are given by

$$\begin{cases} T_R = \frac{0.3}{2}\left\{\dot{u}_{des} - \frac{0.01}{2}(u - u_{des}) - \left(\frac{\partial V_1}{\partial \mathbf{x}_1}\right)^T g_u(\mathbf{x}_1)\right\} \\ \qquad\quad + \frac{0.4}{0.2}\left\{\dot{r}_{des} - \frac{0.01}{2}(r - r_{des}) - \left(\frac{\partial V_1}{\partial \mathbf{x}_1}\right)^T g_r(\mathbf{x}_1)\right\} \\ T_L = \frac{0.3}{2}\left\{\dot{u}_{des} - \frac{0.01}{2}(u - u_{des}) - \left(\frac{\partial V_1}{\partial \mathbf{x}_1}\right)^T g_u(\mathbf{x}_1)\right\} \\ \qquad\quad - \frac{0.4}{0.2}\left\{\dot{r}_{des} - \frac{0.01}{2}(r - r_{des}) - \left(\frac{\partial V_1}{\partial \mathbf{x}_1}\right)^T g_r(\mathbf{x}_1)\right\} \end{cases} , \quad \text{for } \mathbf{x}_1(t) \in \mathcal{R}_i, \tag{6.20}$$

where

$$\begin{matrix} \dot{u}_{des} = 0 \\ \dot{r}_{des} = K_i(c_c)\dot{\mathbf{x}}_1 \end{matrix} , \quad \text{for } \mathbf{x}_1(t) \in \mathcal{R}_i, \tag{6.21}$$

and

$$\left(\frac{\partial V_1}{\partial \mathbf{x}_1}\right)^T = 2P_1(c_c)\mathbf{x}_1, \tag{6.22}$$

and

$$g_u(\mathbf{x}_1)\begin{bmatrix} 0 \\ \cos\theta \\ \sin\theta \end{bmatrix}, \qquad g_r(\mathbf{x}_1) = \begin{bmatrix} 1 \\ 0 \\ 0 \end{bmatrix}. \tag{6.23}$$

The augmented control Lyapunov function $V_2(\mathbf{x}_2, c_c)$ in (5.24) is described by

$$\begin{aligned} V_2(\mathbf{x}_2, c_c) &= (\mathbf{x}_2 - \mathbf{x}_2^{cl})^T P_2(c_c)(\mathbf{x}_2 - \mathbf{x}_2^{cl}) \\ &= \begin{bmatrix} u - u_{des} \\ r - r_{des} \\ \mathbf{x}_1 - \mathbf{x}_1^{cl} \end{bmatrix}^T \begin{bmatrix} \frac{1}{2} & 0 & 0 \\ 0 & \frac{1}{2} & 0 \\ 0 & 0 & P_1(c_c) \end{bmatrix} \begin{bmatrix} u - u_{des} \\ r - r_{des} \\ \mathbf{x}_1 - \mathbf{x}_1^{cl} \end{bmatrix} . \end{aligned} \tag{6.24}$$

The next section gives the input voltage laws V_R and V_L.

6.3 Actuator Controller Synthesis

The WMR parameterized path kinematics, WMR dynamics, and actuator dynamics (5.30) are given by

$$\begin{cases} \dot{T}_R = -\frac{10.0}{0.001} i_R - \frac{0.0001}{0.001}\dot{\phi}_R + \frac{1.0}{0.001} V_R \\ \dot{T}_L = -\frac{10.0}{0.001} i_L - \frac{0.0001}{0.001}\dot{\phi}_L + \frac{1.0}{0.001} V_L \\ \dot{u} = \frac{1}{0.3}(T_R + T_L) \\ \dot{r} = \frac{0.1}{0.4}(T_R - T_L) \\ \dot{\theta} = r - 0.10 c_c(t) \\ \dot{s}_1 = 0.10\cos\theta + 0.10 c_c(t) y_1 - 0.10 \\ \dot{y}_1 = 0.10\sin\theta - 0.10 c_c(t) s_1 \end{cases} . \tag{6.25}$$

The actuator control laws (5.31) are given by

$$\begin{cases} V_R = \frac{0.001}{1.0}\dot{T}_{R_{des}} - \frac{0.00001}{2}(T_R - T_{R_{des}}) \\ \qquad -\frac{0.001}{1.0}\left(\frac{\partial V_2}{\partial \mathbf{x}_2}\right)^T g_{T_R}(\mathbf{x}_2) + 0.0001\dot{\phi}_R + 10.0 i_R \\ V_L = \frac{0.001}{1.0}\dot{T}_{L_{des}} - \frac{0.00001}{2}(T_L - T_{L_{des}}) \\ \qquad -\frac{0.001}{1.0}\left(\frac{\partial V_2}{\partial \mathbf{x}_2}\right)^T g_{T_L}(\mathbf{x}_2) + 0.0001\dot{\phi}_L + 10.0 i_L \end{cases} , \quad \text{for } \mathbf{x}_1(t) \in \mathcal{R}_i, \tag{6.26}$$

where

$$\begin{aligned}\left(\frac{\partial V_2}{\partial \mathbf{x}_2}\right)^T &= 2P_2(c_c)(\mathbf{x}_2 - \mathbf{x}_2^{cl}) \\ &= 2\begin{bmatrix}\frac{1}{2} & 0 & 0 \\ 0 & \frac{1}{2} & 0 \\ 0 & 0 & P_1(c_c)\end{bmatrix}\begin{bmatrix}u - u_{des} \\ r - r_{des} \\ \mathbf{x}_1 - \mathbf{x}_1^{cl}\end{bmatrix}\end{aligned} \tag{6.27}$$

and

$$g_{T_R}(\mathbf{x}_2) = \begin{bmatrix}\frac{1}{0.3} \\ \frac{0.1}{0.4} \\ 0 \\ 0 \\ 0\end{bmatrix}, \qquad g_{T_R}(\mathbf{x}_2) = \begin{bmatrix}\frac{1}{0.3} \\ \frac{-0.1}{0.4} \\ 0 \\ 0 \\ 0\end{bmatrix}, \tag{6.28}$$

and

$$\begin{cases} \dot{T}_{R_{des}} = \frac{0.3}{2}\left\{\ddot{u}_{des} - \frac{0.01}{2}\dot{\xi}_u - \frac{d}{dt}\left[\left(\frac{\partial V_1}{\partial \mathbf{x}_1}\right)^T\right] g_u(\mathbf{x}_1) - \left(\frac{\partial V_1}{\partial \mathbf{x}_1}\right)^T \frac{d}{dt}\left[g_u(\mathbf{x}_1)\right]\right\} \\ \qquad\quad +\frac{0.4}{0.2}\left\{\ddot{r}_{des} - \frac{0.01}{2}\dot{\xi}_r - \frac{d}{dt}\left[\left(\frac{\partial V_1}{\partial \mathbf{x}_1}\right)^T\right] g_r(\mathbf{x}_1) - \left(\frac{\partial V_1}{\partial \mathbf{x}_1}\right)^T \frac{d}{dt}\left[g_r(\mathbf{x}_1)\right]\right\} \\ \dot{T}_{L_{des}} = \frac{0.3}{2}\left\{\ddot{u}_{des} - \frac{0.01}{2}\dot{\xi}_u - \frac{d}{dt}\left[\left(\frac{\partial V_1}{\partial \mathbf{x}_1}\right)^T\right] g_u(\mathbf{x}_1) - \left(\frac{\partial V_1}{\partial \mathbf{x}_1}\right)^T \frac{d}{dt}\left[g_u(\mathbf{x}_1)\right]\right\} \\ \qquad\quad -\frac{0.4}{0.2}\left\{\ddot{r}_{des} - \frac{0.01}{2}\dot{\xi}_r - \frac{d}{dt}\left[\left(\frac{\partial V_1}{\partial \mathbf{x}_1}\right)^T\right] g_r(\mathbf{x}_1) - \left(\frac{\partial V_1}{\partial \mathbf{x}_1}\right)^T \frac{d}{dt}\left[g_r(\mathbf{x}_1)\right]\right\} \end{cases}, \tag{6.29}$$

for $\mathbf{x}_1(t) \in \mathcal{R}_i$, with

$$\begin{aligned}\frac{d}{dt}\left[\left(\frac{\partial V_1}{\partial \mathbf{x}_1}\right)^T\right] &= 2\dot{c}_c\frac{dP_1}{dc_c}\mathbf{x}_1 + 2P_1(c_c)\dot{\mathbf{x}}_1 \\ &= -2\dot{c}_c[P_1(c_c)\overline{Q0}P_1(c_c)]\mathbf{x}_1 + 2P_1(c_c)\dot{\mathbf{x}}_1\end{aligned} \tag{6.30}$$

and

$$\frac{d}{dt}\left[g_u(\mathbf{x}_1)\right] = \begin{bmatrix}0 \\ -\dot{\theta}\sin\theta \\ \dot{\theta}\cos\theta\end{bmatrix}, \quad \frac{d}{dt}\left[g_r(\mathbf{x}_1)\right] = \begin{bmatrix}0 \\ 0 \\ 0\end{bmatrix}. \tag{6.31}$$

The augmented control Lyapunov function $V_3(\mathbf{x}_3, c_c)$ in (5.32) is described by

$$\begin{aligned} V_3(\mathbf{x}_3, c_c) &= (\mathbf{x}_3 - \mathbf{x}_3^{cl})^T P_3(c_c)(\mathbf{x}_3 - \mathbf{x}_3^{cl}) \\ &= \begin{bmatrix} T_R - T_{R_{des}} \\ T_L - T_{L_{des}} \\ \mathbf{x}_2 - \mathbf{x}_2^{cl} \end{bmatrix}^T \begin{bmatrix} \frac{1}{2} & 0 & 0 \\ 0 & \frac{1}{2} & 0 \\ 0 & 0 & P_2(c_c) \end{bmatrix} \begin{bmatrix} T_R - T_{R_{des}} \\ T_L - T_{L_{des}} \\ \mathbf{x}_2 - \mathbf{x}_2^{cl} \end{bmatrix}. \end{aligned} \tag{6.32}$$

The next section presents the simulation results for a time-varying curvature.

6.4 Simulation Results

The desired trajectory is shown in the top part of Figure 6.2 and is defined by a series of straight lines and circles. The curvature function that describes the desired trajectory is plotted with respect to time in Figure 6.3, where it can be seen that the curvature function is always within the bounds $c_{c_{min}} = -1.0\ m^{-1}$ and $c_{c_{max}} = +1.0\ m^{-1}$. Figure 6.4 plots the curvature rate of change with respect to time, with the curvature function shown in Figure 6.3 underneath it. It can be seen from Figure 6.4 that the magnitude of the curvature rate of change is always within the bound $c_{c_{max}} = +2.0\ m^{-1}s^{-1}$. A diagram of the closed-loop WMR system is shown in Figure 6.5.

Simulations were performed using 5 different sets of initial conditions, shown in the bottom part of Figure 6.2, to demonstrate the effectiveness of the path following controller synthesis method proposed in this thesis. In particular, consider the case where the WMR begins on the desired path, but with a heading error $\theta = \pi\ rad$, as shown in the bottom part of Figure 6.6. The remaining results pertain to this particular case.

The time response of the WMR parameterized path kinematics θ, s_1, and y_1 in (5.1) is shown in Figure 6.7. It can be seen from Figure 6.7 that the parameterized

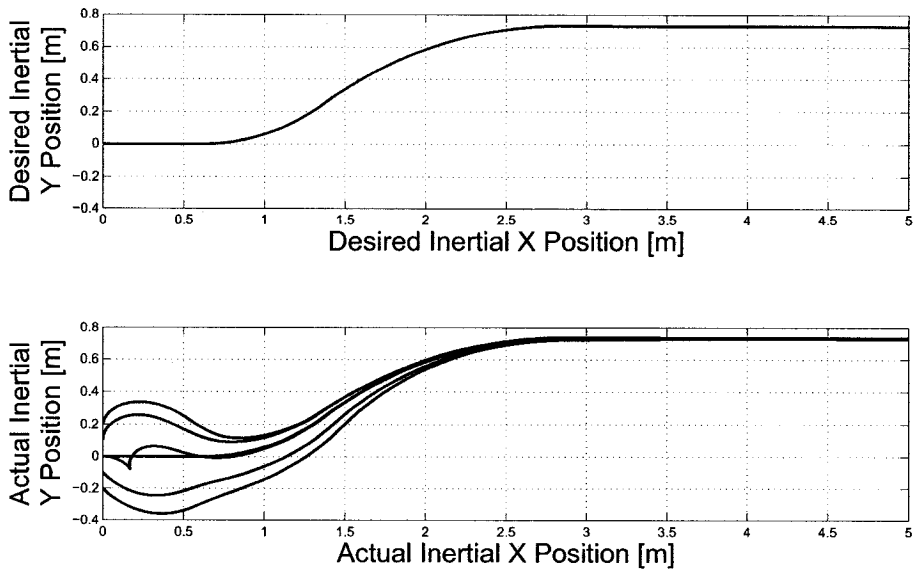

Figure 6.2: Plot of desired and actual trajectories (multiple cases)

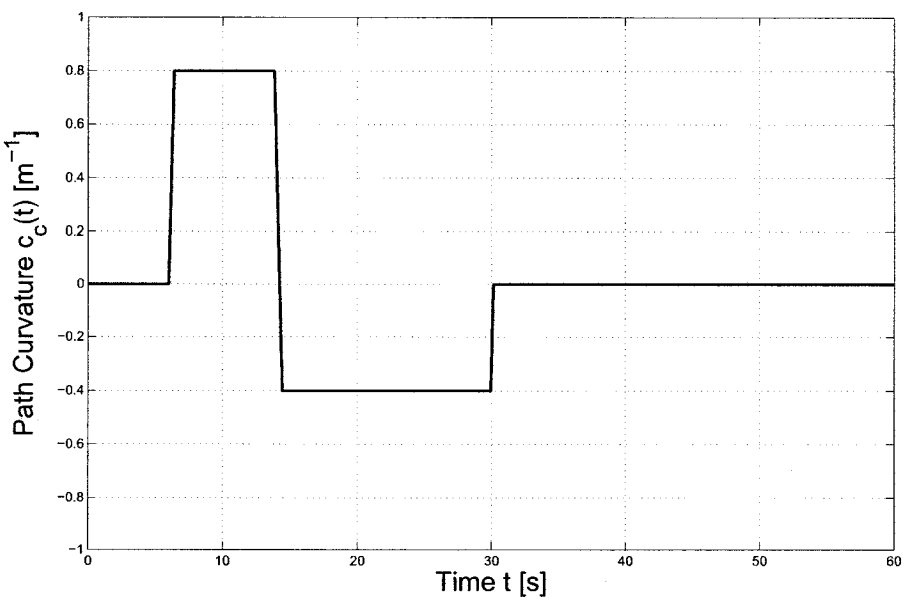

Figure 6.3: Plot of time-varying curvature function

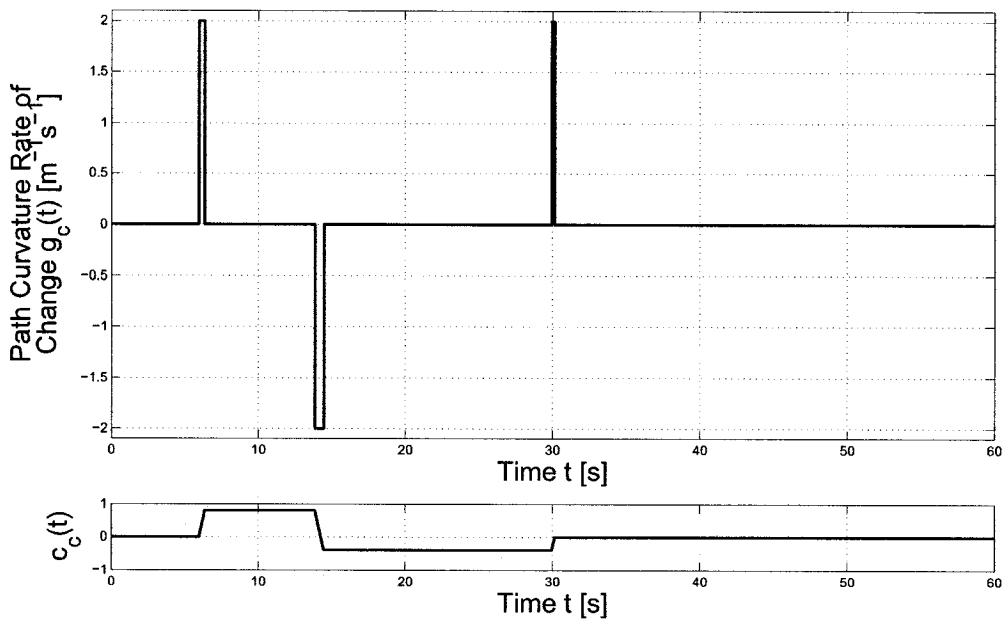

Figure 6.4: Plot of curvature rate of change

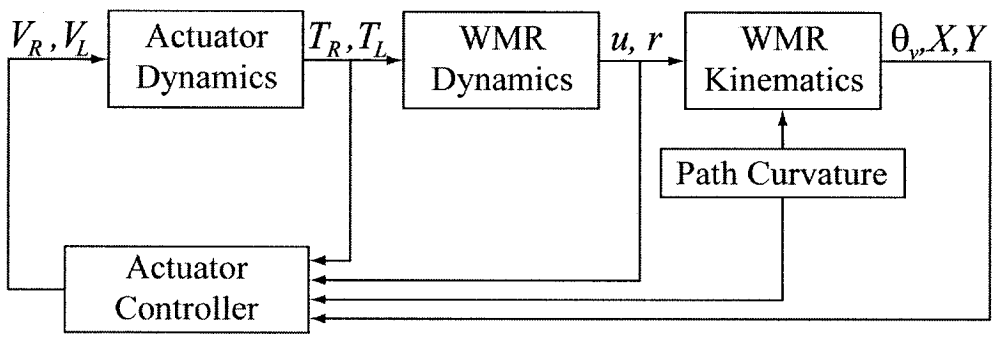

Figure 6.5: Diagram of closed-loop WMR system

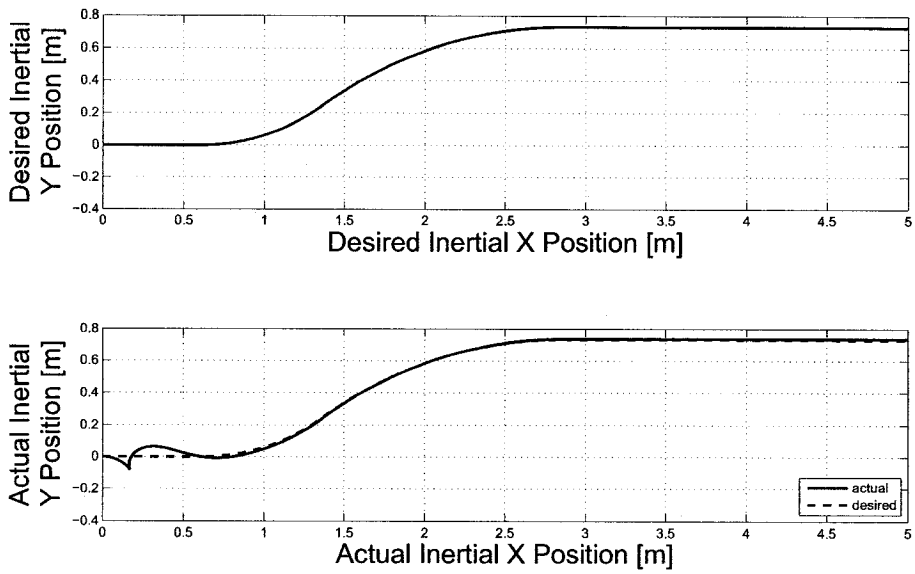

Figure 6.6: Plot of actual trajectory (particular case)

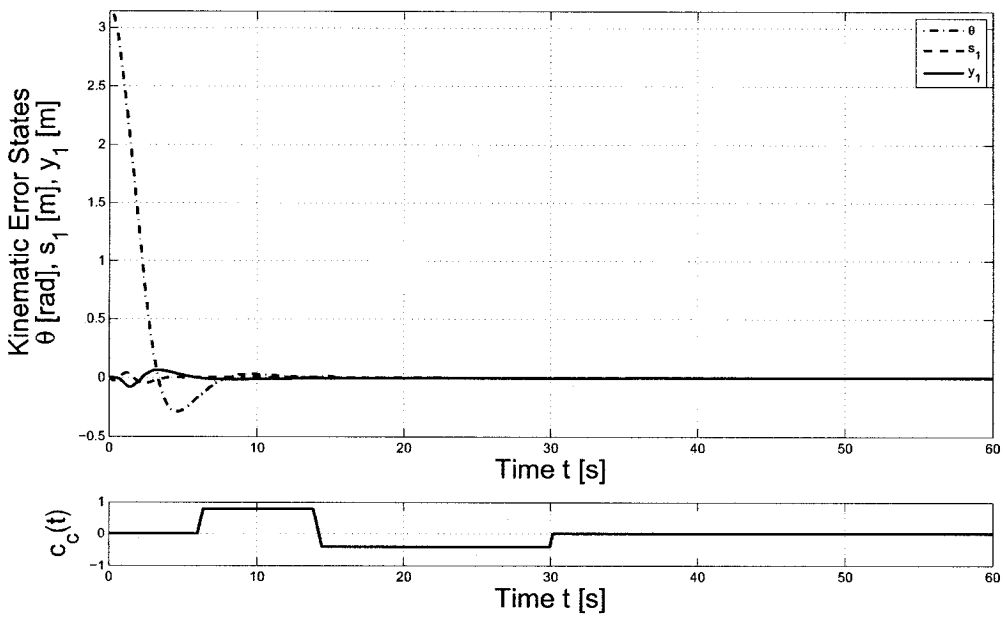

Figure 6.7: Plot of kinematic error states θ, s_1, y_1

kinematics, which represent the difference in the actual position and orientation of the WMR with respect to the desired position and orientation, converge to zero. The dynamic states u and r in (5.16) are plotted in Figure 6.8 with respect to time. It can be seen that the forward velocity converges to the desired value of $u_{des} = 0.10\ m/s$. It can also be seen from this figure that the rotational velocity varies each time the desired path curvature changes and finally converges to zero, which is the desired rotational velocity for the last segment of the path. The actuator states, the right and left motor torques T_R and T_L in (5.30), are plotted in Figure 6.9 with respect to time. The actuator control inputs, the right and left motor voltages V_R and V_L, are plotted with respect to time in Figure 6.10. Note in Figures 6.9 and 6.10 that the actuator states and input voltages vary when the desired path curvature changes. It can be seen from Figure 6.10 that the input voltages required to bring the WMR to the desired trajectory is less than 20 V.

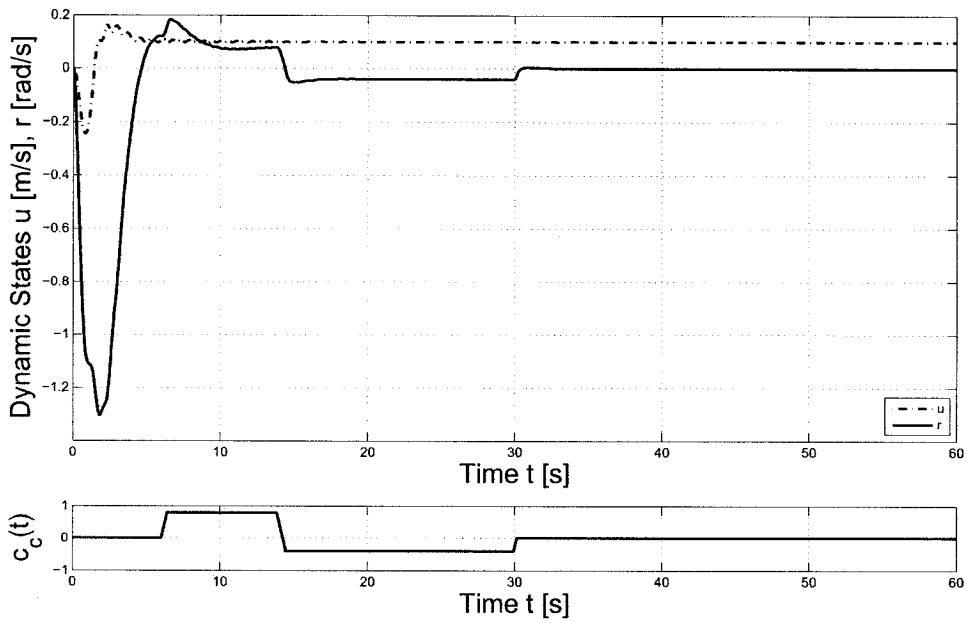

Figure 6.8: Plot of dynamic states u, r

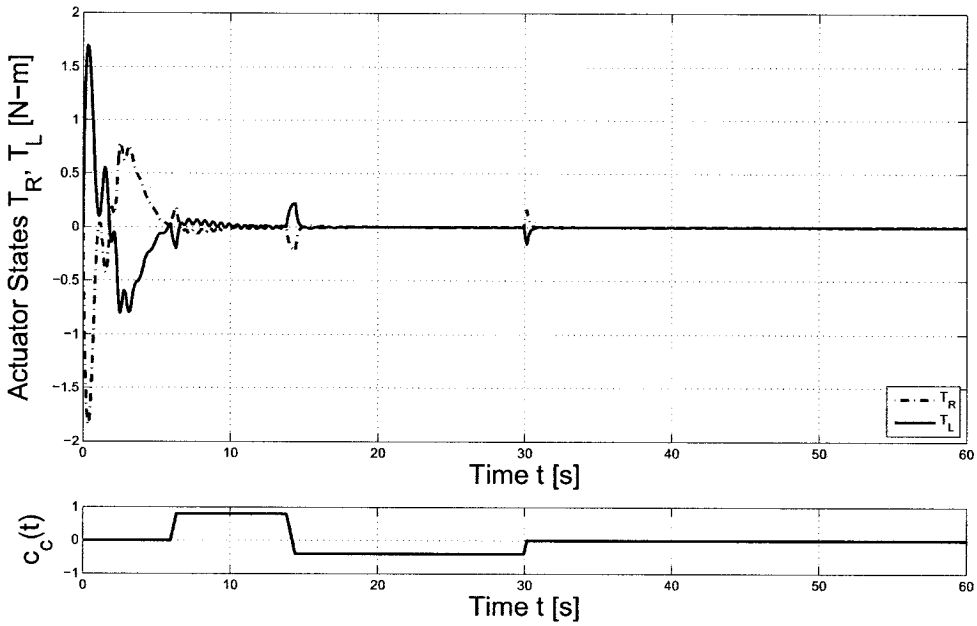

Figure 6.9: Plot of actuator states T_R, T_L

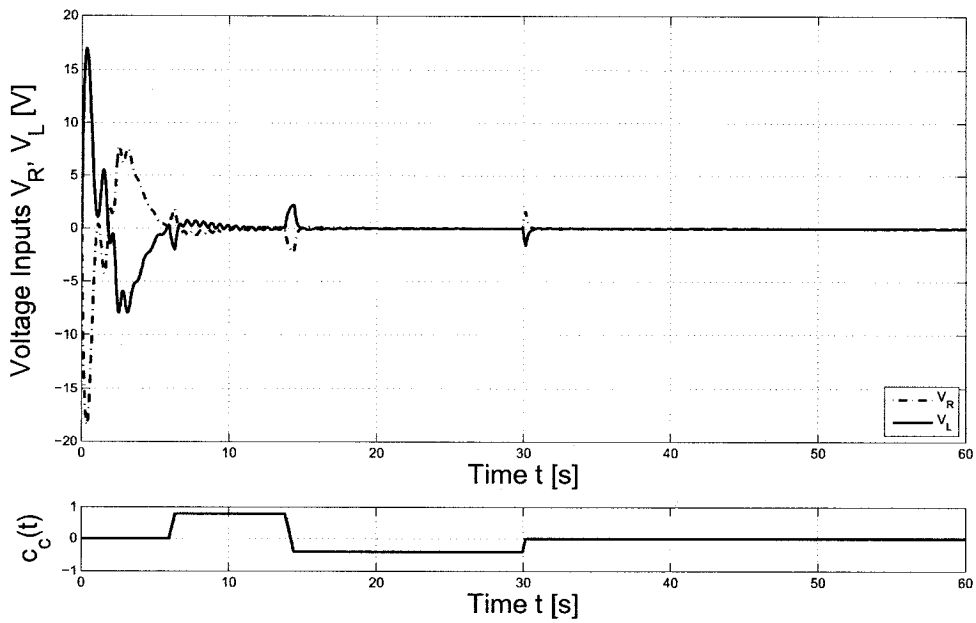

Figure 6.10: Plot of actuator voltage inputs V_R, V_L

The desired PWAPV steering control input, r_{des}, is plotted in Figure 6.11, while the corresponding switching signal, given by the regions $\mathcal{R}_i$, is plotted in Figure 6.12. It is seen in Figure 6.11 that the desired PWAPV steering input goes to zero and in Figure 6.12 that the switching signal goes to region $\mathcal{R}_3$, which is the region in which $\theta = 0\ rad$ is located.

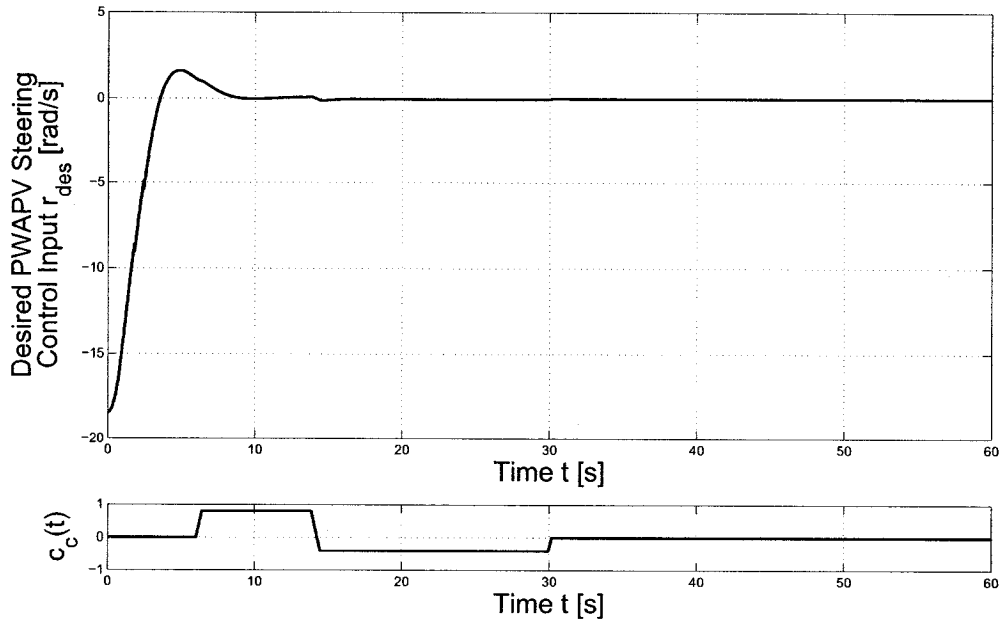

Figure 6.11: Plot of PWAPV steering control input r_{des}

The next section presents simulation results using the method developed by Soeanto *et al.* [2] as a means of comparison.

6.5 Comparison of Simulation Results

Using the method of Soeanto *et al.* [2], simulations were performed for the desired time-varying curvature shown in Figure 6.3. It should be noted that the method developed by Soeanto *et al.* does not include the actuator dynamics; although

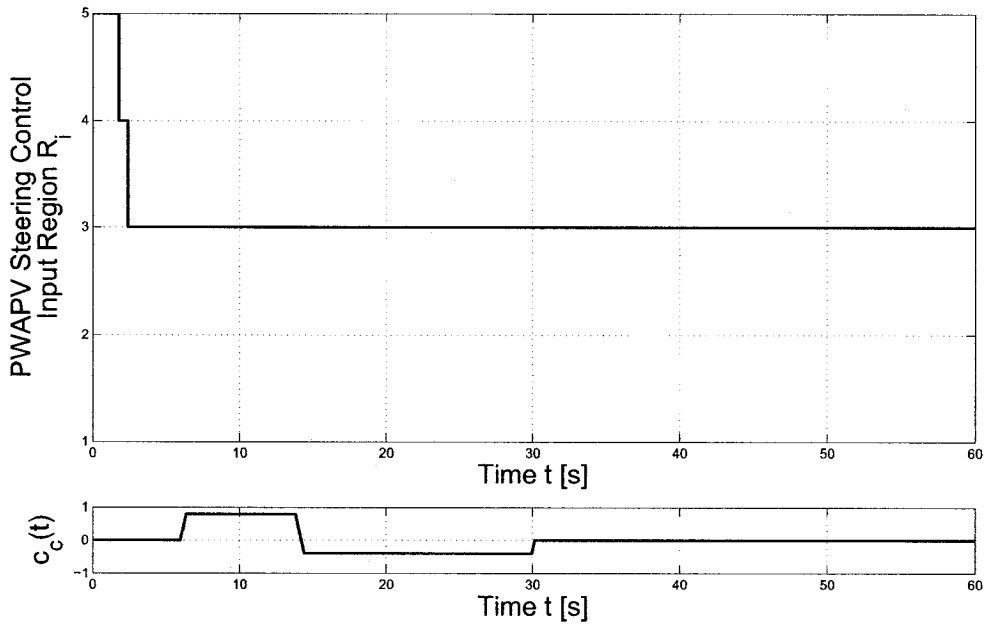

Figure 6.12: Plot of PWAPV switching signal $\mathcal{R}_i$

backstepping could be used, higher-order derivatives of the states are required and therefore the inputs in the following simulations are the right and left wheel torques T_R and T_L. The WMR begins on the desired path with a heading error $\theta = \pi$ *rad.*

The desired trajectory is shown in the top part of Figure 6.13, while the actual trajectory is shown in the bottom part of the figure. The time response of the WMR parameterized path kinematics θ, s_1, and y_1 in (5.1) is shown in Figure 6.14. It can be seen from Figure 6.14 that the parameterized kinematics, which represent the difference in the actual position and orientation of the WMR with respect to the desired position and orientation, converge to zero. The dynamic states u and r in (5.16) are plotted in Figure 6.15 with respect to time. It can be seen from this figure that the forward velocity converges to the desired value of $u_{des} = 0.10\ m/s$ while the rotational velocity converges to zero, which is the desired velocity for the final straight line segment of the path. The wheel control inputs, the right and left motor

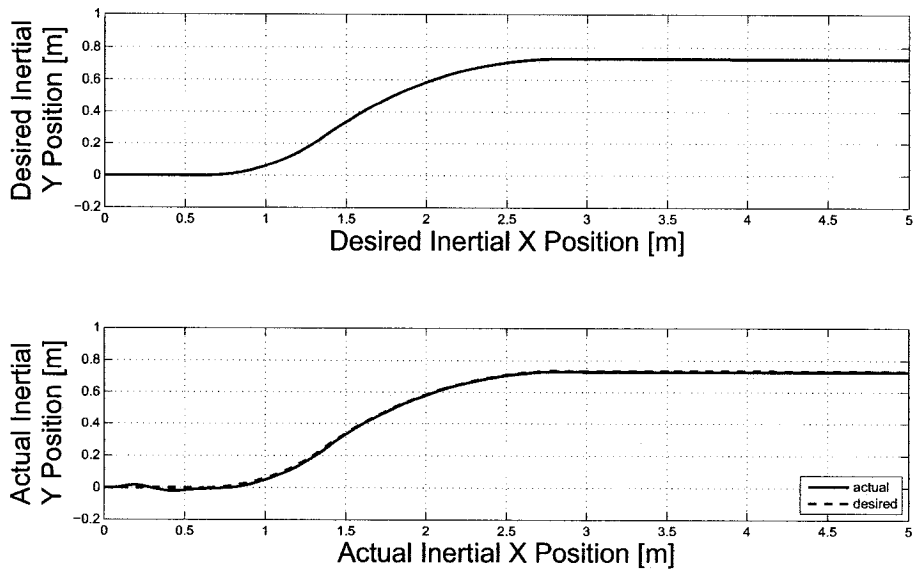

Figure 6.13: Plot of desired and actual trajectories (Soeanto's method)

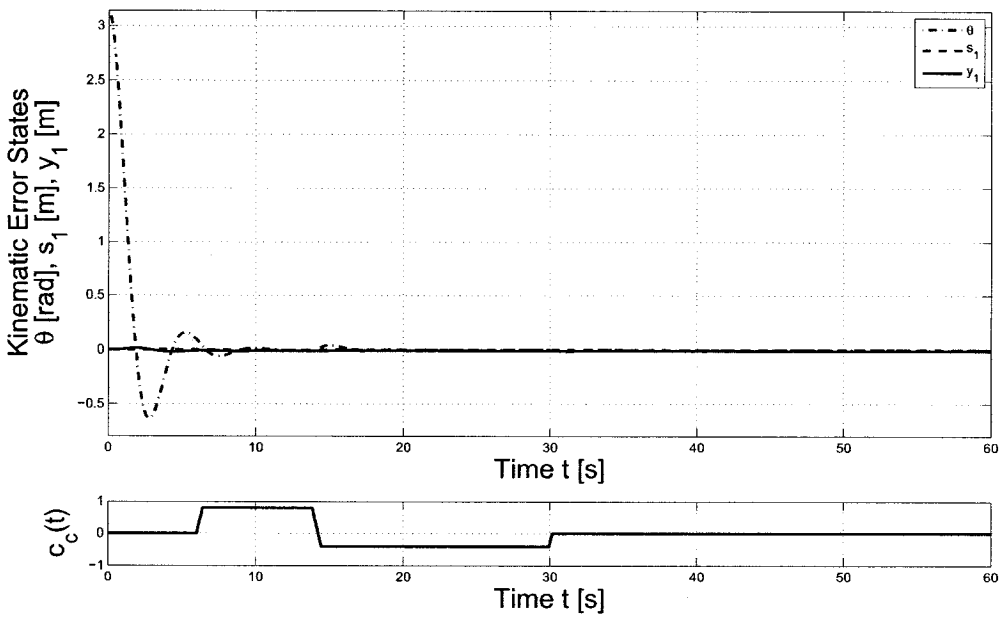

Figure 6.14: Plot of kinematic error states θ, s_1, y_1 (Soeanto's method)

torques T_R and T_L, are plotted with respect to time in Figure 6.16. Note in Figure 6.16 that the torque inputs vary when the desired path curvature changes. It can be seen from this last figure that the input torques required to bring the WMR to the desired trajectory using the method of Soeanto *et al.* are greater than those required using the method proposed in this thesis.

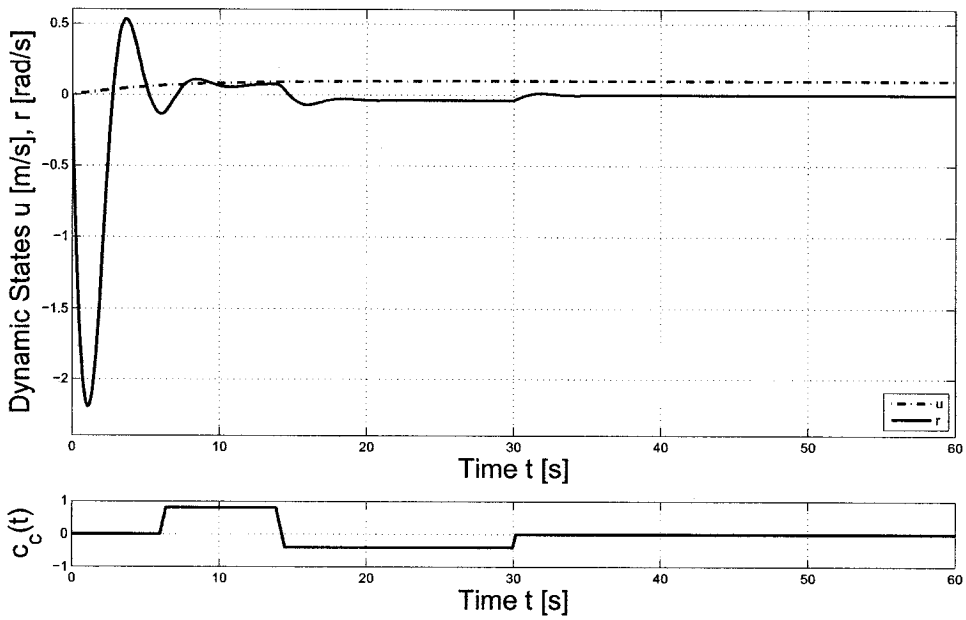

Figure 6.15: Plot of dynamic states u, r (Soeanto's method)

This chapter presented numerical simulations that demonstrate the effectiveness of the path following controller synthesis method proposed in this thesis and presented simulations using the method of Soeanto *et al.* [2] as a basis of comparison. The next chapter states the conclusions and suggestions for future work.

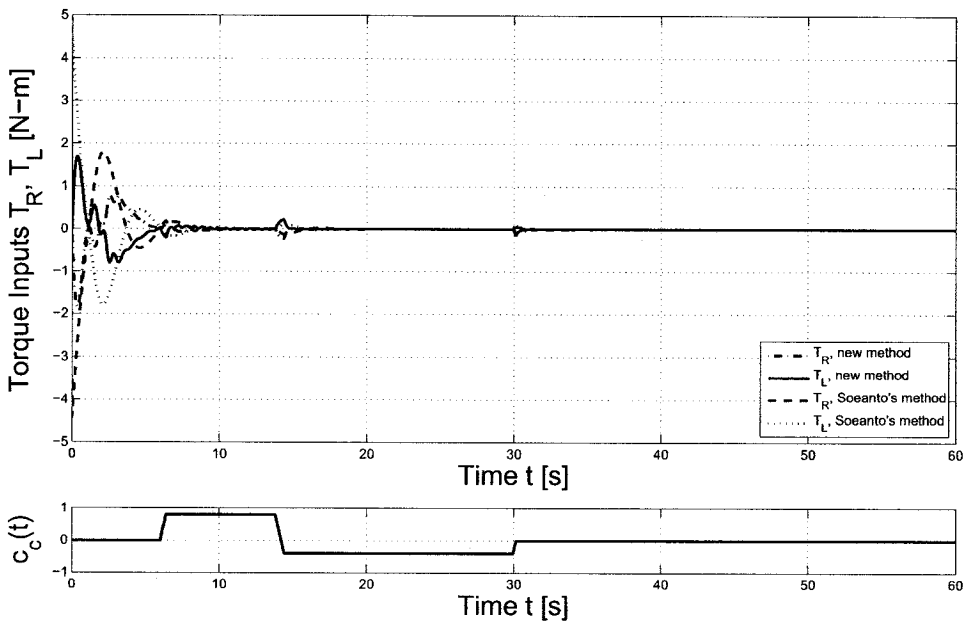

Figure 6.16: Plot of wheel torque inputs T_R, T_L (Soeanto's method)

Chapter 7

Conclusions and Future Work

This thesis proposed a path following control method consisting of a three-step procedure mixing piecewise-affine (PWA) and linear parameter-varying (LPV) techniques with backstepping. In the first step, two curvature limits and a curvature rate of change limit were defined for the desired path and the nonlinear WMR parameterized path kinematics were approximated by an uncertain piecewise-affine parameter-varying (PWAPV) system, while assuming that the WMR forward velocity is constant. A numerical method were proposed for determining PWA bounds on the uncertainty terms such that the original nonlinear parameter-dependent system is contained in the uncertain PWAPV system. Then, a PWAPV steering control law was designed using a parameter-dependent quadratic Lyapunov function. In the second step, a backstepping-type approach was used to include the vehicle dynamics and design the wheel control torques that guarantee convergence of the WMR forward and rotational velocities to the desired values. Finally, in the third step, the actuator dynamics were included and the input voltages are designed using backstepping. The effectiveness of the proposed path following control method was demonstrated through numerical simulations.

There are four primary advantages to the path following controller synthesis method proposed in this thesis. First, the PWAPV controller synthesis method can be formulated as a convex optimization program subject to a parameterized set of Linear Matrix Inequalities (LMIs), which was approximated by a finite set of LMIs using LPV theory and then solved efficiently using available software. Second, it included both a general, non-singular path parameterization and the actuator dynamics. Third, the PWAPV control law can also stabilize the type of nonlinear parameter-dependent system considered here. And fourth, it is a first step toward including hard nonlinearities in the actuator dynamics, which are important PWA characteristics.

Despite the advantages just mentioned, there are some limitations to the methods proposed in this thesis. This work does not include PWA characteristics in the actuator dynamics, does not study the robustness of the closed-loop system to disturbances, uses a general form for the uncertainties, requires knowledge of all the states, considers a unicycle-type vehicle, and does not validate the proposed method through hardware experiments. Therefore, the following topics are proposed for future work, with comments regarding possible difficulties or approaches in each case:

- Include PWA characteristics in the actuator dynamics. Note that, in the case of a series combination of PWA systems, the number of regions of each of the subsystems is multiplied together, thus increasing the complexity of the overall system.

- Examine the robustness of the overall system to disturbances using methods such as differential inclusions or $\mathcal{H}_\infty$. Two possible approaches are foreseen: one is to consider each step of the path following controller synthesis method individually, while the other is to consider the overall closed-loop system.

- Consider particular types of modelling uncertainties. It would be interesting to add more structure to the uncertainties, such as for example, polynomial or polytopic, which could simplify the methods proposed in this thesis.

- Extend the current state feedback approach to output feedback. Although output feedback synthesis methods have been developed for PWA systems, difficulties may result when combining PWA and backstepping methods.

- Extend the methods to more complex WMR kinematic models. The path parameterization method used in this thesis was developed for a unicycle-type vehicle and should be extended to more complex models. Factors that should be taken into account include, for example, the tire dynamics and the effects of non-horizontal surfaces on the lateral, forward and vertical dynamics.

- Validate the proposed path following controller synthesis method through hardware experiments. The use of proper sensors is always an issue that must be considered when developing hardware testbeds.

Bibliography

[1] Courtesy NASA/JPL-Caltech, "Mars Exploration Rover Mission: Multimedia." [Online]. Available: http://marsrovers.nasa.gov/gallery/artwork/

[2] D. Soeanto, L. Lapierre, and A. M. Pascoal, "Adaptive, Non-Singular Path-Following, Control of Dynamic Wheeled Robot," in *Proc. of the 11th Int. Conf. on Advanced Robotics ICAR'03*, Coimbra, Portugal, 30 June–3 July 2003.

[3] J. F. Sturm, "Using SeDuMi 1.02, a MATLAB Toolbox for Optimization Over Symmetric Cones (Updated for Version 1.05)," *Optimization Methods and Software*, vol. 11–12, pp. 625–653, 1999.

[4] M. Aicardi, G. Casalino, A. Bicchi, and A. Balestrino, "Closed Loop Steering of Unicycle-Like Vehicles Via Lyapunov Techniques," *IEEE Robotics and Automation Magazine*, vol. 2, no. 1, pp. 27–35, March 1995.

[5] A. Micaelli and C. Samson, "Trajectory Tracking for Unicycle-Type and Two-Steering-Wheels Mobile Robots," *Technical Report No. 2097*, 1993.

[6] K. D. Do and J. Pan, "Robust Path Following of Underactuated Ships Using Serret-Frenet Frame," in *Proc. of the 2003 American Control Conf.*, vol. 3, 4–6 June 2003, pp. 2000–2005.

[7] P. Encarnação and A. M. Pascoal, "3D Path Following Control of Autonomous Underwater Vehicles," in *Proc. of the 39th IEEE Conf. on Decision and Control*, vol. 3, Sydney, Australia, 12–15 December 2000, pp. 2977–2982.

[8] S. Al-Hiddabi and N. McClamroch, "Tracking and Maneuver Regulation Control for Nonlinear Nonminimum Phase Systems: Application to Flight Control," *IEEE Trans. on Control Systems Technology*, vol. 10, no. 6, pp. 780–792, November 2002.

[9] J. Hauser and R. Hindman, "Aggressive Flight Maneuvers," in *Proc. of the 36th IEEE Conf. on Decision and Control*, vol. 5, San Diego, U.S.A., 12–15 December 1997, pp. 4186–4191.

[10] S. Shehab and L. Rodrigues, "Preliminary results on UAV path following using piecewise-affine control," in *Proc. of the 2005 IEEE Conf. on Control Applications*, Toronto, Canada, 28–31 August 2005, pp. 358–363.

[11] Y. Zhao and S. L. BeMent, "Kinematics, Dynamics and Control of Wheeled Mobile Robots," in *Proc. of the 1992 IEEE Int. Conf. on Robotics and Automation*, vol. 1, Nice, France, 12–14 May 1992, pp. 91–96.

[12] C. Canudas de Wit and O. J. Sørdalen, "Exponential stabilization of mobile robots with nonholonomic constraints," *IEEE Trans. on Automatic Control*, vol. 37, no. 11, pp. 1791–1797, November 1992.

[13] R. T. M'Closkey and R. M. Murray, "Exponential Stabilization of Driftless Nonlinear Control Systems Using Homogeneous Feedback," *IEEE Trans. on Automatic Control*, vol. 42, no. 5, pp. 614–628, May 1997.

[14] W. E. Dixon, D. M. Dawson, and E. Zergeroglu, "Tracking and Regulation Control of a Mobile Robot System With Kinematic Disturbances: A Variable Structure-Like Approach," *J. of Dynamic Systems, Measurement, and Control*, vol. 122, no. 4, pp. 616–623, December 2000.

[15] J.-M. Yang and J.-H. Kim, "Sliding Mode Control for Trajectory Tracking of Nonholonomic Wheeled Mobile Robots," *IEEE Trans. on Robotics and Automation*, vol. 15, no. 3, pp. 578–587, June 1999.

[16] B. D'Andréa-Novel, G. Bastin, and G. Campion, "Control of Nonholonomic Wheeled Mobile Robots by State Feedback Linearization," *Int. J. Robotics Research*, vol. 14, no. 6, pp. 543–559, December 1995.

[17] A. D. Luca and M. D. D. Benedetto, "Control of Nonholonomic Systems Via Dynamic Compensation," *Kybernetica*, vol. 29, no. 6, pp. 593–608, 1993.

[18] E. Yang, D. Gu, T. Mita, and H. Hu, "Nonlinear Tracking Control of a Car-Like Mobile Robot Via Dynamic Feedback Linearisation," in *Proc. of Control 2004*, University of Bath, U.K., 6–9 September 2004.

[19] I. Kolmanovsky and N. H. McClamroch, "Developments in Nonholonomic Control Problems," *IEEE Control Systems Magazine*, vol. 15, no. 6, pp. 20–36, December 1995.

[20] R. Fierro and F. L. Lewis, "Control of a Nonholonomic Mobile Robot: Backstepping Kinematics Into Dynamics," in *Proc. of the 34th IEEE Conf. on Decision and Control*, vol. 4, New Orleans, U.S.A., 13–15 December 1995, pp. 3805–3810.

[21] Y.-C. Chang and B.-S. Chen, "Adaptive Tracking Control Design of Nonholonomic Mechanical Systems," in *Proc. of the 35th IEEE Conf. on Decision and Control*, vol. 4, Kobe, Japan, 11–13 December 1996, pp. 4739–4744.

[22] W. E. Dixon, D. M. Dawson, F. Zhang, and E. Zergeroglu, "Global Exponential Tracking Control of a Mobile Robot System via a PE Condition," *IEEE Trans. on Systems, Man, and Cybernetics – Part B: Cybernetics*, vol. 30, no. 1, pp. 129–142, February 2000.

[23] T. Fukao, H. Nakagawa, and N. Adachi, "Adaptive Tracking Control of a Nonholonomic Mobile Robot," *IEEE Trans. on Robotics and Automation*, vol. 16, no. 5, pp. 609–615, October 2000.

[24] S. V. Gusev, I. A. Makarov, I. E. Paromtchik, V. A. Yakubovich, and C. Laugier, "Adaptive Motion Control of a Nonholonomic Vehicle," in *Proc. of the IEEE Int. Conf. on Robotics and Automation*, Leuven, Belgium, 16–20 May 1998, pp. 3285–3290.

[25] H. G. Tanner and K. J. Kyriakopoulos, "Discontinuous Backstepping for Stabilization of Nonholonomic Mobile Robots," in *Proc. of the 2002 IEEE Int. Conf. on Robotics and Automation*, vol. 4, Washington, U.S.A., 11–15 May 2002, pp. 3948–3953.

[26] G. Oriolo, A. De Luca, and M. Vendittelli, "WMR Control via Dynamic Feedback Linearization: Design, Implementation and Experimental Validation," *IEEE Trans. Control Systems Technology*, vol. 10, no. 6, pp. 835–852, November 2002.

[27] S. He, "Feedback Control Design of Differential-Drive Wheeled Mobile Robots," in *Proc. of the 12th Int. Conf. on Advanced Robotics ICAR'05*, Seattle, U.S.A., 18–20 July 2005, pp. 135–140.

[28] D. Chwa, "Sliding-Mode Tracking Control of Nonholonomic Wheeled Mobile Robots in Polar Coordinates," *IEEE Trans. on Control Systems Technology*, vol. 12, no. 4, pp. 637–644, July 2004.

[29] M. Bak, N. Poulsen, and O. Ravn, "Path Following Mobile Robot in the Presence of Velocity Constraints," in *Proc. of European Control Conf.*, Porto, Portugal, 4–7 September 2001.

[30] K. C. Koh and H. S. Cho, "A Smooth Path Tracking Algorithm for Wheeled Mobile Robots with Dynamic Constraints," *J. Intelligent and Robotic Systems*, vol. 24, pp. 367–385, 1999.

[31] M. Oya, C.-Y. Su, and R. Katoh, "Robust Adaptive Motion/Force Tracking Control of Uncertain Nonholonomic Mechanical Systems," *IEEE Trans. on Robotics and Automation*, vol. 19, no. 1, pp. 175–181, February 2003.

[32] X. Yun and Y. Yamamoto, "Stability Analysis of the Internal Dynamics of a Wheeled Mobile Robot," vol. 14, no. 10, pp. 697–709, 1997.

[33] D. Wang and G. Xu, "Full-State Tracking and Internal Dynamics of Nonholonomic Wheeled Mobile Robots," *IEEE/ASME Trans. on Mechatronics*, vol. 8, no. 2, pp. 203–214, June 2003.

[34] G. Ishigami, A. Miwa, and K. Yoshida, "Steering Trajectory Analysis of Planetary Exploration Rovers Based on All-Wheel Dynamics Model," in *Proc. of*

the 8th Int. Symposium on Artificial Intelligence, Robotics and Automation in Space, Munich, Germany.

[35] G. Ishigami and K. Yoshida, "Steering Characteristics of an Exploration Rover on Loose Soil Based on All-Wheel Dynamics Model," in *2005 IEEE/RSJ Int. Conf. on Intelligent Robots and Systems*, Alberta, Canada, 2–6 August 2005, pp. 3099–3104.

[36] K. Yoshida and G. Ishigami, "Steering Characteristics of a Rigid Wheel for Exploration on Loose Soil," in *2004 IEEE/RSJ Int. Conf. on Intelligent Robots and Systems*, vol. 4, Miyagi, Japan, 28 September–2 October 2004, pp. 3995 – 4000.

[37] A. Aguiar, A. Atassi, and A. Pascoal, "Regulation of a Nonholonomic Dynamic Wheeled Mobile Robot With Parametric Modeling Uncertainty Using Lyapunov Functions," in *Proc. of the 39th IEEE Conf. on Decision and Control*, Sydney, Australia, 12–15 December 2000.

[38] W. Dong and Y. Guo, "Dynamic Tracking Control of Uncertain Nonholonomic Mobile Robots," in *Proc. of IEEE Int. Conf. on Intelligent Robots and Systems*, Edmonton, Canada, 2–6 August 2005.

[39] M. Egerstedt, X. Hu, and A. Stotsky, "Control of a Car-Like Robot Using a Dynamic Model," in *Proc. 1998 IEEE Int. Conf. on Robotics and Automation*, vol. 4, Leuven, Belgium, 16–20 May 1998, pp. 3273–3278.

[40] ——, "Control of a Car-Like Robot Using a Virtual Vehicle Approach," in *Proc. of the 37th IEEE Conf. on Decision and Control*, vol. 2, Tampa, U.S.A., 16–18 December 1998, pp. 1502–1507.

[41] Y. Zhang, D. Hong, J. Chung, and S. Velinsky, "Dynamic Model Based Robust Tracking Control of a Differentially Steered Wheeled Mobile Robot," in *Proc. of the 1998 American Control Conf.*, vol. 2, Philidelphia, U.S.A., 24–26 June 1998, pp. 850–855.

[42] Y. Bestaoui, "An optimal velocity generation of a rear wheel drive tricycle along a specified path," in *Proc. of the 2000 American Control Conf.*, vol. 4, Chicago, U.S.A., 28–30 June 2000, pp. 2907–2911.

[43] C.-F. Chang, C.-I. Huang, and L.-C. Fu, "Nonlinear Control of a Wheeled Mobile Robot with Nonholonomic Constraints," *2004 IEEE Int. Conf. on Systems, Man and Cybernetics*, vol. 6, pp. 5404–5410, 10–13 October 2004.

[44] K. Kozłowski and D. Pazderski, "Modeling and Control of a 4-Wheel Skid-Steering Mobile Robot," *Int. J. Appl. Math. Comput. Sci.*, vol. 14, no. 4, pp. 477–496, 2004.

[45] A. Albagul and W. Martono, "Dynamic Modelling and Adaptive Traction Control for Mobile Robots," in *Int. J. of Advanced Robotic Systems*, vol. 1, no. 3, 2004, pp. 149–154.

[46] A. D. Luca, G. Oriolo, and M. Vendittelli.

[47] B. M. Kim and P. Tsiotras, "Controllers for Unicycle-Type Wheeled Robots - Theoretical Results and Experimental Validation," *IEEE Trans. on Robotics and Automation*, vol. 18, no. 3, pp. 294–307, June 2002.

[48] Z.-H. Luo, K. Machida, and M. Funaki, "Design and Control of a Cartesian Nonholonomic Robot," *J. of Robotic Systems*, vol. 15, no. 2, pp. 85–95, 1998.

[49] V. M. Peri and D. Simon, "Fuzzy Logic Control for an Autonomous Robot," in *2005 Annual Meeting of the North American Fuzzy Information Processing Society NAFIPS 2005*, 26–28 June 2005, pp. 337–342.

[50] G. S. Sukhatme, S. Brizius, and G. A. Bekey, "Mobility Evaluation of a Wheeled Microrover using a Dynamic Model," in *1997 IEEE/RSJ Int. Conf. on Intelligent Robots and Systems*, vol. 3, Grenoble, France, 7–11 September 1997, pp. 1506–1512.

[51] A. Hassibi and S. P. Boyd, "Quadratic Stabilization and Control of Piecewise-Linear Systems," in *Proc. of the 1998 American Control Conf.*, vol. 6, Philadelphia, U.S.A., 24–26 June 1998, pp. 3659–3664.

[52] M. Johansson, *Piecewise Linear Control Systems.* Berlin, Heidelberg: Springer, 2003.

[53] N. B. O. L. Pettit and P. E. Wellstead, "Analyzing Piecewise Linear Dynamical Systems," *IEEE Control Systems Magazine*, vol. 15, no. 5, pp. 43–50, October 1995.

[54] L. Rodrigues, "Stability Analysis of Piecewise-Affine Systems Using Controlled Invariant Sets," *Systems and Control Letters*, vol. 53, no. 2, pp. 157–169, October 2004.

[55] S. LeBel, L. Rodrigues, and A. Ng, "Piecewise-Affine Controller Synthesis for a Model of 2D Orbital Path Following," in *Proc. of the 2005 IEEE Conf. on Control Applications*, Toronto, Canada, 28–31 August 2005, pp. 571–576.

[56] A. Rantzer and M. Johansson, "Piecewise Linear Quadratic Optimal Control," *IEEE Trans. on Automatic Control*, vol. 45, no. 4, pp. 629–637, April 2000.

[57] L. Rodrigues and J. How, "Synthesis of Piecewise-Affine Controllers for Stabilization of Nonlinear Systems," in *Proc. of the 42nd IEEE Conf. on Decision and Control*, vol. 3, Maui, Hawaii, 9–12 December 2003, pp. 2071–2076.

[58] L. Rodrigues and S. P. Boyd, "Piecewise-Affine State Feedback for Piecewise-Affine Slab Systems Using Convex Optimization," *Systems and Control Letters*, vol. 54, no. 9, pp. 835–853, September 2005.

[59] L. Rodrigues, "State Feedback Control of Piecewise-Affine Systems with Norm Bounded Noise," in *Proc. of 2005 American Control Conf.*, Portland, U.S.A., 8–10 June 2005.

[60] C. A. Yfoulis, A. Muir, N. B. O. L. Pettit, and P. E. Wellstead, "Stabilization of Orthogonal Piecewise Linear Systems Using Piecewise Lyapunov-Like Function," in *Proc. of 37th IEEE Conf. on Decision and Control*, vol. 2, Tampa, U.S.A., 16–18 December 1998, pp. 1476–1481.

[61] A. Pavlov, N. van de Wouw, and H. Nijmeijer, "Convergent Piecewise Affine Systems: Analysis and Design, Part I: Continuous Case," in *Proc. of 44th IEEE Conf. on Decision and Control and European Control Conf.*, Seville, Spain, 12–15 December 2005, pp. 5391–5396.

[62] L. Rodrigues, A. Hassibi, and J. P. How, "Output Feedback Controller Synthesis for Piecewise-Affine Systems with Multiple Equilibria," in *Proc. of 2000 American Control Conf.*, vol. 3, Chicago, U.S.A., 28–30 June 2000, pp. 1784–1789.

[63] L. Rodrigues and J. How, "Observer-Based Control of Piecewise-Affine Systems," *Int. J. of Control*, vol. 76, pp. 459–477, March 2003.

[64] M. Johansson and A. Rantzer, "Computation of Piecewise Quadratic Lyapunov Functions for Hybrid Systems," *IEEE Trans. on Automatic Control*, vol. 43, no. 4, pp. 555–559, April 1998.

[65] G. Feng, "Controller Design and Analysis of Uncertain Piecewise-Linear Systems," *IEEE Trans. on Circuits and Systems – I: Fundamental Theory and Applications*, vol. 49, no. 2, pp. 224–232, February 2002.

[66] G. Feng, G. P. Lu, and S. S. Zhou, "An Approach to H_∞ Controller Synthesis of Piecewise Linear Systems," *Communications in Information and Systems*, vol. 2, no. 3, pp. 245–254, December 2002.

[67] G. Feng, "Controller Synthesis of Fuzzy Dynamic Systems Based on Piecewise Lyapunov Functions and Bilinear Matrix Inequalities," *IEEE Trans. on Fuzzy Systems*, vol. 11, no. 5, pp. 605–612, October 2003.

[68] M. Chen, C. R. Zhu, and G. Feng, "Linear-Matrix-Inequality–Based Approach to H_∞ Controller Synthesis of Uncertain Continuous-Time Piecewise Linear Systems," *IEE Proc. Control Theory Applications*, vol. 151, no. 3, pp. 295–301, May 2004.

[69] G. Feng, C.-L. Chen, D. Sun, and Y. Zhu, "H_∞ Controller Synthesis of Fuzzy Dynamic Systems Based on Piecewise Lyapunov Functions and Bilinear Matrix Inequalities," *IEEE Trans. on Fuzzy Systems*, vol. 13, no. 1, pp. 94–103, February 2005.

[70] S. LeBel and L. Rodrigues, "Path Following of a Wheeled Mobile Robot Combining Piecewise-Affine Synthesis and Backstepping Approaches," in *Proc. of the 2007 American Control Conf.*, New York, U.S.A., 11–13 July 2007, pp. 4518–4523.

[71] S. Shehab and L. Rodrigues, "UAV Path Following Using a Mixed Piecewise-Affine and Backstepping Control Approach," in *Proc. of the European Control Conf.*, Kos, Greece, 2–5 July 2007, pp. 301–306.

[72] J. Shamma, "Analysis and Design of Gain Scheduled Control Systems," Ph.D. dissertation, Massachusetts Institute of Technology, 1998.

[73] J. Shamma and M. Athans, "Analysis of Gain Scheduled Control for Nonlinear Plants," *IEEE Trans. on Automatic Control*, vol. 35, no. 8, pp. 898–907, August 1990.

[74] D. Leith and W. Leithead, "Survey of Gain Scheduling Analysis & Design," *Int. J. of Control*, 1999.

[75] R. Gao, K. Ohtsubo, and H. Kajiwara, "LPV Design for a Space Vehicle Attitude Control Benchmark Problem," in *SICE 2003 Annual Conference*, vol. 2, 4–6 August 2003, pp. 1461–1464.

[76] A. S. Ghersin and R. S. S. P. na, "LPV Control of a 6-DOF Vehicle," *IEEE Trans. on Control Systems Technology*, vol. 10, no. 6, pp. 883–887, November 2002.

[77] S. Lim, "New Quaternion Feedback Control for Efficient Large Angle Maneuvers," in *Proc. of the AIAA Guidance, Navigation, and Control Conference*, Montreal, Canada, 6–9 August 2001.

[78] A. Marcos and G. J. Balas, "Development of Linear-Parameter-Varying Models for Aircraft," *J. of Guidance, Control, and Dynamics*, vol. 27, no. 2, pp. 218–228, March–April 2004.

[79] J.-Y. Shin, G. J. Balas, and M. A. Kaya, "Blending Methodology of Linear Parameter Varying Control Synthesis of F-16 Aircraft System," *J. of Guidance, Control, and Dynamics*, vol. 25, no. 6, pp. 1040–1048, November–December 2002.

[80] S. Lim and J. How, "Modeling and $\mathcal{H}_\infty$ Control for Switched Linear Parameter-Varying Missile Autopilot," *IEEE Trans. Control Systems Technology*, vol. 11, no. 6, pp. 830–838, November 2003.

[81] F. Wu, A. Packard, and G. Balas, "LPV Control Design for Pitch Axis Missile Autopilot," in *Proc. of the 34th IEEE Conf. on Decision and Control*, vol. 1, New Orleans U.S.A., 13–15 December 1995, pp. 188–191.

[82] Q. Song and K. M. Grigoriadis, "Diesel Engine Speed Regulation Using Linear Parameter Varying Control," in *Proc. of the 2003 American Control Conf.*, vol. 1, Denver, U.S.A., 4–6 June 2003, pp. 779–784.

[83] G. Becker and A. Packard, "Robust Performance of Linear Parametrically Varying Systems Using Parameterically-Dependent Linear Feedback," *System and Control Letters*, vol. 23, no. 3, pp. 205–215, September 1994.

[84] E. Feron, P. Apkarian, and P. Gahinet, "$\mathcal{S}$-Procedure for the Analysis of Control Systems with Parametric Uncertainties via Parameter-Dependent Lyapunov Functions," in *Proc. of the 1995 American Control Conf.*, vol. 1, Seattle, U.S.A., 21–23 June 1995, pp. 968–972.

[85] P. Gahinet, P. Apkarian, and M. Chilali, "Affine Parameter-Dependent Lyapunov Functions and Real Parametric Uncertainty," *IEEE Trans. on Automatic Control*, vol. 41, no. 3, pp. 437–442, March 1996.

[86] F. Wu, "Control of Linear Parameter Varying Systems," Ph.D. dissertation, University of California at Berkeley, Berkeley, U.S.A., 1995.

[87] S. Lim and J. How, "Analysis of LPV Systems using a Piecewise Affine Parameter-Dependent Lyapunov Function," in *Proc. of the 36th IEEE Conf. on Decision and Control*, vol. 2, San Diego, U.S.A., 10–12 December 1997, pp. 978–983.

[88] S. Lim and K. Chan, "Analysis of Hybrid Linear Parameter-Varying Systems," in *Proc. of the 2003 American Control Conf.*, vol. 6, Denver, U.S.A., 4–6 June 2003, pp. 4822–4827.

[89] S. Lim and J. P. How, "Control of LPV Systems Using a Quasi-Piecewise Affine Parameter-Dependent Lyapunov Function," in *Proc. of the 1998 American Control Conf.*, vol. 2, Philadelphia, U.S.A., 24–26 June 1998, pp. 1200–1204.

[90] B. Lu and F. Wu, "Switching LPV Control Designs Using Multiple Parameter-Dependent Lyapunov Functions," *Automatica*, vol. 40, no. 11, pp. 1973–1980, November 2004.

[91] F. P. Beer, W. E. Clausen, and P. J. Cornwell, *Vector Mechanics for Engineers: Dynamics*, 8th ed. McGraw-Hill, 2006.

[92] R. Dorf and R. Bishop, *Modern Control Systems*, 9th ed. Prentice Hall, 2001.

[93] L. Rodrigues and J. How, "Automated Control Design for a Piecewise-Affine Approximation of a Class of Nonlinear Systems," in *Proc. of 2001 American Control Conf.*, vol. 4, Arlington, U.S.A., 25–27 June 2001, pp. 3189–3194.

[94] S. Pettersson, "Analysis and design of hybrid systems," Ph.D. dissertation, Chalmers University of Technology, Göteborg, Sweden, June 1999.

[95] B. Samadi and L. Rodrigues, "Extension of a Local Linear Controller to a Stabilizing Semi-Global Piecewise-Affine Controller," in *7th Portuguese Conf. on Automatic Control*, Lisbon, Portugal, 11–13 September 2006.

[96] E.-K. Boukas and Z.-K. Liu, *Deterministic and Stochastic Time-Delay Systems.* New York, U.S.A.: Birkhäuser, 2002.

[97] S. Boyd, L. E. Ghaoui, E. Feron, and V. Balakrishnan, *Linear Matrix Inequalities in System and Control Theory.* Philadelphia, U.S.A.: SIAM (Studies in Applied Mathematics), 1994.

[98] S. M. Selby, *Standard Mathematical Tables.* CRC Press, 1974.

[99] M. Krstić, I. Kanellakopoulos, and P. Kokotović, *Nonlinear and Adaptive Control Design.* New York, U.S.A.: John Wiley & Sons, Inc., 1995.